Title
Transcriptional control of the recombination activating genes Rag1 and Rag2 in B lymphocytes and non-lymphoid cells

Author
Timblin, Greg Alan

Publication Date
2014

Peer reviewed|Thesis/dissertation

Transcriptional control of the recombination activating genes *Rag1* and *Rag2* in B lymphocytes and non-lymphoid cells.

by

Greg Alan Timblin

A dissertation submitted in partial satisfaction of the requirements for a degree in

Doctor of Philosophy

in

Molecular and Cell Biology

in the

Graduate Division

of

The University of California, Berkeley

Committee in charge:

Professor Mark S. Schlissel, co-chair

Professor Robert Tjian, co-chair

Professor David Raulet
Professor Donald Rio
Professor David Schaffer

Spring 2014

Abstract

Transcriptional control of the recombination activating genes *Rag1* and *Rag2* in B lymphocytes and non-lymphoid cells.

by

Greg Alan Timblin

Doctor of Philosophy in Molecular and Cell Biology

University of California, Berkeley

Professor Mark S. Schlissel and Professor Robert Tjian, co-chairs

Expression of the recombination activating genes *Rag1* and *Rag2* (*Rag*) is essential for generation of a diverse B cell antigen receptor repertoire necessary for effective adaptive immune responses. The *Rag* genes are among the first lineage-specific genes expressed in lymphocyte progenitors, and their expression strongly correlates with commitment to the B lineage. Because V(D)J recombination involves generation of DNA breaks by the RAG proteins, *Rag* expression must be tightly controlled throughout B cell development to maintain genomic integrity. Using Abelson Murine Leukemia Virus-transformed B cells as a model system, we sought to identify factors that repress *Rag* transcription during pre-B cell differentiation, a period of B cell development marked by rapid proliferation during which the *Rag* genes are transiently repressed and then reactivated upon differentiation. A screen identified Ebf1 and c-Myb, two well-studied transcription factors in the context of early B cell development, as repressors of *Rag* transcription in these highly proliferative cells. As we found no evidence for direct *Rag* repression by Ebf1, we investigated how Ebf1 influences the expression of factors previously implicated in the regulation *Rag* transcription. We discovered that Ebf1 achieves *Rag* repression through both negative regulation of the *Rag* activator Foxo1, and positive regulation of the *Rag* repressor Gfi1b. In addition to influencing Foxo1 and Gfi1b expression in a similar manner, we found that c-Myb directly binds to the E*rag* enhancer in the *Rag* locus and antagonizes Foxo1 binding to this *cis* regulatory element. Together this work reveals previously unappreciated roles for Ebf1 and c-Myb in the transcriptional repression of the *Rag* genes during pre-B cell differentiation. In addition to screening for factors that regulate *Rag* expression during B cell development, we also performed a screen for factors capable of activating the *Rag* genes in non-lymphoid cells. Given the close connection between *Rag* expression and B lineage commitment in lymphocyte progenitors, we reasoned that if we were able to induce *Rag* transcription in non-lymphoid cells such as fibroblast, these cells might be activating a host of B cell-specific genes and undergoing direct reprogramming to the B lineage. While we identified factors that could readily induce *Rag* expression when overexpressed in primary fibroblasts, we could detect no evidence of a reprogramming event involving activation of additional B lineage genes. Together our work identified novel repressors of *Rag* transcription in developing B cells, and factors capable of activating *Rag* transcription in non-lymphoid cells that may inform future fibroblast-to-B cell reprogramming experiments.

For Mom, Dad, and Angie,
your love and unwavering support of everything I do means the world to me.

Acknowledgements

First and foremost I thank my mentor Mark Schlissel for making me the scientist I am today. I'm not sure if he sees it this way or noticed a progression and improvement over time, but personally I feel I have come a LONG way in terms of simply being able to "think like a scientist" since I joined Schlissel Lab in the spring of 2009. In hindsight I see myself at that time as having the ability to move liquids from one tube to another with a pipette, but not much else. I now have the confidence in my abilities to design and carry out good experiments, evaluate and make all possible interpretations of the data, and draw appropriate conclusions that can be used to ask the next question. The majority of credit for instilling this confidence in my scientific abilities goes to Mark. Not only did I learn how to be a scientist through observing and interacting with him, but perhaps more importantly through the process of my own trial and error, which were made possible by Mark allowing me the freedom work on and pursue the things I found interesting in lab.

In addition, the tenacity and passion with which he attacks his work, whether it be scientific or administrative, is extremely inspiring, motivating, and sometimes confounding. Timestamps on emails often make me wonder if he ever sleeps. I hope that throughout life I am able to do things that interest and excite me to the degree that I can put forth at least half the effort that Mark pours into his work. One simple yet powerful quote from a conversation with Mark about a future experiment has really stuck with me in particular: "You don't know until you try". This simple mantra has become something I strive to live by and apply to all situations, scientific or otherwise. Thank you Mark.

I am extremely grateful for the support and generosity of my co-mentor Robert Tjian. Tij and members of his lab welcomed me and afforded me the opportunity finish the final year of my thesis work in a fantastic lab environment. Though I was only a part of the Tij lab for a short period, I am a much better scientist for it as a result of the learning and interactions that took place during that time.

I am very appreciative of the efforts put forth by the other members of my thesis committee: David Raulet, Don Rio, and Dave Schaffer. Your time, support, and ideas were crucial to the progress I made on projects during my time as a MCB graduate student.

The Schlissel Lab was an enjoyable place to work because of the people just as much as the science. Thank you to all the Schlissel Lab members whom I had the pleasure to work with, you each brought something special to the table that created a wonderful environment to do science. Whether I was doing experiments in my tiny end-of-bench workspace, enjoying yet another delicious birthday cake and the conversation that always came with it, or sneaking out for beverages and science talk in the afternoon sun, lab was always a good place for me to be because of the people there. I sincerely thank you all.

I owe a special thanks to certain members of the MCB Class of 2008 who were crucial to my success as a grad student. Michael Sanchez, who I met in the summer of 2007 during our participation in the Amgen Scholars Program at Berkeley, has been a great friend, roommate, and all-around inspiration to me over the last 7 years. His integrity, work ethic, and perseverance

are second to none. While most of our time together was spent complaining about grad school and science, I always left any interaction with Mike with a sense of positivity and eagerness to attack the next challenge that lie ahead.

As Margaux Bennett and Nikki Kong also dabbled in B cell development and transformation in their graduate research, our paths crossed frequently. Many reagents, ideas, and stories of great experimental success and failures were shared between us. These interactions provided me with both chances to commiserate, and hope that my experiments might some day pan out, too.

Finally I am most grateful for the love and support provided by my family. Having a Mom who was also kindergarten/1st grade teacher was such blessing as she understood the importance of education and reading in my development as an all-around person. Thanks to her, summer days spent in places like libraries, museums, and zoos sparked my curiosity and passion for learning at a young age and ultimately fueled my desire to become a scientist. While my original aspirations of becoming a paleontologist didn't come to fruition (all those dinosaur books read for nothing!), molecular biologist is a nice compromise. Thank you Mom.

Dad taught me that it is a good thing to be busy. Whether it was a new landscaping project in the yard or tinkering with a vehicle in the shed, Dad always went about his business with little to say and intense focus on the task at hand. Not that he didn't have time for a game of catch or one-on-one, or to help coach my youth baseball and basketball teams. His workman-like approach to all things inspired me to apply great focus to athletics and academics, and to always give my best effort without worry or complaining about things out of my control. A simple "good job bud" and pat on the back from him always made any big win or aced test that much sweeter. Thank you Dad.

Growing up I always looked up to and was inspired by my older sister Angie. Her success, whether it was in the classroom, at a speech tournament, or on the softball field or golf course, made me so proud and inspired me to put forth my best efforts in my own academic and athletic activities. While I am jealous of her higher ACT mark to this day, maybe a Ph.D. evens the score? I am probably the only one still keeping score, as she is too busy being a great mother to my wonderful niece and nephew Ellie and Quinn, and a loving wife to Kyle, who has been a great brother-in-law to get to know over the past several years. Thanks big sister.

Table of Contents

List of Figures

Chapter 1

Introduction

Background

The Innate and Adaptive Immune Systems

Interactions between organisms shape their behavior and evolution. While some interactions are beneficial to one or both of the organisms involved, interactions exist where one organism benefits at the expense of the other. This is often the case in host-pathogen interactions, as pathogens by definition cause disease in their host. Co-evolution of pathogens (microorganisms such viruses, bacteria, fungi and protozoa) and their hosts (often more complex organisms such as plants and animals) has lead to the development of host immune systems that are responsible for the detection and clearance of harmful pathogens.

The immune system of higher mammals is divided into two arms: the innate and adaptive immune systems (Figure 1.1). The innate immune system is an ancient, evolutionary conserved system of cell surface and intracellular receptors that relies on the detection of invariant features shared among pathogens (Janeway and Medzhitov., 2002). Examples of ligands include genetic material such as DNA and RNA, structural components such as lipopolysaccharide (LPS), and byproducts of pathogen invasion and replication in host cells such as membrane damage (Vance et al., 2009). The advantage of the innate immune system is speed: a fixed number of germline-encoded innate receptors are expressed in a variety of cell types from birth, ready to sense potential invaders. This comes at a cost however, as pathogens can quickly evolve and potentially mutate around the specificity of a given innate receptor. Moreover, if the feature detected by an innate immune sensor is not unique to pathogens but is also present in the host (ex. DNA), the receptor has the potential to initiate an autoimmune response against the host (Barton et al., 2006).

Unlike the innate immune system, the adaptive immune system relies on vast repertoire of receptors that are somatically generated in B and T lymphocytes, clonally expressed, highly specific, and bind with high affinity to their targets, referred to as antigens (Tonegawa., 1983, Flajnik and Kasahara., 2010). The adaptive immune system is a feature unique to jawed vertebrates, where innate immune responses play a crucial role in activating and shaping the adaptive immune response following initial detection of invading pathogens (Iwasaki and Medzhitov., 2010). While the cost of adaptive immunity comes in the time lag needed to activate and expand the cells expressing antigen receptors that can mediate pathogen clearance, the enormous diversity of the receptor repertoire affords protection against an almost limitless number of pathogens. The process that gives rise to antigen receptor repertoire diversity occurs during B and T lymphocyte development and is known as V(D)J recombination.

Lymphocyte Antigen Receptors and V(D)J recombination

Antigen receptors on B and T lymphocytes are structurally and functionally distinct (Figure 1.2). The B cell receptor (BCR) or immunoglobulin (Ig) molecule is a tetrameric complex consisting of two identical heavy (H) chain and two identical light (L) chains. Both H and L chain proteins possess invariant constant (C) regions, and variable (V) regions that form the antigen-binding surface that differ between individual antibody molecules (discussed below). Whether in a

membrane-bound or secreted form, the BCR typically recognizes soluble antigens in their native forms.

T cell receptors (TCR) are made up of either α and β chains or γ and δ chains in αβ and γδ T cells, respectively (Figure 1.2). Like heavy and light chain proteins, the TCR chains posses C and V regions. αβ TCRs recognize peptide antigens derived from proteins processed by intracellular proteases and chaperoned to the cell surface by major histocompatibility (MHC) molecules. Unlike the BCR, the αβ TCR is always expressed as a membrane-bound receptor.

The seven loci that encode for B and T cell receptor components (Ig H, κ, λ, and TCR α, β, γ, and δ loci) span several megabases on different chromosomes and are made up of numerous variable (V), diversity (D), and joining (J) gene segments (Figure 1.3). Each segment is flanked by a recombination signal sequence (RSS) that consist of a conserved heptamer and nonamer sequence separated by a 12 or 23 base pair spacer. The products of the recombination activating genes *Rag1* and *Rag2* (collectively referred to as the *Rag* genes) are responsible for the rearrangement of Ig and TCR gene segments during V(D)J recombination (Schatz et al., 1989, Oettinger et al., 1990).

The biochemistry of RAG-mediated recombination at the Ig and TCR loci is well-characterized (Schatz and Swanson., 2011)(Figure 1.4). The RAG proteins bind to RSS sequences adjacent to two gene segments that have been brought into close proximity by DNA looping and make double-stranded DNA breaks, producing blunt, 5'-phosphorylated signal ends and hairpin coding ends. The coding end hairpins are open by the Artemis endonuclease and joined by DNA Ligase IV and other components of the nonhomologous end-joining (NHEJ) pathway to produce complete coding regions. The signal ends are also joined by NHEJ and the DNA between recombined gene segments is lost.

The end result of V(D)J recombination and Ig/TCR gene segment rearrangement is a vast array of different V(D)J joints within large populations of B and T lymphocytes. These joints, which differ both combinatorially (they use different gene segments) and junctionally (loss and addition of nucleotides occurs during the DNA repair process), encode for the variable (V) regions of the Ig and TCR molecules responsible for binding soluble antigens and peptide/MHC complexes, respectively. Thus the combinatorial and junctional diversity generated during V(D)J recombination gives rise to the vast array of binding specificities in the receptor repertoire of adaptive immune system cells.

Regulation of V(D)J recombination

V(D)J recombination is regulated on several levels (Schlissel., 2003). First, the expression of the *Rag* genes is lymphocyte-specific. Thus, antigen receptor loci will only be recombined in developing B cells in the fetal liver, neonatal gut (Wesemann et al., 2013), and adult bone marrow, and in developing T cells in the thymus.

Secondly, rearrangement of Ig and TCR loci is cell-type specific. All evidence to date suggests the proteins that carry out V(D)J recombination do not differ between B and T cells. This implies that the accessibility of the recombinase machinery to the antigen receptor loci must differ

between the two cell types, giving rise to the so-called "accessibility hypothesis". Indeed *in vitro* studies with purified chromatin from both cell types reveals only Ig loci are accessible to RAG proteins in B cells, and only TCR loci are accessible in T cells (Stanhope-Baker et al., 1996). A complex interplay of germline transcription, chromatin remodeling and looping, and epigenetic marks such as histone modifications and DNA methylation contribute to this cell type-specific locus accessibility in processes directed by lineage-specific transcription factors (Bossen et al., 2012).

Third, V(D)J recombination occurs in a highly ordered fashion. Certain loci rearrange before others during lymphocyte development, and within these loci the order with which gene segments rearrange is fixed. For example, D-J rearrangement occurs before V-DJ rearrangement at the Ig H locus, and Ig L does not initiate until Ig H recombination is complete in developing B cells (Hardy et al., 1991). This regulation is achieved in part by the "12/23 Rule" in which gene segments flanked by a RSS with a 12 base pair spacer will only recombine with gene segments flanked by an RSS with a 23 base pair spacer (van Gent et al., 1996). Moreover, numerous studies have described how germline transcription, chromatin dynamics, and epigenetics cooperate to control the order with which antigen receptor loci rearrange (Schlissel and Baltimore., 1989, Guo et al., 2011, Mandal et al., 2011, Lin et al., 2012).

Fourth, antigen receptor loci are subject to allelic exclusion, meaning that if successful rearrangement occurs at one Ig or TCR allele, recombination at and expression of the second allele is actively repressed (Vettermann and Schlissel., 2010). This mode of regulation is more prevalent at the Ig H and TCR β loci, as it is estimated that 1-10% of B and T cells show allelic inclusion of the Ig κ and TCR α loci, respectively (Brady et al., 2010). Nevertheless, allelic exclusion ensures that the majority of cells of the adaptive immune system are clonal ("one cell, one receptor, one specificity"), which is thought to be crucial for self-tolerance and the prevention of autoimmunity (Fournier et al., 2012).

Finally, the expression of *Rag* genes is tightly controlled (Kuo and Schlissel., 2009). This mode of regulation operates at both the transcriptional and post-translational levels, ensuring *Rag* mRNA and RAG proteins are expressed only during specific periods of B and T cell development. The significance of this control in the context of B cell development and oncogenic transformation is discussed in more detail below.

Rag **locus structure and control of** ***Rag*** **transcription**

Rag1 and *Rag2* are physically linked and convergently transcribed genes, each giving rise to transcripts with large single-exon open reading frames (Figure 1.5). This unique genomic structure, along with the similarities between V(D)J recombination and DNA transposition reactions, suggests the *Rag* locus is a "captured and tamed" mobile DNA element that entered the genome of a common ancestor of jawed vertebrates during very recent evolution (Fugmann., 2010). Indeed, the RAG proteins are capable of catalyzing transposition of cleaved DNA fragments with signal ends into target sites on independent DNA molecules (Hiom et al., 1998, Agrawal et al., 1998).

The *trans*-acting factors and *cis*-regulatory elements that control transcription during B and T cell development differ between the two cell types. While the *Rag1* promoter drives reporter gene expression in a variety of cell types, the *Rag2* promoter is active only in lymphocyte cell lines and is regulated by different transcription factors in B versus T cells (Lauring and Schlissel., 1999, Wang et al., 2000, Kishi et al., 2000). Much attention has been focused on characterization of more distal *cis* regulatory elements 5' of *Rag2* that control both *Rag1* and *Rag2* expression. The 10 kb region 5' of *Rag2* is important for *Rag* expression in developing B cells and $CD4^-$ $CD8^-$ double negative (DN) T cells, but not $CD4^+CD8^+$ double positive (DP) T cells (Yu et al., 1999). In agreement with this, regions 0-2 kb and 2-7 kb 5' of *Rag2* can independently rescue B but not T cell development in $Rag2^{-/-}$ mice (Monroe et al., 1999), though deletion of the 0-2 kb region had to effect on B and T cell development or *Rag* expression *in vivo*. Consistent with the idea that more distal elements are required for *Rag* expression during later stages of T cell development, a T cell-specific enhancer 55 kb 5' of *Rag2* known as ASE directs RAG expression in DP T cells (Yannoutsos et al., 2004). Finally, our lab identified a B cell-specific enhancer 23 kb 5' of *Rag2* known as E*rag* (Hsu et al., 2003)(Figure 1.5). Deletion of E*rag* results in a partial block in B cell development, while T cell development is unaffected.

Numerous transcription factors have been shown to bind the *Rag* promoters and *cis* regulatory elements and drive *Rag* expression during B cell development, including E2A, Ebf1, Pax5, Foxo1, Foxp1, Lef1, c-Myb, Ikaros, and Bcl11A (Lauring and Schlissel., 1999, Jin et al., 2002, Hsu et al., 2003, Hu et al., 2006, Dengler et al., 2008a, Reynaud et al., 2008, Zandi et al., 2008, Lee et al., 2013). The method used to show binding differs between these studies (e.g., *in vitro* gel shift versus *ex vivo* chromatin immunoprecipitation), as does the method used to show functionality (e.g., reporter constructs in transfected non-lymphoid cell lines versus activation of the endogenous *Rag* locus in B cell lines). Thus for many of these factors, the connection between occupancy and function remains unclear. Further work is needed to delineate factors absolutely necessary for *Rag* expression, along with factors important for negatively regulating the *Rag* genes, during B cell development *in vivo*.

V(D)J Recombination and *Rag* expression during B cell development

The development of B lymphocytes from hematopoietic stem cells in the bone marrow is a complex process during which transcription factors and signaling pathways drive commitment to the B lineage and loss of alternative lineage potentials (Mandel and Grosschedl., 2010)(Figure 1.6). The *Rag* genes are among the earliest B lineage genes expressed in the common lymphoid progenitor (CLPs) compartment (Igarashi et al., 2002), and the level of *Rag* expression in CLPs correlates with B lineage restriction (Mansson et al., 2010). Ig H locus D-J rearrangement occurs as CLPs differentiate into pre-pro-B cells, with Ig H V-DJ rearrangement occurring in committed CD19+ pro-B cells (Hardy et al., 1991).

If Ig H locus rearrangement in pro-B cells results in production of a stable heavy chain protein, it pairs with surrogate light chain components VpreB and λ5 and traffics to the cell surface as a precursor B cell antigen receptor (pre-BCR), signifying the transition to the pre-B cell stage (Herzog et al., 2009). If competent for signaling, the pre-BCR induces proliferation and the clonal expansion of cells that have produced a functional heavy chain protein. *Rag* mRNA and RAG protein levels are downregulated during this proliferative burst (discussed

below)(Grawunder et al., 1995). Following several rounds of cell division, these large cycling pre-B cells exit the cell cycle, reexpress the *Rag* genes, and progress to the small resting pre-B cell stage where Ig κ locus rearrangement is initiated.

If rearrangement of the Ig κ locus in small pre-B cells results in production of a light chain protein that can successfully pair with the heavy chain, these proteins are expressed on the cell surface as a fully assembled B cell receptor (BCR), marking transition to the immature B cell stage. If rearrangement at either of the Ig κ alleles fails to produce a functional light chain, rearrangement will proceed at the Ig λ loci. Regardless of whether a fully assembled BCR contains a κ or λ light chain protein, *Rag* transcription is terminated if the BCR is not autoreactive (Grawunder et al., 1995)

If the BCR expressed on the cell surface of an immature B cell is autoreactive, the *Rag* genes will continue to be expressed and cells will undergo a process known as receptor editing (Luning Prak et al., 2011). During editing, additional rearrangements occur at the Ig κ and/or Ig λ loci that lead to the production of new light chain proteins that may pair with the heavy chain to form an alternative BCR. If this BCR is still autoreactive and rearrangement options have been exhausted, the developing B cells will undergo negative selection and apoptosis. This process is critical for purging the B cell repertoire of autoreactive B cells and maintaining self-tolerance.

Rag expression during pre-B cell differentiation

Rag expression and DSB generation are restricted to lymphocytes in the G_0-G_1 phases of cell cycle such that repair of DNA coding ends in the RAG-stabilized post-cleavage complex is carried out by the non-homologous end-joining (NHEJ) pathway (Lee et al., 2004). RAG-induced DSBs produced during S phase have the potential to be repaired by homologous recombination, a process that can lead to chromosomal translocations and oncogenic transformation (Kuppers and Dalla-Favera., 2001, Zhang et al., 2011). As lymphocytes go through periods of clonal expansion during their development, the expression of the *Rag* genes must be tightly regulated to maintain genomic integrity

As mentioned above, the pre-BCR checkpoint is a stage of B cell development during which cells undergo rapid proliferation followed by differentiation. The pre-BCR activates signaling pathways that synergize with interleukin-7 receptor (IL-7R) signaling to direct two processes (Johnson et al., 2008). The first is clonal expansion of pre-BCR+ progenitors, a stage during which RAG protein and *Rag* mRNA levels are negatively regulated upon entry of these large, cycling pre-B cells into S phase (Grawunder et al., 1995, Li et al., 1996). The second process is differentiation to the small pre-B cell stage, which involves coordinated cell cycle exit, re-expression of *Rag1* and *Rag2*, and increased chromatin accessibility at the Ig *kappa* light-chain locus to allow light chain gene recombination
(Mandal et al., 2009).

Phosphorylation and proteasome-dependent degradation of RAG2 controls recombinase protein levels during this proliferative burst (Lee and Desiderio., 1999). However, the mechanism by which *Rag* transcription is repressed by pre-BCR and IL-7R signaling has yet to be completely described. One way repression is achieved is through inactivation of positive regulators of the

Rag genes. PI(3)K-Akt signaling downstream of these receptors has been implicated in the repression of *Rag* transcription via antagonism of Foxo transcription factors including Foxo1 (Amin and Schlissel., 2008, Dengler et al., 2008b, Herzog et al., 2008, Ochiai et al., 2012). Phosphorylation of Foxo1 by Akt results cytoplasmic sequestration, though increases in Foxo1 protein and *Foxo1* mRNA levels observed upon pre-B cell differentiation show *Foxo1* is also regulated at the transcriptional level (Heng et al., 2008, Ochiai et al., 2012, Timblin and Schlissel., 2013). Attenuation of pre-BCR and IL-7R signaling leads to strong binding of Foxo1 to a site in the E*rag* enhancer in small pre-B cells (Ochiai et al., 2012), an event that is likely crucial for *Rag* expression in these cells. The MEK/ERK pathway has been shown to negatively regulate E2A proteins (Novak et al., 2010), which like Foxo1 have been implicated in the activation of *Rag* transcription through binding to E*rag* (Hsu et al., 2003).

Negative regulators of *Rag* transcription in large pre-B cells have also been described. Stat5, which represses premature recombinase accessibility at the Ig κ locus (Mandal et al., 2011), has been shown to repress *Rag* potentially through binding to regions upstream of the *Rag1* promoter in large pre-B cells (Johnson et al., 2012). Stat5 is activated by IL-7R signaling (Goetz et al., 2004), consistent with the ability of IL-7 to repress *Rag* transcription (Amin and Schlissel., 2008, Johnson et al., 2008). The transcriptional repressor Gfi1b has also been described as a negative regulator of *Rag* transcription (Schulz et al., 2012). Gfi1b achieves repression via a dual mechanism: directly via binding near E*rag* and recruiting chromatin-modifying enzymes that alter E*rag* accessibility, and indirectly via negative regulation of *Foxo1* expression. The pathways and factors controlling Gfi1b expression and activity are largely unknown, though the observation that *Gfi1b* mRNA levels peak in large pre-B cells suggests the involvement of pre-BCR and IL-7R signaling (Schulz et al., 2012).

In closing, the aforementioned factors clearly play important roles in *Rag* transcriptional regulation based on experimental findings. However, the interplay between these positive and negative regulators, and how pre-BCR and IL-7R signals are integrated to regulate their activity and achieve dynamic transcriptional activation and repression of the *Rag* genes in pre-B cells, remains to be fully elucidated.

AMuLV-transformed B cells as a model to study *Rag* transcriptional regulation during pre-B cell differentiation

To date, much has been learned about the molecular circuitry that controls the decision between pre-B cell proliferation and differentiation (Clark et al., 2014). As large cycling pre-B cells exist only in a transient state *in vivo* (Winkler et al., 1995), the majority of studies use cells isolated from mice lacking genes required for pre-B cell differentiation such as the signaling adaptor BLNK (SLP-65) and IRF transcription factors (Jumaa et al., 1999, Pappu et al., 1999, Lu et al., 2003). B lymphocytes isolated from these mice and cultured in IL-7 are arrested in a highly proliferative, pre-BCR+ state where the *Rag* genes are repressed. Cytokine withdrawal or gene reconstitution induces pre-B cell differentiation in these cultures, yielding a robust *in vitro* system to dissect the pathways controlling cell cycle, *Rag* transcription, and Ig κ locus recombination.

In addition to these mutant cell lines, another *in vitro* tool used to study the dynamic regulation of *Rag* transcription during pre-B cell differentiation are Abelson Murine Leukemia Virus (AMuLV)-transformed B cell lines. AMuLV was discovered as a virus that selectively transforms lymphoid cells *in vitro* (Rosenberg et al., 1975). The viral oncogene encoded by AMuLV is v-Abl, a constitutively active form of the non-receptor tyrosine kinase c-Abl, which has a well-characterized role as an oncogene in human malignancies (Heisterkamp et al., 1983). When total mouse bone marrow is infected with AMuLV, v-Abl selectively transforms and arrests developing B lymphocytes in a highly proliferative, cytokine-independent, large pre-B cell-like state where the *Rag* genes are repressed. Treatment of AMuLV-transformed cells with a small molecule inhibitor of v-Abl kinase, STI-571 (Gleevec), induces cell cycle exit, reexpression of the *Rag* genes, and differentiation to a small pre-B cell-like state where recombination at the Ig κ locus is initiated (Muljo and Schlissel., 2003). Thus like the aforementioned mutant cell lines, the AMuLV system represents a robust *in vitro* system to study pre-B cell differentiation and the regulation of *Rag* transcription during this developmental transition (Duy et al., 2010).

Purpose

The work in Chapter 2 of this thesis is focused on better understanding the molecular mechanisms controlling *Rag* transcription during B cell development. More specifically, we sought to identify factors that control the dynamic regulation of *Rag* transcription during pre-B differentiation using AMuLV-transformed B cells as our model system. To do so, we performed a screen for factors that actively repress *Rag* transcription in these highly proliferative cells. We identified Ebf1 and its downstream target c-Myb, two transcription factors well-studied in the context of early B cell development and the activation of B lineage genes in lymphocyte progenitors, as strong repressor of *Rag* transcription (Timblin and Schlissel., 2013). Experiments show that Ebf1 achieves repression through negative regulation of the *Rag* activator Foxo1, and positive regulation of the *Rag* repressor Gfi1b. This work reveals a previously unappreciated role for Ebf1 and c-Myb in restricting *Rag* expression during this highly proliferative stage of B cell development and preventing RAG-induced DNA breaks that could be aberrantly repaired and lead to oncogenic transformation.

In Chapter 3, we set out to learn more about the mechanism by which c-Myb represses *Rag* transcription. Experiments comparing the activity of wild-type c-Myb to a mutant c-Myb protein that lacks repressive activity show that c-Myb represses *Rag* transcription by a dual mechanism: indirectly by negatively regulating the expression of Foxo1, and directly by occupying the E*rag* enhancer element in the *Rag* locus and antagonizing Foxo1 binding. This work provides new insight into c-Myb biology and the mechanism by which this factor represses *Rag* transcription during B cell development.

Finally, Chapter 4 of this thesis describes attempts to utilize *Rag* transcription as a reporter in the direct reprogramming of fibroblasts to B lymphocytes. *Rag* transcription is closely tied with the commitment of lymphocyte progenitors to the B lineage. We reasoned that if we were able to induce *Rag* expression in non-lymphoid cells such as fibroblasts, these cells might be undergoing direct reprogramming to the B lineage. Thus we designed a screening strategy aimed at identifying a set of defined factors capable of directly reprogramming fibroblasts to B lymphocytes using activation of the *Rag* locus as a marker for reprogramming. While we failed to achieve full or partial reprogramming of target fibroblasts, we identified factors that can induce *Rag* expression in these cells in a robust and reproducible manner. This information may prove useful in the development of an efficient fibroblast-to-B cell reprogramming system. Such a system would be of great use in the context of regenerative medicine as it could provide an unlimited source of patient-specific B cells for the treatment of various immunodeficiencies, autoimmune disorders, and malignant conditions.

References

Agrawal, A., Q.M. Eastman, and D.G. Schatz. 1998. Transposition mediated by RAG1 and RAG2 and its implications for the evolution of the immune system. *Nature* 394:744-751.

Amin, R.H., and M.S. Schlissel. 2008. Foxo1 directly regulates the transcription of recombination-activating genes during B cell development. *Nat. Immunol.* 9:613-622.

Barton, G.M., J.C. Kagan, and R. Medzhitov. 2006. Intracellular localization of Toll-like receptor 9 prevents recognition of self DNA but facilitates access to viral DNA. *Nat. Immunol.* 7:49-56.

Bossen, C., R. Mansson, and C. Murre. 2012. Chromatin topology and the regulation of antigen receptor assembly. *Annu. Rev. Immunol.* 30:337-356.

Brady, B.L., N.C. Steinel, and C.H. Bassing. 2010. Antigen receptor allelic exclusion: an update and reappraisal. *J. Immunol.* 185:3801-3808.

Clark, M.R., M. Mandal, K. Ochiai, and H. Singh. 2014. Orchestrating B cell lymphopoiesis through interplay of IL-7 receptor and pre-B cell receptor signalling. *Nat. Rev. Immunol.* 14:69-80.

Dengler, H.S., G.V. Baracho, S.A. Omori, S. Bruckner, K.C. Arden, D.H. Castrillon, R.A. DePinho, and R.C. Rickert. 2008a. Distinct functions for the transcription factor Foxo1 at various stages of B cell differentiation. *Nat. Immunol.* 9:1388-1398.

Dengler, H.S., G.V. Baracho, S.A. Omori, S. Bruckner, K.C. Arden, D.H. Castrillon, R.A. DePinho, and R.C. Rickert. 2008b. Distinct functions for the transcription factor Foxo1 at various stages of B cell differentiation. *Nat. Immunol.* 9:1388-1398.

Duy, C., J.J. Yu, R. Nahar, S. Swaminathan, S.M. Kweon, J.M. Polo, E. Valls, L. Klemm, S. Shojaee, L. Cerchietti, W. Schuh, H.M. Jack, C. Hurtz, P. Ramezani-Rad, S. Herzog, H. Jumaa, H.P. Koeffler, I.M. de Alboran, A.M. Melnick, B.H. Ye, and M. Muschen. 2010. BCL6 is critical for the development of a diverse primary B cell repertoire. *J. Exp. Med.* 207:1209-1221.

Flajnik, M.F., and M. Kasahara. 2010. Origin and evolution of the adaptive immune system: genetic events and selective pressures. *Nat. Rev. Genet.* 11:47-59.

Fournier, E.M., M.G. Velez, K. Leahy, C.L. Swanson, A.V. Rubtsov, R.M. Torres, and R. Pelanda. 2012. Dual-reactive B cells are autoreactive and highly enriched in the plasmablast and memory B cell subsets of autoimmune mice. *J. Exp. Med.* 209:1797-1812.

Fugmann, S.D. 2010. The origins of the Rag genes--from transposition to V(D)J recombination. *Semin. Immunol.* 22:10-16.

Goetz, C.A., I.R. Harmon, J.J. O'Neil, M.A. Burchill, and M.A. Farrar. 2004. STAT5 activation underlies IL7 receptor-dependent B cell development. *J. Immunol.* 172:4770-4778.

Grawunder, U., T.M. Leu, D.G. Schatz, A. Werner, A.G. Rolink, F. Melchers, and T.H. Winkler. 1995. Down-regulation of RAG1 and RAG2 gene expression in preB cells after functional immunoglobulin heavy chain rearrangement. *Immunity* 3:601-608.

Guo, C., H.S. Yoon, A. Franklin, S. Jain, A. Ebert, H.L. Cheng, E. Hansen, O. Despo, C. Bossen, C. Vettermann, J.G. Bates, N. Richards, D. Myers, H. Patel, M. Gallagher, M.S. Schlissel, C. Murre, M. Busslinger, C.C. Giallourakis, and F.W. Alt. 2011. CTCF-binding elements mediate control of V(D)J recombination. *Nature* 477:424-430.

Hardy, R.R., C.E. Carmack, S.A. Shinton, J.D. Kemp, and K. Hayakawa. 1991. Resolution and characterization of pro-B and pre-pro-B cell stages in normal mouse bone marrow. *J. Exp. Med.* 173:1213-1225.

Heisterkamp, N., J.R. Stephenson, J. Groffen, P.F. Hansen, A. de Klein, C.R. Bartram, and G. Grosveld. 1983. Localization of the c-ab1 oncogene adjacent to a translocation break point in chronic myelocytic leukaemia. *Nature* 306:239-242.

Heng, T.S., M.W. Painter, and Immunological Genome Project Consortium. 2008. The Immunological Genome Project: networks of gene expression in immune cells. *Nat. Immunol.* 9:1091-1094.

Herzog, S., E. Hug, S. Meixlsperger, J.H. Paik, R.A. DePinho, M. Reth, and H. Jumaa. 2008. SLP-65 regulates immunoglobulin light chain gene recombination through the PI(3)K-PKB-Foxo pathway. *Nat. Immunol.* 9:623-631.

Herzog, S., M. Reth, and H. Jumaa. 2009. Regulation of B-cell proliferation and differentiation by pre-B-cell receptor signalling. *Nat. Rev. Immunol.* 9:195-205.

Hiom, K., M. Melek, and M. Gellert. 1998. DNA transposition by the RAG1 and RAG2 proteins: a possible source of oncogenic translocations. *Cell* 94:463-470.

Hsu, L.Y., J. Lauring, H.E. Liang, S. Greenbaum, D. Cado, Y. Zhuang, and M.S. Schlissel. 2003. A conserved transcriptional enhancer regulates RAG gene expression in developing B cells. *Immunity* 19:105-117.

Hu, H., B. Wang, M. Borde, J. Nardone, S. Maika, L. Allred, P.W. Tucker, and A. Rao. 2006. Foxp1 is an essential transcriptional regulator of B cell development. *Nat. Immunol.* 7:819-826.

Igarashi, H., S.C. Gregory, T. Yokota, N. Sakaguchi, and P.W. Kincade. 2002. Transcription from the RAG1 locus marks the earliest lymphocyte progenitors in bone marrow. *Immunity* 17:117-130.

Iwasaki, A., and R. Medzhitov. 2010. Regulation of adaptive immunity by the innate immune system. *Science* 327:291-295.

Janeway, C.A.,Jr, and R. Medzhitov. 2002. Innate immune recognition. *Annu. Rev. Immunol.* 20:197-216.

Jin, Z.X., H. Kishi, X.C. Wei, T. Matsuda, S. Saito, and A. Muraguchi. 2002. Lymphoid enhancer-binding factor-1 binds and activates the recombination-activating gene-2 promoter together with c-Myb and Pax-5 in immature B cells. *J. Immunol.* 169:3783-3792.

Johnson, K., J. Chaumeil, M. Micsinai, J.M. Wang, L.B. Ramsey, G.V. Baracho, R.C. Rickert, F. Strino, Y. Kluger, M.A. Farrar, and J.A. Skok. 2012. IL-7 functionally segregates the pro-B cell stage by regulating transcription of recombination mediators across cell cycle. *J. Immunol.* 188:6084-6092.

Johnson, K., T. Hashimshony, C.M. Sawai, J.M. Pongubala, J.A. Skok, I. Aifantis, and H. Singh. 2008. Regulation of immunoglobulin light-chain recombination by the transcription factor IRF-4 and the attenuation of interleukin-7 signaling. *Immunity* 28:335-345.

Jumaa, H., B. Wollscheid, M. Mitterer, J. Wienands, M. Reth, and P.J. Nielsen. 1999. Abnormal development and function of B lymphocytes in mice deficient for the signaling adaptor protein SLP-65. *Immunity* 11:547-554.

Kishi, H., X.C. Wei, Z.X. Jin, Y. Fujishiro, T. Nagata, T. Matsuda, and A. Muraguchi. 2000. Lineage-specific regulation of the murine RAG-2 promoter: GATA-3 in T cells and Pax-5 in B cells. *Blood* 95:3845-3852.

Kuo, T.C., and M.S. Schlissel. 2009. Mechanisms controlling expression of the RAG locus during lymphocyte development. *Curr. Opin. Immunol.* 21:173-178.

Kuppers, R., and R. Dalla-Favera. 2001. Mechanisms of chromosomal translocations in B cell lymphomas. *Oncogene* 20:5580-5594.

Lauring, J., and M.S. Schlissel. 1999. Distinct factors regulate the murine RAG-2 promoter in B- and T-cell lines. *Mol. Cell. Biol.* 19:2601-2612.

Lee, B.S., J.D. Dekker, B.K. Lee, V.R. Iyer, B.P. Sleckman, A.L. Shaffer 3rd, G.C. Ippolito, and P.W. Tucker. 2013. The BCL11A transcription factor directly activates RAG gene expression and V(D)J recombination. *Mol. Cell. Biol.* 33:1768-1781.

Lee, G.S., M.B. Neiditch, S.S. Salus, and D.B. Roth. 2004. RAG proteins shepherd double-strand breaks to a specific pathway, suppressing error-prone repair, but RAG nicking initiates homologous recombination. *Cell* 117:171-184.

Lee, J., and S. Desiderio. 1999. Cyclin A/CDK2 regulates V(D)J recombination by coordinating RAG-2 accumulation and DNA repair. *Immunity* 11:771-781.

Li, Z., D.I. Dordai, J. Lee, and S. Desiderio. 1996. A conserved degradation signal regulates RAG-2 accumulation during cell division and links V(D)J recombination to the cell cycle. *Immunity* 5:575-589.

Lin, Y.C., C. Benner, R. Mansson, S. Heinz, K. Miyazaki, M. Miyazaki, V. Chandra, C. Bossen, C.K. Glass, and C. Murre. 2012. Global changes in the nuclear positioning of genes and intra- and interdomain genomic interactions that orchestrate B cell fate. *Nat. Immunol.* 13:1196-1204.

Lin, Y.C., S. Jhunjhunwala, C. Benner, S. Heinz, E. Welinder, R. Mansson, M. Sigvardsson, J. Hagman, C.A. Espinoza, J. Dutkowski, T. Ideker, C.K. Glass, and C. Murre. 2010. A global network of transcription factors, involving E2A, EBF1 and Foxo1, that orchestrates B cell fate. *Nat. Immunol.* 11:635-643.

Lu, R., K.L. Medina, D.W. Lancki, and H. Singh. 2003. IRF-4,8 orchestrate the pre-B-to-B transition in lymphocyte development. *Genes Dev.* 17:1703-1708.

Luning Prak, E.T., M. Monestier, and R.A. Eisenberg. 2011. B cell receptor editing in tolerance and autoimmunity. *Ann. N. Y. Acad. Sci.* 1217:96-121.

Mandal, M., S.E. Powers, M. Maienschein-Cline, E.T. Bartom, K.M. Hamel, B.L. Kee, A.R. Dinner, and M.R. Clark. 2011. Epigenetic repression of the Igk locus by STAT5-mediated recruitment of the histone methyltransferase Ezh2. *Nat. Immunol.* 12:1212-1220.

Mandal, M., S.E. Powers, K. Ochiai, K. Georgopoulos, B.L. Kee, H. Singh, and M.R. Clark. 2009. Ras orchestrates exit from the cell cycle and light-chain recombination during early B cell development. *Nat. Immunol.* 10:1110-1117.

Mandel, E.M., and R. Grosschedl. 2010. Transcription control of early B cell differentiation. *Curr. Opin. Immunol.* In Press, Corrected Proof:

Mansson, R., S. Zandi, E. Welinder, P. Tsapogas, N. Sakaguchi, D. Bryder, and M. Sigvardsson. 2010. Single-cell analysis of the common lymphoid progenitor compartment reveals functional and molecular heterogeneity. *Blood* 115:2601-2609.

Monroe, R.J., F. Chen, R. Ferrini, L. Davidson, and F.W. Alt. 1999. RAG2 is regulated differentially in B and T cells by elements 5' of the promoter. *Proc. Natl. Acad. Sci. U. S. A.* 96:12713-12718.

Muljo, S.A., and M.S. Schlissel. 2003. A small molecule Abl kinase inhibitor induces differentiation of Abelson virus-transformed pre-B cell lines. *Nat. Immunol.* 4:31-37.

Novak, R., E. Jacob, J. Haimovich, O. Avni, and D. Melamed. 2010. The MAPK/ERK and PI3K pathways additively coordinate the transcription of recombination-activating genes in B lineage cells. *J. Immunol.* 185:3239-3247.

Ochiai, K., M. Maienschein-Cline, M. Mandal, J.R. Triggs, E. Bertolino, R. Sciammas, A.R. Dinner, M.R. Clark, and H. Singh. 2012. A self-reinforcing regulatory network triggered by limiting IL-7 activates pre-BCR signaling and differentiation. *Nat. Immunol.* 13:300-307.

Oettinger, M.A., D.G. Schatz, C. Gorka, and D. Baltimore. 1990. RAG-1 and RAG-2, adjacent genes that synergistically activate V(D)J recombination. *Science* 248:1517-1523.

Pappu, R., A.M. Cheng, B. Li, Q. Gong, C. Chiu, N. Griffin, M. White, B.P. Sleckman, and A.C. Chan. 1999. Requirement for B cell linker protein (BLNK) in B cell development. *Science* 286:1949-1954.

Reynaud, D., I.A. Demarco, K.L. Reddy, H. Schjerven, E. Bertolino, Z. Chen, S.T. Smale, S. Winandy, and H. Singh. 2008. Regulation of B cell fate commitment and immunoglobulin heavy-chain gene rearrangements by Ikaros. *Nat. Immunol.* 9:927-936.

Rosenberg, N.\., D.\. Baltimore, and C.D.\. Scher. 1975. In vitro transformation of lymphoid cells by Abelson murine leukemia virus.\. *Proc. Natl. Acad. Sci. U. S. A.* 72\:1932-6\.

Schatz, D.G., M.A. Oettinger, and D. Baltimore. 1989. The V(D)J recombination activating gene, RAG-1. *Cell* 59:1035-1048.

Schatz, D.G., and P.C. Swanson. 2011. V(D)J recombination: mechanisms of initiation. *Annu. Rev. Genet.* 45:167-202.

Schlissel, M.S. 2003. Regulating antigen-receptor gene assembly. *Nat. Rev. Immunol.* 3:890-899.

Schlissel, M.S., and D. Baltimore. 1989. Activation of immunoglobulin kappa gene rearrangement correlates with induction of germline kappa gene transcription. *Cell* 58:1001-1007.

Schulz, D., L. Vassen, K.T. Chow, S.M. McWhirter, R.H. Amin, T. Moroy, and M.S. Schlissel. 2012. Gfi1b negatively regulates Rag expression directly and via the repression of FoxO1. *J. Exp. Med.* 209:187-199.

Stanhope-Baker, P., K.M. Hudson, A.L. Shaffer, A. Constantinescu, and M.S. Schlissel. 1996. Cell type-specific chromatin structure determines the targeting of V(D)J recombinase activity in vitro. *Cell* 85:887-897.

Timblin, G.A., and M.S. Schlissel. 2013. Ebf1 and c-Myb repress rag transcription downstream of Stat5 during early B cell development. *J. Immunol.* 191:4676-4687.

Tonegawa, S. 1983. Somatic generation of antibody diversity. *Nature* 302:575-581.

van Gent, D.C., D.A. Ramsden, and M. Gellert. 1996. The RAG1 and RAG2 proteins establish the 12/23 rule in V(D)J recombination. *Cell* 85:107-113.

Vance, R.E., R.R. Isberg, and D.A. Portnoy. 2009. Patterns of pathogenesis: discrimination of pathogenic and nonpathogenic microbes by the innate immune system. *Cell. Host Microbe* 6:10-21.

Vettermann, C., and M.S. Schlissel. 2010. Allelic exclusion of immunoglobulin genes: models and mechanisms. *Immunol. Rev.* 237:22-42.

Wang, Q.F., J. Lauring, and M.S. Schlissel. 2000. c-Myb binds to a sequence in the proximal region of the RAG-2 promoter and is essential for promoter activity in T-lineage cells. *Mol. Cell. Biol.* 20:9203-9211.

Wesemann, D.R., A.J. Portuguese, R.M. Meyers, M.P. Gallagher, K. Cluff-Jones, J.M. Magee, R.A. Panchakshari, S.J. Rodig, T.B. Kepler, and F.W. Alt. 2013. Microbial colonization influences early B-lineage development in the gut lamina propria. *Nature* 501:112-115.

Winkler, T.H., A. Rolink, F. Melchers, and H. Karasuyama. 1995. Precursor B cells of mouse bone marrow express two different complexes with the surrogate light chain on the surface. *Eur. J. Immunol.* 25:446-450.

Yannoutsos, N., V. Barreto, Z. Misulovin, A. Gazumyan, W. Yu, N. Rajewsky, B.R. Peixoto, T. Eisenreich, and M.C. Nussenzweig. 2004. A cis element in the recombination activating gene locus regulates gene expression by counteracting a distant silencer. *Nat. Immunol.* 5:443-450.

Yu, W., Z. Misulovin, H. Suh, R.R. Hardy, M. Jankovic, N. Yannoutsos, and M.C. Nussenzweig. 1999. Coordinate regulation of RAG1 and RAG2 by cell type-specific DNA elements 5' of RAG2. *Science* 285:1080-1084.

Zandi, S., R. Mansson, P. Tsapogas, J. Zetterblad, D. Bryder, and M. Sigvardsson. 2008. EBF1 is essential for B-lineage priming and establishment of a transcription factor network in common lymphoid progenitors. *J. Immunol.* 181:3364-3372.

Zhang, L., T.L. Reynolds, X. Shan, and S. Desiderio. 2011. Coupling of V(D)J recombination to the cell cycle suppresses genomic instability and lymphoid tumorigenesis. *Immunity* 34:163-174.

Figures

Figure 1.1

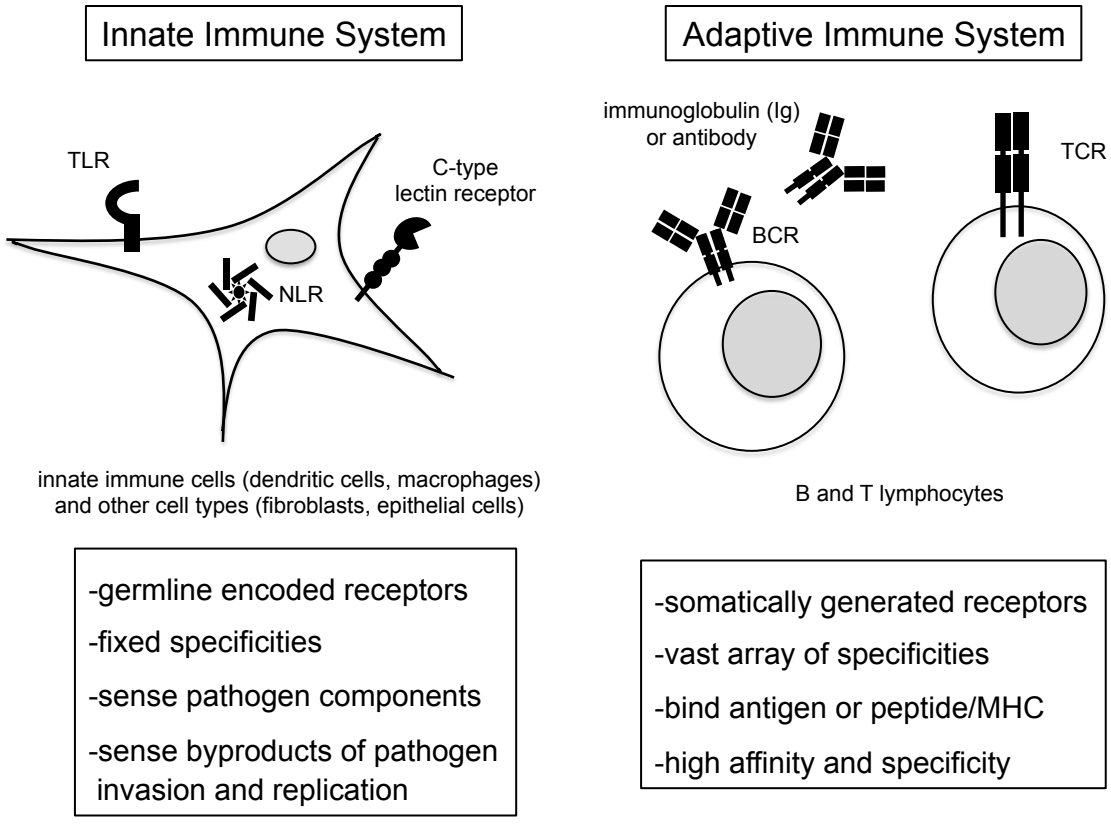

Figure 1.1. Comparison of the innate and adaptive immune systems.

Figure 1.2

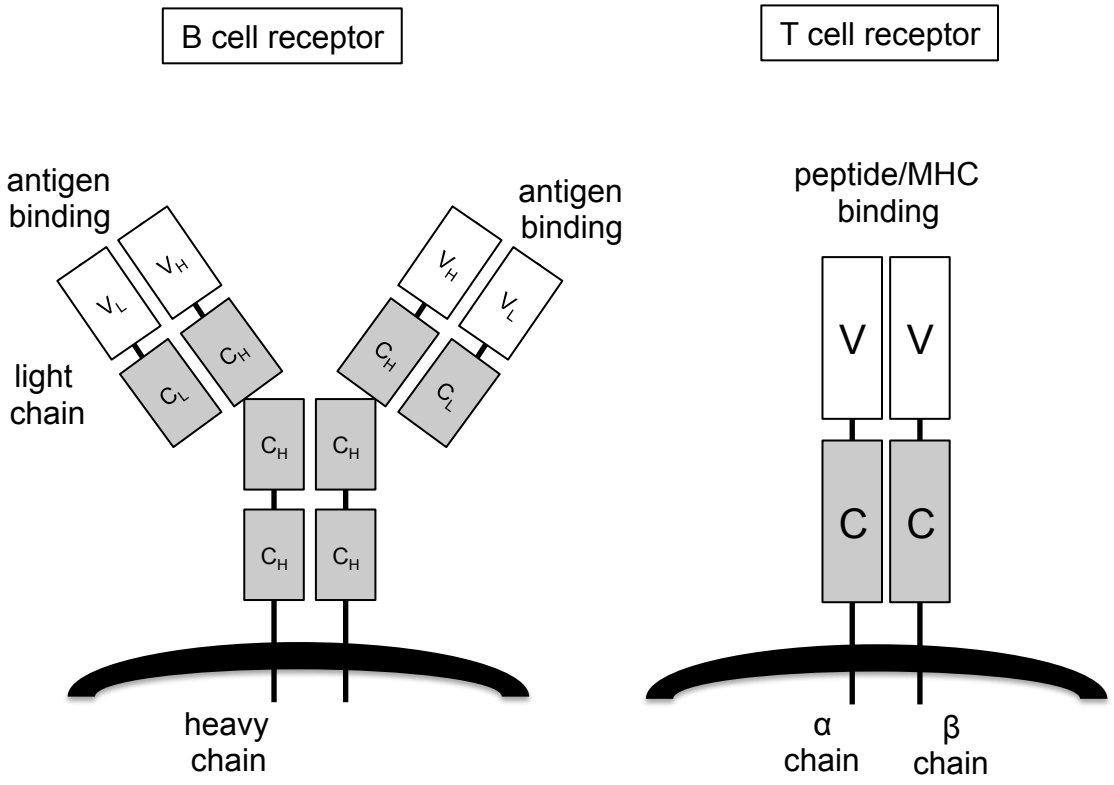

Figure 1.2. Structure of B and T cell antigen receptors. BCR structure (left) showing constant regions (gray), variable regions (white), and two antigen binding domains formed by the variable regions of the heavy and light chains. αβ TCR structure (right) showing constant regions (gray) and variable regions (white) of the two chains. The variable regions form the peptide/MHC binding domain.

Figure 1.3

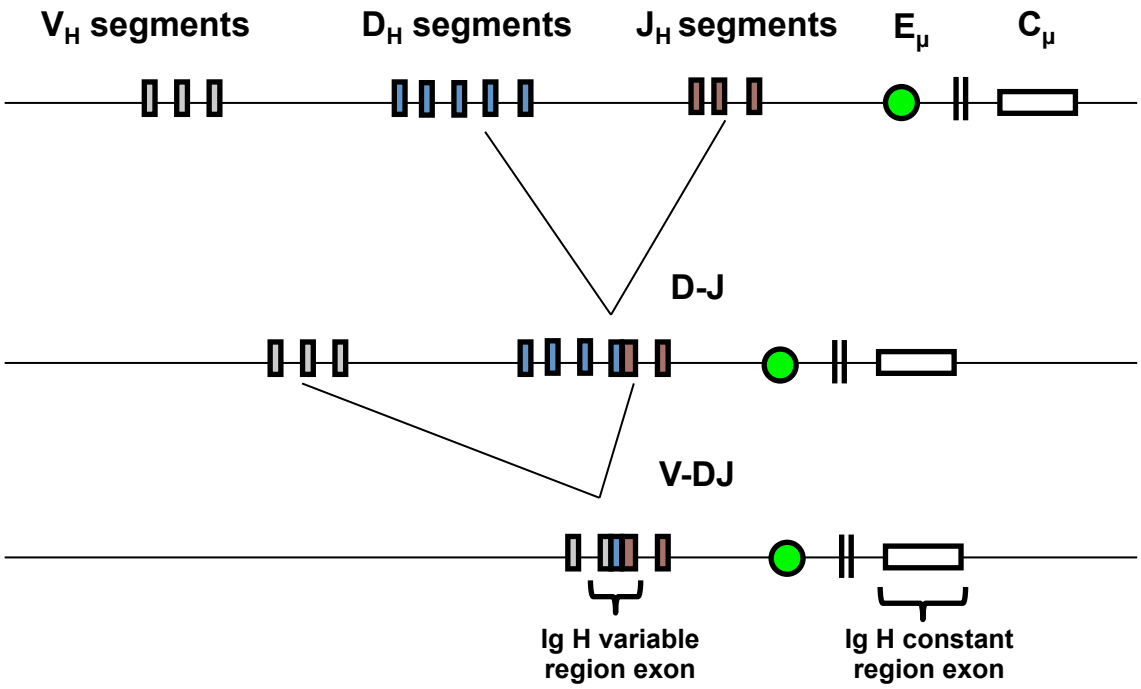

Figure 1.3. Antigen receptor locus organization. Schematic of the immunoglobulin heavy chain (Ig H) locus showing the basic features of the various antigen receptor loci. In the germline configuration, clusters of variable (V), diversity (D), and joining (J) gene segments lie separated by several kilobases of DNA. D-J, followed by V-DJ rearrangement creates a VDJ joint that encodes for the variable region of Ig H. Transcription through the rearranged locus driven by the Eμ enhancer produces a mRNA that is spliced to bring together the VDJ exon with the Ig H constant region exon Cμ. (note: only the Ig H and TCR β and δ loci have D segments; the remaining loci consist of only V and J segments)

Figure 1.4

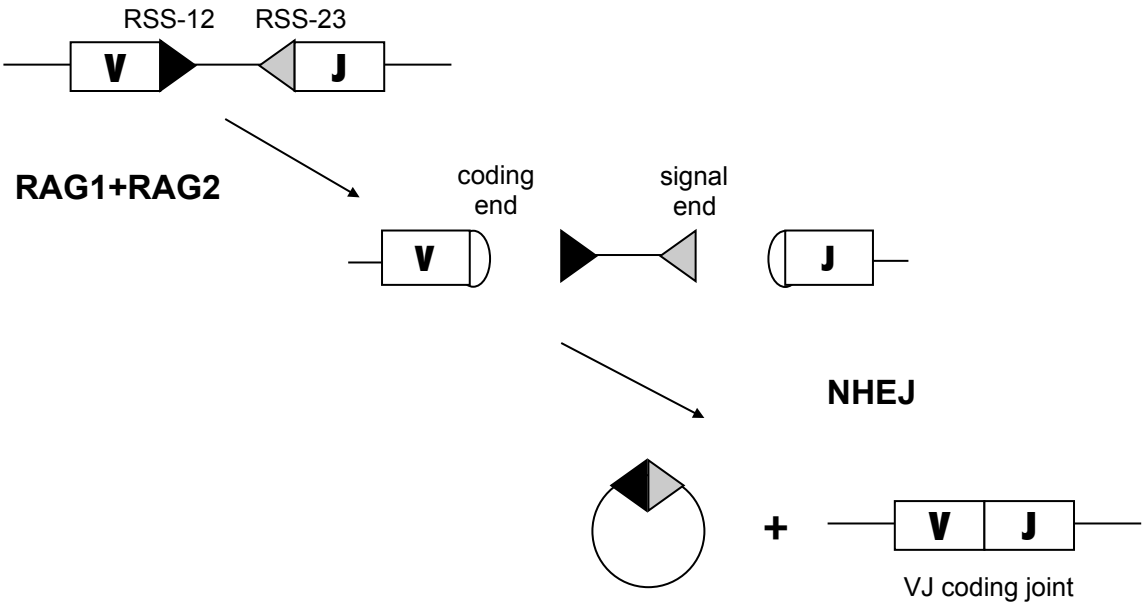

Figure 1.4. Biochemistry of V(D)J recombination. Representation of V(D)J recombination between individual V and J gene segments at the Ig κ locus is shown. RAG1 and RAG2 form a complex on the recombination signal sequences (RSSs – black and gray triangles) adjacent to each of the two gene segments undergoing recombination and make double-stranded DNA breaks. This produces blunt, 5'-phosphorylated signal ends and hairpinned coding ends. Opening of the coding ends allows for repair and formation of a VJ joint, while the signal end DNA is also repaired and lost from the genome. The nonhomologous end-joining pathway (NHEJ) carries out both repair processes.

Figure 1.5

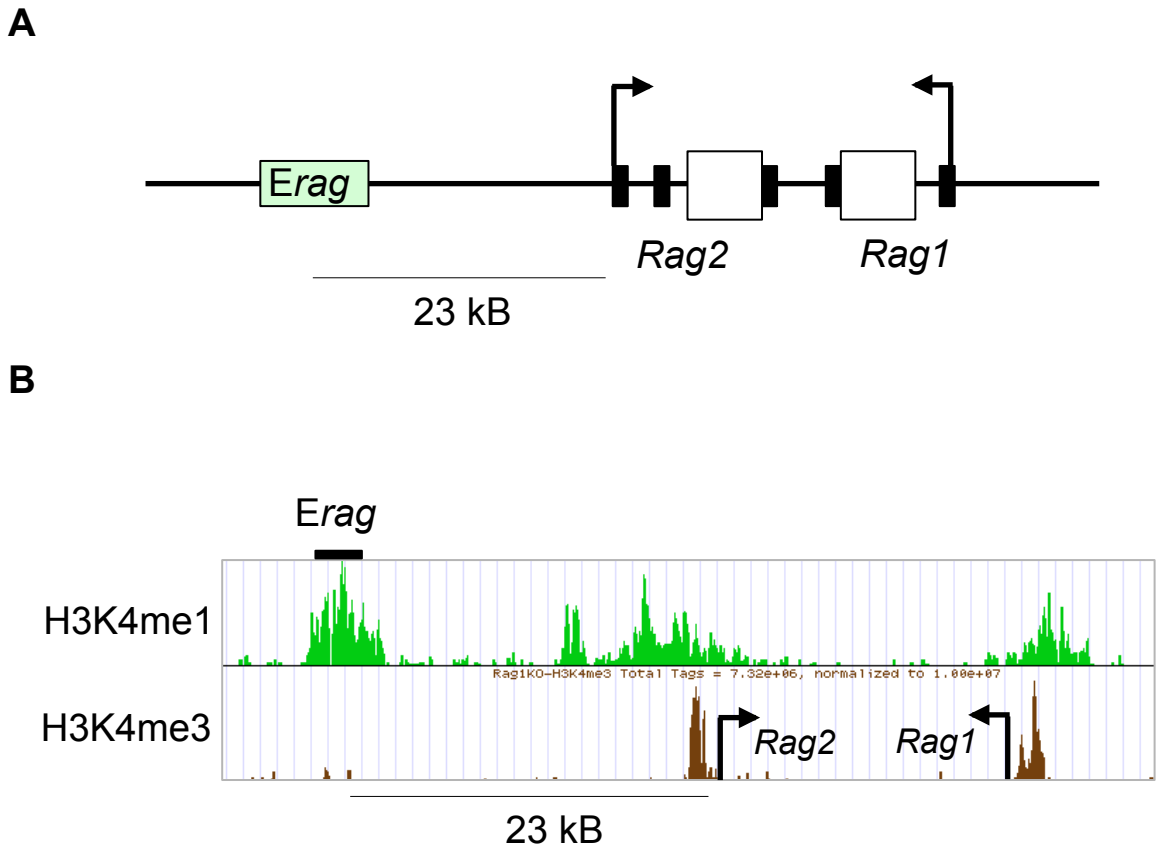

Figure 1.5. Organization of the *Rag* locus. (A) *Rag* locus schematic showing convergently transcribed *Rag1* and *Rag2* promoters (arrows), coding and non-coding exons, (white and black), and location of E*rag* enhancer element (green). **(B)** ChIP-seq data (Lin et al., 2010) for histone modifications marking active promoters (H3K4me3) and enhancers (H3K4me1) in the *Rag* locus. Approximate locations of the *Rag1* and *Rag2* promoters (arrows) and E*rag* (black line) are indicated.

Figure 1.6

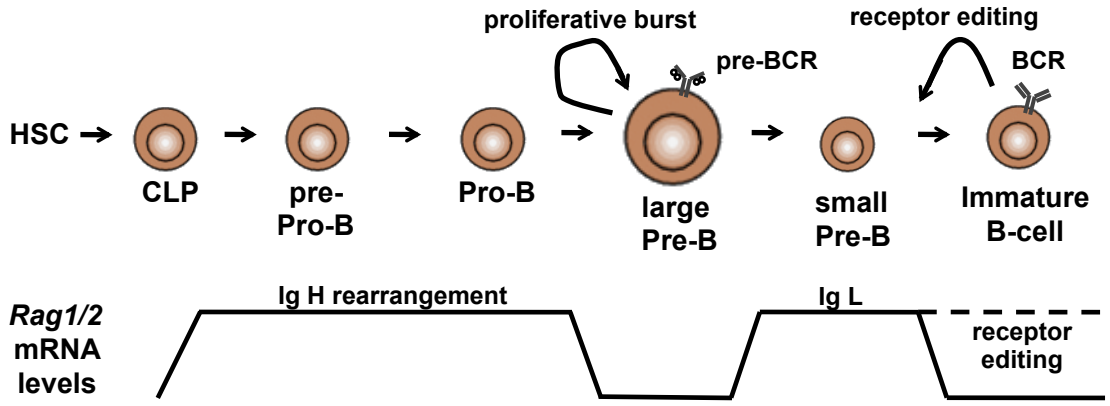

Figure 1.6. *Rag* expression during B cell development. Successive stages of early B cell development are shown with the line below the stages indicating when the *Rag* genes are expressed to mediate V(D)J recombination at the Ig H and Ig L loci.

Chapter 2

Ebf1 and c-Myb repress *Rag* transcription downstream of Stat5 during early B cell development

Background

The generation of diverse B and T cell antigen (Ag) receptor repertoires is dependent on the expression of the recombination-activating genes *Rag1* and *Rag2* (collectively known as *Rag*) during early lymphocyte development (Schlissel., 2003). RAG1 and RAG2 proteins form a complex that binds to conserved recombination signal sequences (RSSs) flanking a pair of Ag receptor gene segments and synchronously generates double-stranded DNA breaks (DSBs) between each RSS and its corresponding gene segment (Schatz and Swanson., 2011). *Rag* expression and DSB generation are restricted to the G0-G1 phases of cell cycle such that repair of DNA coding ends in the RAG-stabilized post-cleavage complex is carried out by the non-homologous end-joining (NHEJ) pathway resulting in assembly of the variable domain exons of Ag receptor genes (Lee et al., 2004). RAG-induced DSBs produced during S phase have the potential to be repaired by homologous recombination, a process that can lead to chromosomal translocations and transformation (Kuppers and Dalla-Favera., 2001, Zhang et al., 2011). As lymphocytes go through periods of clonal expansion during their development, the balance between proliferation and differentiation, along with the expression of *Rag*, must be tightly regulated to maintain genomic integrity and ensure the production of diverse pools of B and T cells to mediate adaptive immune responses.

Following productive immunoglobulin (Ig) heavy-chain gene rearrangement in developing pro-B cells in the bone marrow, expression of the precursor B cell antigen receptor (pre-BCR) activates signaling pathways that synergize with interleukin-7 receptor (IL-7R) signaling to direct two processes (Johnson et al., 2008, Herzog et al., 2009). The first is clonal expansion of pre-BCR+ progenitors, a stage during which RAG protein and *Rag* mRNA levels are negatively regulated upon entry of these large, cycling pre-B cells into S phase (Li et al., 1996, Grawunder et al., 1995). The second process is differentiation to the small pre-B cell stage, which involves coordinated cell cycle exit, re-expression of *Rag1* and *Rag2*, and increased chromatin accessibility at the Ig *kappa* light-chain locus (Mandal et al., 2009) to allow light chain gene recombination and ultimately the assembly of a complete B cell receptor (BCR).

Phosphorylation and proteasome-dependent degradation of RAG2 controls recombinase protein levels during this proliferative burst (Lee and Desiderio., 1999). However, the mechanism by which *Rag1* and *Rag2* transcription is repressed by IL-7R and pre-BCR signaling is ill-defined. Activation of the PI(3)K-Akt pathway downstream of these receptors has been implicated in the inactivation of *Rag* transcription via antagonism of Foxo transcription factors (Amin and Schlissel., 2008, Herzog et al., 2008, Ochiai et al., 2012). Gfi1b and Stat5 have been implicated as direct negative regulators of *Rag* transcription (Schulz et al., 2012, Johnson et al., 2012). Stat5 is activated by IL-7R signaling (Goetz et al., 2004), consistent with the ability of IL-7 to repress *Rag* transcription (Amin and Schlissel., 2008, Johnson et al., 2008).

Abelson Murine Leukemia Virus (AMuLV)-transformed B cell lines provide an *in vitro* model system to study the dynamics of *Rag* transcription during the developmental transition from the large to small pre-B cell stage. The constitutively active v-Abl kinase transforms B cell progenitors in a highly proliferative state where *Rag* expression is low, mimicking the large, cycling pre-B cell stage of development. This developmental block can be released by inhibition of v-Abl with the small molecule kinase inhibitor STI-571 (STI) (Muljo and Schlissel., 2003).

STI treatment induces cell cycle arrest, upregulation of *Rag* transcription, and differentiation to a small pre-B cell-like state where initiation of Ig *kappa* light-chain gene recombination occurs. In this study, we utilized the AMuLV system to identify novel pathways and factors responsible for the repression of *Rag* transcription. A gain-of-function screen identified unexpected roles for Early B Cell Factor 1 (Ebf1) and c-Myb in the repression of *Rag* transcription. The expression of these factors is driven by the IL-7R signaling effector Stat5, linking the negative regulation of *Rag* transcription by IL-7 to a novel repressive pathway involving Ebf1 and c-Myb. These results, which reveal previously unappreciated roles for Ebf1 and c-Myb in the repression of *Rag* transcription, were originally published in the *Journal of Immunology* (Timblin and Schlissel., 2013. Ebf1 and c-Myb repress *Rag* transcription downstream of Stat5 during early B cell development. J. Immunol. Vol. 191(9): 4676-4687. Copyright © 2013 The American Association of Immunologists, Inc.).

Results

Ebf1 overexpression negatively regulates *Rag* transcription

To screen for transcriptional regulators of *Rag*, we used retroviruses to individually overexpress a panel of transcription factors important for B cell development in a previously described AMuLV-transformed *Rag1*-GFP reporter B cell line (Amin and Schlissel., 2008). This line was derived from a heterozygous *Rag1*-GFP knock-in mouse that has a GFP cDNA in place of the coding exon at one *Rag1* allele (Igarashi et al., 2002), allowing changes in *Rag* transcription to be monitored by flow cytometry. We assessed *Rag1*-GFP levels following overexpression of the different factors in both untreated and STI-treated reporter cells.

To our surprise, Early B Cell Factor 1 (Ebf1), a transcription factor implicated as a positive regulator of *Rag* transcription during early B cell development (Zandi et al., 2008), repressed baseline *Rag1*-GFP levels when overexpressed in the reporter cell line as compared to empty vector control cells (Figure 2.1A, top row). Moreover, when the Ebf1-overexpressing cells were treated with STI, *Rag1*-GFP induction was severely blunted compared to STI-treated control cells (Figure 2.1A, bottom row). DNA binding by Ebf1 was required for *Rag1*-GFP repression as mutation of H157 in the Ebf1 zinc-finger motif abolished activity (Fields et al., 2008) (Figure 2.1A, right). The repression of both *Rag1* and *Rag2* by Ebf1 was confirmed by quantitative realtime PCR (qPCR) (Figure 2.1B), and the repressive effect of Ebf1 overexpression on *Rag* transcription was validated in independently generated Abelson cell lines (data not shown). Interestingly, Ebf1 overexpression did not affect other aspects of STI-induced differentiation, such as the upregulation of *Irf4* and *Spi-B* expression, or the induction of Ig *kappa* germline transcription (κGT)(Figure 2.2).

To test if Ebf1 overexpression represses *Rag* transcription in primary cells, we transduced cultured pro-B cells isolated from heterozygous *Rag1*-GFP mouse bone marrow with Ebf1 or empty vector control retroviruses. In cultures with a high concentration of IL-7, flow cytometry analysis revealed that the Ebf1-overexpressing cells had a lower GFP mean fluorescence intensity (MFI) than empty vector control cells (Figure 2.3A, left). When the IL-7 concentration in these cultures was lowered to induce *Rag* expression and differentiation to the pre-B cell stage, an increase in the GFP MFI was seen in the control cells but not the Ebf1-overexpressing cells (Figure 2.3A, right), confirming that Ebf1 represses *Rag* induction upon IL-7 withdrawal. The repression of both *Rag1* and *Rag2* by Ebf1 in primary IL-7-cultured pro-B cells from wildtype C57/B6 mice was confirmed by qPCR (Figure 2.3B). Together these data show that Ebf1 overexpression in Abelson cells and committed primary pro- and pre-B cells represses *Rag* transcription.

Ebf1 levels are inversely correlated with *Rag* expression at the large-to-small pre-B cell transition

Ebf1 mRNA levels are low in lymphoid progenitors, increase during progression through the pro-, pre-, and immature B cell stages, and decrease in mature and peripheral B cell subsets (Heng et al., 2008, Vilagos et al., 2012). Our Ebf1 overexpression results prompted us to assess *Ebf1* mRNA and Ebf1 protein expression levels with respect to *Rag* expression in developing B

cells. In agreement with microarray data that shows *Ebf1* transcript levels increasing from Fraction C' (large pre-B) to Fraction D (small pre-B) (Heng et al., 2008) both STI treatment of Abelson cells and IL-7 withdrawal in primary cell cultures resulted in an induction of *Ebf1* mRNA (Figure 2.4B,D). However, we observed a decrease in Ebf1 protein levels upon STI treatment and IL-7 withdrawal in lysates prepared from these same cells (Figure 2.4A,C), indicating that Ebf1 protein levels are inversely correlated with *Rag* expression in both Abelson cells and IL-7-cultured primary cells.

To further confirm the inverse relationship between Ebf1 and *Rag* expression, we performed intracellular staining for Ebf1 in primary B cells isolated from wildtype C57BL/6 mouse bone marrow. Ebf1 expression in pro-B cells (IgM-, B220+, CD43+) was lower than in large cycling pre-B cells (IgM-, B220+, CD43-, forward scatter high) (Figure 2.4). And in agreement with our western blot data, small resting pre-B cells (IgM-, B220+, CD43-, forward scatter low) expressed less Ebf1 than large pre-B cells (Figure 2.4E). These data suggest that Ebf1 protein levels peak in large cycling pre-B cells in which *Rag* transcription is repressed, and that Ebf1 protein levels decrease upon differentiation to the small resting pre-B cell stage when *Rag* transcription is upregulated to initiate Ig light-chain gene recombination. This inverse relationship between Ebf1 and *Rag* expression strongly correlates with our observation that Ebf1 overexpression negatively influences *Rag* transcription in Abelson cells and IL-7-cultured primary cells.

Ebf1 knockdown is sufficient to induce *Rag* transcription in Abelson cells

Upon STI-induced differentiation of Abelson cell lines, a multitude of changes in gene expression takes place, several of which are important for the induction of *Rag* transcription. If a decrease in Ebf1 protein levels is one of the changes essential for this induction, we reasoned that knockdown of Ebf1 might be sufficient to upregulate *Rag* transcription even in the absence of other STI-mediated effects. This was indeed the case as shRNA knockdown of Ebf1 was sufficient to induce *Rag* transcription in the *Rag1*-GFP reporter cell line, while a control luciferase shRNA had no effect on *Rag* levels (Figure 2.5A). Reduction of *Ebf1* mRNA levels by the Ebf1 shRNA was confirmed by qPCR (Figure 2.5B). Thus Ebf1 is a *bona fide* repressor of *Rag* transcription in Abelson cells.

The Ebf1 target gene *c-Myb* represses *Rag* transcription in Abelson cells

Conditional deletion in pro-B cells revealed that Ebf1 is critical for their proliferation and survival (Gyory et al., 2012). In agreement with this, Ebf1 overexpression enhanced proliferation in our *Rag1*-GFP reporter cell line, while Ebf1 knockdown was deleterious to survival as Ebf1 shRNA-transduced cells could not be expanded in culture (Figure 2.6). The same study showed that the Ebf1 target gene *c-Myb* was important for cell survival, and that c-Myb overexpression rescued cell death in *Ebf1*-deficient AMuLV-transformed B cells. Consistent with c-Myb being downstream of Ebf1, qPCR analysis revealed that *c-Myb* mRNA levels decreased significantly upon Ebf1 knockdown (Figure 2.7A). Although c-Myb has been previously described as a positive regulator of *Rag* transcription (Wang et al., 2000, Kishi et al., 2002), we found that c-Myb overexpression in the *Rag1*-GFP reporter cell line both decreased baseline *Rag* levels and severely blunted STI-induced *Rag* transcription (Figure 2.7B).

To test if c-Myb is a *bona fide* repressor of *Rag* transcription, we performed shRNA knockdown of c-Myb in the *Rag1*-GFP reporter line. As was the case for Ebf1 knockdown, c-Myb knockdown was sufficient to induce *Rag* transcription in the absence of STI treatment (Figure 2.7C). Conditional deletion of *c-Myb* in lymphoid progenitors showed that this factor positively regulates Ebf1 expression during early B cell development (Fahl et al., 2009). However in our cell line, c-Myb knockdown does not affect *Ebf1* transcript levels (Figure 2.7D), suggesting that the observed increase in *Rag* transcription is due to c-Myb knockdown alone and not a concurrent decrease in Ebf1 expression. Thus during later stages of B cell development represented by our Abelson cell line, c-Myb is downstream of Ebf1 in a pathway that represses *Rag* transcription.

Ebf1 and c-Myb independently repress *Rag* transcription

The observation that c-Myb is downstream of Ebf1 (Figure 2.7A) suggested that upon Ebf1 knockdown, the increase in *Rag* transcription may be due to the subsequent decrease in c-Myb levels. To test if a decrease in Ebf1 levels that occurs independent of a decrease in c-Myb levels would be sufficient to induce *Rag* transcription, we transduced cells overexpressing a c-Myb cDNA with our Ebf1 shRNA or control luciferase shRNA. qPCR confirmed that the expression level of *c-Myb* mRNA was stable upon Ebf1 knockdown due to rescue by the exogenous c-Myb cDNA (Figure 2.8A). However, Ebf1 knockdown still induced higher levels of *Rag* transcription in the absence of STI as compared to luciferase shRNA control cells (Figure 2.8B, left). Moreover, while STI treatment was unable to fully upregulate *Rag* transcription in the luciferase shRNA control cells due to the repressive effects of c-Myb overexpression, STI-induced *Rag* transcription in the Ebf1 knockdown cells is robust (Figure 2.8B, right). This result, along with the c-Myb knockdown result, shows that an independent decrease in either Ebf1 or c-Myb levels in our *Rag1*-GFP reporter Abelson cell line is sufficient to activate *Rag* transcription.

Ebf1 and c-Myb antagonize Foxo1 binding to the *Rag* locus upon STI-induced differentiation of Abelson cells

We hypothesized that Ebf1 and c-Myb might repress *Rag* transcription by antagonizing the activity of positive regulators of *Rag*. A recent study using *Irf4*$^{-/-}$*Irf8*$^{-/-}$ pre-B cells implicated Foxo1 and Pax5 as critical factors for the upregulation of *Rag* transcription during the large to small pre-B cell transition (Ochiai et al., 2012). Individual overexpression of Foxo1 or Pax5 is sufficient to increase *Rag1*-GFP levels in the reporter Abelson cell line, and knockdown of either factor severely blunts STI-induced *Rag* transcription (Figure 2.9) (Amin and Schlissel., 2008). Genome-wide ChIP-seq analysis in the *Irf4*$^{-/-}$*Irf8*$^{-/-}$ pre-B cells identified Foxo1 and Pax5 binding sites in the *Rag* locus that are inducibly bound by these factors upon IL-7 withdrawal and pre-B cell differentiation (Ochiai et al., 2012). These sites included previously identified elements such as the E*rag* enhancer (Hsu et al., 2003) and *Rag2* promoter Pax5 binding site (Kishi et al., 2002), along with novel promoter (P) and intergenic (I) binding sites (see *Rag* locus schematic in Figure 2.10). We performed ChIP in untreated and STI-treated Abelson cells and observed increased occupancy of both Pax5 and Foxo1 at these *Rag* locus sites following STI treatment (Figure 2.11A, Figure 2.12A). We also observed increased Foxo1 occupancy at sites in the *Blnk* and *Syk* loci, two other genes identified as direct Foxo1 targets during *Irf4*$^{-/-}$*Irf8*$^{-/-}$ pre-B cell differentiation (Ochiai et al., 2012)(Figure 2.12A). Together, these experiments implicate Foxo1

and Pax5 as direct transcriptional activators of *Rag* and other genes involved in pre-B cell differentiation in the AMuLV system following STI treatment.

We then tested if Ebf1 and c-Myb overexpression affected the binding of Pax5 or Foxo1 to the *Rag* locus sites upon STI treatment. Pax5 ChIP experiments showed that binding of this factor to the *Rag* locus upon STI treatment was not affected by Ebf1 or c-Myb overexpression (Figure 2.11C). However, Foxo1 ChIP experiments revealed that overexpression of either Ebf1 or c-Myb clearly reduced the amount of Foxo1 bound to the *Rag* locus upon STI treatment (Figure 2.12B, left). Ebf1 or c-Myb overexpression did not affect Foxo1 binding to the *Blnk* and *Syk* loci (Figure 2.12B, right), suggesting these factors repress *Rag* induction but not other aspects of pre-B cell differentiation. Thus Ebf1 and c-Myb negatively regulate *Rag* transcription by antagonizing Foxo1 binding to the *Rag* locus.

Ebf1 and c-Myb negatively regulate *Foxo1* expression

ImmGen microarray data shows that Foxo1 mRNA levels are high in Fractions B and C, decrease in Fraction C', and increase again in Fraction D (Heng et al., 2008). In agreement with this, we found that *Foxo1* transcript levels increase upon differentiation of primary B cell cultures and AMuLV cells following IL-7 withdrawal and STI treatment, respectively (Figure 2.13). Together these data suggest that factors actively repress *Foxo1* transcription in large cycling pre-B cells. Reduced Foxo1 binding to the *Rag* locus in STI-treated Ebf1- and c-Myb-overexpressing cell lines prompted us to assess Foxo1 expression levels in these cells. Western blotting revealed lower levels of Foxo1 protein in cells overexpressing Ebf1 or c-Myb compared to control empty vector-transduced cells (Figure 2.14), suggesting that these factors act as negative regulators of *Foxo1* expression. To further assess the relationship between Ebf1, c-Myb, and Foxo1, we assayed *Foxo1* mRNA levels in cells transduced with shRNAs targeting either Ebf1 or c-Myb. Indeed either Ebf1 and c-Myb knockdown resulted in an increase in *Foxo1* transcript levels compared to cells transduced with a control luciferase shRNA (Figure 2.15), supporting the notion that Ebf1 and c-Myb are negative regulators of *Foxo1* transcription in Abelson cells.

Genome-wide ChIP-seq analysis in pro-B and splenic B cells revealed Ebf1 binding sites in both the *Foxo1* promoter and downstream intergenic sites (Lin et al., 2010, Gyory et al., 2012)(Figure 2.16A). Conventional ChIP in cells overexpressing a 3XFLAG-tagged Ebf1 protein revealed strong Ebf1 binding to these sites, but not to a control site in the *Rag1* promoter (Figure 2.16B). Furthermore, ChIP with an anti-Ebf1 antibody revealed that endogenous Ebf1 is bound to these sites in resting Abelson cells, and that Ebf1 occupancy decreases upon STI-induced differentiation (Figure 2.16C). These experiments suggest that Ebf1 represses *Foxo1* transcription directly and that this repression is relieved upon STI treatment thus allowing induction of *Foxo1* mRNA and *Rag* transcription.

Ebf1 and c-Myb positively regulate *Gfi1b expression*

In spite of their negative influence on *Foxo1* expression, Foxo1 binding to non-*Rag* locus targets upon STI-induced differentiation was unaffected by Ebf1 or c-Myb overexpression (Figure 2.12B), suggesting Ebf1 and c-Myb influence chromatin accessibility at the *Rag* locus but not

other Foxo1 target genes. Gfi1b is both a direct negative regulator of *Rag* transcription, and an indirect regulator of the *Rag* genes via its antagonism of *Foxo1* expression (Schulz et al., 2012). Gfi1b directly represses *Rag* transcription by biding near the I*rag2* and E*rag* elements also bound by Foxo1 (Figure 2.12) and recruiting chromatin modifiers that deposit H3K9me2, a chromatin mark associated with transcriptional repression (Schulz et al., 2012). Given the effects of Ebf1 and c-Myb on both *Foxo1* expression and Foxo1 binding to the *Rag* locus, we hypothesized that these factors may also regulate *Gfi1b* expression. Indeed, knockdown of either Ebf1 and c-Myb resulted in a strong decrease of *Gfi1b* mRNA levels (Figure 2.17), suggesting that Ebf1 and c-Myb repress *Rag* and *Foxo1* in part by driving *Gfi1b* expression. *Gfi1b* has been previously identified as a direct target of Ebf1 in both pro-B and splenic B cells, with ChIP-seq revealing Ebf1 binding sites the *Gfi1b* promoter (Lin et al., 2010, Gyory et al., 2012)(Figure 2.18A). Conventional ChIP in cells overexpressing a 3XFLAG-tagged Ebf1 protein revealed strong binding of Ebf1 to this site (Figure 2.18B), suggesting that Ebf1's positive influence on *Gfi1b* expression is direct.

Ebf1 does not bind E*rag* or other sites in the *Rag* locus

The overexpression, knockdown, and ChIP experiments described above suggest Ebf1 is a direct negative regulator of Foxo1, and a direct positive regulator of Gfi1b. Previous work suggested Ebf1 positively regulates *Rag* expression during early B cell development by binding to the E*rag* enhancer (Zandi et al., 2008). Thus we wanted to test if we could detect Ebf1 binding to E*rag*, or to other potential Ebf1 binding sites in the *Rag* locus, in AMuLV B cells. We selected potential Ebf1 binding sites using the aforementioned ChIP-seq data (Figure 2.19A). We then performed conventional ChIP in cells overexpressing a 3XFLAG-tagged Ebf1 protein to test if Ebf1 occupied any of these sites, using the *Foxo1* and *Gfi1b* locus Ebf1 binding sites as positive controls. We were unable to detect Ebf1 binding to E*rag* or any of the other candidate sites in the *Rag* locus (Figure 2.19B), suggesting Ebf1 does not negatively regulate the *Rag* genes in a direct manner in AMuLV B cells.

Stat5 represses *Rag* through upregulation of Ebf1

The IL-7R signaling pathway has been implicated in both the control of *Ebf1* expression (Dias et al., 2005, Kikuchi et al., 2005, Roessler et al., 2007, Tsapogas et al., 2011) and the repression of *Rag* transcription (Amin and Schlissel., 2008, Johnson et al., 2012) during B cell development. Signaling through the IL-7R and transformation by v-Abl both result in the phosphorylation and activation of Stat5 (Danial et al., 1995, Goetz et al., 2004). Our IL-7 withdrawal and STI-treatment experiments showed that both IL-7R and v-Abl signaling positively regulate Ebf1 protein expression (Figure 2.4). Thus, we hypothesized that Stat5 is the downstream effector in these signaling pathways that upregulates Ebf1 to repress *Rag* transcription. As with Ebf1 and c-Myb, overexpression of a constitutively active form of Stat5 (CA-STAT5B) (Onishi et al., 1998) in the *Rag1*-GFP reporter cell line repressed baseline *Rag* levels and severely blunted STI-induced *Rag* transcription (Figure 2.20A). When we compared Ebf1 protein levels in sorted empty vector control and CA-STAT5B-transduced cells, Stat5 overexpression clearly upregulated Ebf1 (Figure 2.20B, left lanes). Upon inhibition of v-Abl with STI, levels of phosphorylated endogenous Stat5a decrease (Figure 2.20B, top 100kDa band), and this correlates with a decrease in Ebf1 levels in empty vector control cells as observed in Figure 2.4. However

in cells overexpressing CA-STAT5B, Ebf1 expression is rescued and remains high despite v-Abl inhibition and loss of active endogenous Stat5a (Figure 2.20B, right lanes). This result is consistent with a model in which activation of Stat5 downstream of v-Abl (and likely the IL-7 receptor) drives high levels of Ebf1 expression that mediate the transcriptional repression of *Rag1* and *Rag2*.

Based on our data we propose the following model for the role Ebf1 in regulating *Rag* transcription during B cell development (Figure 2.21). Initial IL-7R signaling events minimally activate the *Ebf1* locus during the early stages of B cell development. Low levels of Ebf1 drive B lineage specification through activation of genes including *Foxo1* and *Rag* and the initiation of Ig heavy-chain gene rearrangement. Enhanced IL-7R signaling in late pro-B cells undergoing transient proliferative bursts upon exposure to high local concentrations of IL-7, or in pre-BCR(+) large pre-B cells undergoing clonal expansion, strongly upregulates Ebf1 expression. Increased Ebf1 dosage drives proliferation through activation target genes involved in cell cycle progression such as cyclin D3 (*Ccnd3*) (Cooper et al., 2006, Gyory et al., 2012) while simultaneously repressing *Rag* transcription via antagonism of *Foxo1* and activation of *Gfi1b*. Thus the promotion of proliferation by increased Ebf1 dosage is tightly linked with repression of the recombination machinery, ensuring genomic integrity is maintained. Upon the attenuation of IL-7R signaling and differentiation to the small pre-B cell stage, Ebf1 protein levels are reduced and *Rag* expression is upregulated to mediate Ig light-chain gene rearrangement.

Discussion

Restricting expression of the recombinase machinery in developing lymphocytes to non-dividing cells prevents DSBs during S-phase that could be aberrantly repaired and lead to leukemic transformation. During B cell development, signals through the IL-7R and pre-BCR drive proliferation and the repression of *Rag* expression via targeted degradation of RAG2 protein and transcriptional repression of the *Rag* genes. We have identified a novel pathway that adds an additional layer of complexity to how this transcriptional repression is accomplished. While this pathway involves upstream components in IL-7 and Stat5 that have been previously implicated in *Rag* repression, the downstream effectors identified (Ebf1 and c-Myb) paradoxically have been previously described as activators of the *Rag* locus during early B cell development.

Ebf1 was identified as a B lineage-specific factor that bound and activated the *mb-1* promoter (Hagman et al., 1991, Hagman et al., 1993), and *Ebf1*-deficient mice revealed its essential role in early B cell development (Lin and Grosschedl., 1995). Ebf1 promotes specification to the B lineage in multipotent progenitors via simultaneous activation of B lineage genes and repression of genes involved in the development of other lineages (Pongubala et al., 2008, Mansson et al., 2012). Predicted Ebf1 targets during the earliest stages of development include *Rag1*, *Rag2*, and *Foxo1*, as *Ebf1*-deficient common lymphoid progenitors (CLPs) display reduced expression of these genes (Zandi et al., 2008). This raises the question of how Ebf1 is converted to a repressor of *Foxo1* transcription during later stages of B cell development. Our experiments suggest that Ebf1 dosage may play a role, as unexpectedly we found increased levels of Ebf1 in both AMuLV-transformed cells and IL-7-cultured primary B cells result in decreased *Rag* expression (Figure 2.1 and Figure 2.3). While *Ebf1* transcript levels peak in small pre-B cells (Heng et al., 2008), our data show that Ebf1 protein levels are highest in proliferating pro-B and early pre-B cells where *Rag* expression is repressed (Figure 2.4). IL-7R expression levels vary within the pro-B cell compartment (Johnson et al., 2012), and pre-BCR expression enhances IL-7R responsiveness (Marshall et al., 1998, Fleming and Paige., 2001). We hypothesize that brief periods of strong IL-7R signaling in proliferating pro-B and large cycling pre-B cells could cause a spike in Ebf1 dosage that contributes to *Rag* transcriptional repression. Ebf1 dosage has been shown to be important for transcriptional repression of natural killer (NK) cell-specific genes by Ebf1 (Lukin et al., 2011). Perhaps high levels of Ebf1 protein induced by strong IL-7R signaling allow for the formation of repressive complexes at binding sites in the *Foxo1* locus that are not formed under conditions of low Ebf1 expression during earlier stages of development. Stat5 has been shown to simultaneously activate and repress genes in B cells by assembling into distinct dimeric and tetrameric complexes (Mandal et al., 2011). It would be interesting to test biochemically if Ebf1 can form dose-dependent higher-order complexes on *Foxo1* locus binding sites, and if such complexes are competent for co-repressor recruitment.

Alternatively, late pro-B and early pre-B cells may express an Ebf1 co-repressor that is not present at appreciable levels during earlier stages of B cell development to allow for stage-specific *Foxo1* repression. Interestingly, expression levels of the H3K27 methyltransferase Ezh2, which is recruited to the Ig *kappa* locus by tetrameric Stat5 complexes to repress premature recombination in cycling pre-B cells (Mandal et al., 2011), increases throughout early B cell development and peaks in Fraction C' when *Rag* is repressed (Heng et al., 2008). As Ebf1 has been shown to target the repressive H3K27me3 chromatin mark to non-B lineage genes it

actively represses in pro-B cells (Treiber et al., 2010, Banerjee et al., 2013), it would be interesting to test if a stage-specific interaction between Ebf1 and Ezh2 is responsible for *Foxo1* and *Rag* repression in late pro-B and early pre-B cells.

Our experiments also revealed that Ebf1 protein levels decrease upon differentiation to the small pre-B stage and re-expression of *Rag1* and *Rag2* (Figure 2.4). This occurs despite an increase in Ebf1 transcript levels upon differentiation, suggesting Ebf1 protein is actively targeted for degradation at this developmental transition. Interestingly, analysis of GFP expression in mice expressing an Ebf1(1-148aa)-GFP fusion protein revealed high GFP levels in pro-B cells, but greatly reduced GFP expression in pre-B cells (Vilagos et al., 2012). While the authors attribute this to non-specific destabilization of the Ebf1-GFP fusion protein, it is consistent with the decrease in Ebf1 protein levels we observed during pre-B cell differentiation that appears necessary for full re-expression of the *Rag* genes. Identifying the factors and pathways responsible for this post-translational control of Ebf1 will be of considerable interest as disruption of this process could prevent recombinase re-expression and impair Ig light-chain gene rearrangement in resting pre-B cells.

Previous reports by our group and others implicated c-Myb as a positive regulator of *Rag* promoter activity (Wang et al., 2000, Kishi et al., 2002). While these studies relied heavily on reporter constructs containing cloned *Rag* locus elements transfected into both B and non-B lineage cells, our analysis of c-Myb's effects on transcription from the endogenous *Rag* locus in an AMuLV-transformed B cell line clearly shows this factor represses *Rag* expression in this context. Analysis of mice in which *c-Myb* is conditionally deleted in early B cell progenitors, and of mice expressing a hypomorphic *c-Myb* allele, revealed defects in expression of IL-7R and of other early B lymphoid genes (Fahl et al., 2009, Greig et al., 2010). While *Rag* expression was not affected in the B lineage compartments of these mice, it appeared that similar to Ebf1, c-Myb plays a role in B lineage specification via the activation of a large set of genes important for early B cell development. Thus, how c-Myb is co-opted along with Ebf1 as a repressor of the *Rag* genes during a later stage of B cell development will be an important question to answer. Unlike Ebf1, c-Myb protein levels are unchanged following STI treatment of AMuLV cells (Figure 3.4B), suggesting that post-translational modifications or the availability of novel co-repressors control c-Myb activity at this developmental transition. Identifying the factors controlling c-Myb activity, along with the location of functional c-Myb binding sites in the *Rag*, *Foxo1*, and *Gfi1b* loci in B cells, will be essential for understanding the mechanism by which c-Myb represses *Rag* transcription. How c-Myb achieves *Rag* repression is investigated further in Chapter 3.

Foxo1 activity is necessary for the two waves of *Rag* expression that mediate Ig heavy-chain and light-chain gene rearrangement in pro-B and pre-B cells respectively (Dengler et al., 2008). Studies suggest that post-translational mechanisms negatively regulate Foxo1 activity in large pre-B cells, and that upon differentiation this regulation is relieved to allow Foxo1 to activate *Rag* transcription in small pre-B cells (Amin and Schlissel., 2008, Ochiai et al., 2012). However, microarray analysis using RNA from sorted primary cells shows a clear decrease in *Foxo1* transcript levels as pro-B cells (Fractions B/C) differentiate to large cycling pre-B cells (Fraction C'), followed by an increase in *Foxo1* mRNA in small pre-B cells (Fraction D) (Heng et al., 2008). When we quantified *Foxo1* transcripts in both Abelson-transformed and primary cultured pro-B cells, we observed a significant increase in *Foxo1* mRNA levels upon STI- and IL-7

withdrawal-induced differentiation (Figure 2.13), indicating that *Foxo1* is also regulated at the transcription level during this developmental transition. Our experiments suggest that the repression of *Foxo1* transcription by Ebf1 and c-Myb is an important additional level of control of Foxo1 activity (and thus *Rag* expression) in proliferating late pro-B and early pre-B cells.

IL-7R signaling and Stat5 have been implicated in the ordered rearrangement of the Ig loci via activation of chromatin in the heavy-chain locus (Corcoran et al., 1998, Bertolino et al., 2005) and repression of chromatin in the light-chain locus (Malin et al., 2010, Mandal et al., 2011) in pro-B cells. Recent studies have shown that in addition to controlling recombinase accessibility, IL-7R signaling and Stat5 regulate recombination at the level of transcription of the *Rag* genes (Johnson et al., 2008, Amin and Schlissel., 2008, Ochiai et al., 2012, Johnson et al., 2012). Our findings provide additional mechanistic insight into how this negative regulation by Stat5 is accomplished. While potentially acting as a direct negative regulator of *Rag* transcription (Johnson et al., 2012), we showed that Stat5 also activates an Ebf1-dependent pathway that leads to enhanced proliferation and the transcriptional repression of *Foxo1*. Thus, in addition to being controlled post-translationally by the PI(3)K-Akt pathway, Foxo1 is also regulated at the transcriptional level by the IL-7R/Stat5 pathway to prevent *Rag* expression during periods of cellular proliferation.

The transcriptional repressor Gfi1b is an additional downstream factor in the repressive Ebf1-dependent pathway (Figure 2.17). While its ability to negatively regulate *Rag* transcription both directly and through repression of *Foxo1* has been described (Schulz et al., 2012), the pathways controlling *Gfi1b* expression and activity during early B cell development are ill-defined. *Gfi1b* mRNA levels are inversely correlated with *Rag* transcription and peak in large cycling pre-B cells (Schulz et al., 2012). This is consistent with a model where enhanced IL-7R signaling and Stat5 activity at this stage upregulates Ebf1 and c-Myb, which in turn drive increased levels of *Gfi1b* transcription that lead to *Rag* repression. But while our experiments shed light on how *Gfi1b* expression might be regulated during this specific stage of B cell development, it has been reported that Ebf1 is a negative regulator of Gfi1b expression in CLPs (Mansson et al., 2012). So again, the paradox of how Ebf1 switches between transcriptional activator and repressor must be solved to better understand how this factor directs gene expression during distinct developmental stages.

Stat5 is constitutively activated in AMuLV-transformed cells (Danial et al., 1995) and in human hematopoietic malignancies including BCR-ABL(+) acute lymphoblastic leukemia (ALL) (Heltemes-Harris et al., 2011). Stat5 is essential for ALL as Stat5-deficient hematopoietic progenitor cells cannot be transformed by retroviral expression of v-Abl or BCR-ABL oncogenes (Hoelbl et al., 2006). While Stat5 itself directly activates genes involved in proliferation and cell survival, our experiments revealed that Ebf1 and c-Myb act downstream of Stat5 to repress differentiation (as evident by their repression of *Rag* transcription) and promote proliferation and survival of transformed cells. Consistent with other studies (Lidonnici et al., 2008, Gyory et al., 2012, Waldron et al., 2012), reducing Ebf1 and c-Myb levels using shRNAs dramatically reduced proliferation and survival of AMuLV-transformed cells (Figure 2.6B). Thus Ebf1 and c-Myb represent attractive therapeutic targets, and defining the mechanisms regulating their expression and activity during early B cell development will likely contribute to a better understanding of the transformation process.

Materials and Methods

Cell culture and chemicals

AMuLV-transformed B cells were cultured in RPMI 1640 (Gibco) supplemented with 5% vol/vol FCS (Gemini), 100 mg/mL penicillin and streptomycin (Gibco), and 55nM 2-mercaptoethanol (Gibco). Primary B cells isolated from C57/B6 mice were cultured in RPMI with 15% vol/vol FCS and supplemented with 2 ng/mL recombinant mouse IL-7 (R&D Systems). For IL-7 withdrawal experiments, IL-7 concentration was increased to 5 ng/mL for 24 h. Cells were then spun down and resuspended in media with 5 or 0.1 ng/mL IL-7 and cultured for an additional 24 h before harvest or analysis. GP2 retroviral packaging cells (a gift from Greg Barton, UC Berkeley) were cultured in DMEM (Gibco) supplemented with 5% vol/vol FCS, 100 mg/mL penicillin and streptomycin, and 1mM sodium pyruvate (Gibco). All cells were grown at 37°C in 5% CO_2. STI-571 (Novartis) was used at a final concentration of 2.5 uM for 16 h for all experiments.

Expression plasmids

MSCV-based cDNA retroviral expression constructs were previously described (Amin and Schlissel., 2008). All cDNAs were PCR-amplified with Platinum Pfx DNA Polymerase (Invitrogen) and cloned into a multiple cloning site (MCS) upstream of an internal ribosome entry site (IRES). This IRES is followed by coding sequence for either human CD4 (hCD4) or Thy1.1 cell surface proteins to mark infected cells. All cDNA open reading frames (ORFs) were sequenced to confirm the absence of mutations.

Murine c-Myb transcript variant 2 (NM_010848.3) ORF was PCR-amplified from a primary B cell cDNA library, while murine Foxo1, Pax5, and Ebf1 ORFs were PCR amplified from existing plasmids and cloned into CMSCV IRES Thy1.1 or CMSCV IRES hCD4 retroviral vectors. N-terminal 3XFLAG-tagged Ebf1 was created by amplifying the Ebf1 ORF lacking an ATG start codon and cloning it downstream of a 3XFLAG sequence inserted into the MCS of CMSCV IRES hCD4. CA-STAT5B cDNA (a gift from Marcus Clark and Malay Mandal, U. of Chicago) was excised from MIGR1 and cloned into CMSCV IRES hCD4.

MSCV-based shRNA retroviral expression constructs contain a human CD2 (hCD2) cell surface marker cDNA followed by a miR-30 cassette as previously described (Stegmeier et al., 2005). Seed sequences for desired shRNA targets were identified with siRNA Wizard (InvivoGen), and shRNA oligonucleotides containing these seed sequences were designed using RNAi Codex. shRNA oligonucleotides purchased from Elim Biopharm were PCR amplified using Vent Polymerase (NEB) with 5uL DMSO (Sigma-Aldrich) added to each reaction, and cloned into XhoI and EcoRI restriction sites in the miR-30 cassette. Seed sequences were as follows:

Ebf1 shRNA 1*	ACCAAAGGAAGTGATCCTTAAA
Ebf1 shRNA 5	ATGGAAGTCACACTGTCGTACA
c-Myb shRNA 1*	ACCCTTGCAGCTCAAGAAATTA
c-Myb shRNA 2	AGGGAAACTTCTTCTGCTCAAA
c-Myb shRNA 3	ACTGTTATTGCCAAGCACTTAA

Pax5 shRNA 4 ACCAGAACAGACCACAGAGTAT
Foxo1 shRNA ACCATGGACAACAACAGTAAAT

*for Ebf1 and c-Myb, all data presented in figures was generated using these shRNAs. seed sequences for independent shRNAs that successfully knocked down Ebf1 and c-Myb and had similar effects on *Rag* transcription are included. shRNA PCR amplification primers were as follows:

5' XhoI miR-30 F CAGAAGGCTCGAGAAGGTATATTGCTGTTGACAGTGAGCG
3' EcoRI miR-30 R CTAAAGTAGCCCCTTGAATTCCGAGGCAGTAGGCA

Retrovirus production and infection

GP2 packaging cells were transfected with a 5:3 ratio of retroviral:VSVG plasmids using Lipofectamine 2000 (Invitrogen) and placed at 37°C. Cells were moved to 32°C at 24 h. At 48 h, retroviral supernatant was collected and concentrated (1.5 h, 16,800g, 4°C) using a SW 41 Ti rotor and L8-M ultracentrifuge (Beckman). Retroviral pellets were resuspended in media supplemented with 4 ug/mL polybrene (Sigma-Aldrich). Target cells were cultured in concentrated retrovirus at 32°C for 24 h, and then moved to 37°C and expanded. Analysis and sorting were performed 2-4 days post-infection.

Cell sorting, flow cytometry, and intracellular staining

Single-cell suspensions were prepared and cells labeled with fluorochrome-conjugated antibodies using standard techniques. A FC500 (Beckman Coulter) or LSRII (BD Biosciences) flow cytometer was used for analysis, while a MoFlo or Influx cell sorter (Dako-Cytomation) was used for sorting. Data were analyzed with FlowJo software (Tree Star).

Primary B cells were labeled with anti-IgM (II/41), anti-B220 (RA3-6B2), anti-CD43 (S7), and anti-CD19 (1D3) antibodies. Anti-hCD2 (RPA-2.10), anti-hCD4 (RPA-T4) and anti-Thy1.1 (OX-7) antibodies were used to label cells transduced with retrovirus. Anti-B220, anti-CD43, anti-CD19, and anti-Thy1.1 antibodies were obtained from BD Pharmingen. All others were obtained from eBiosciences.

The Fix & Perm Cell Permeabilization Kit (Invitrogen) was used for intracellular staining. Primary antibody was rabbit anti-EBF-1 (Millipore AB10523) or rabbit IgG control (GenScript). Secondary antibody was Alexa Fluor 647 F(ab')2 fragment goat anti-rabbit. Gating strategy was as follows: pro-B cells (IgM-, B220+, CD43+), large cycling pre-B cells (IgM-, B220+, CD43-, forward scatter high), small resting pre-B cells (IgM-, B220+, CD43-, forward scatter low).

Quantitative realtime PCR (qPCR)

Cells were collected by centrifugation and lysed in Trizol, or sorted directly into Trizol LS (both from Invitrogen). RNA was prepared and reverse transcription performed with MMLV-RT (Invitrogen) using random hexamer priming. Quantitative realtime PCR was carried out on an Applied Biosystems 7300 thermocycler using JumpStart Taq (Sigma) and EvaGreen (Biotium).

PCR conditions were as follows: 50°C 2 min, 95°C 10 min, 40 cycles of 95°C 15s, 60°C 1 min. For gene expression analysis, transcript levels of all genes were normalized to *Hprt*. For ChIP qPCR, data is presented as a percentage of ChIP input. Error bars on all plots represent the standard deviation of triplicate qPCR assays. Primer sequences were as follows (forward and reverse primers for each gene shown 5' to 3'):

Hprt	CTGGTGAAAAGGACCTCTCG	TGAAGTACTCATTATAGTCAAGGCA
Rag1	CATTCTAGCACTCTGGCCGG	TCATCGGGTGCAGAACTGAA
Rag2	TTAATTCCTGGCTTGGCCG	TTCCTGCTTGTGGATGTGAAAT
Ebf1	GCCTTCTAACCTGCGGAAATCCAA	GGAGCTGGAGCCGGTAGTGGAT
c-Myb	ACACCGGTGGCAGAAAGTGCT	TGCTTGGCAATAACAGACCAACG
Foxo1	GAAGAGCGTGCCCTACTTCAA	GTTCCTTCATTCTGCACTCGA
Gfi1b	AAGTGCATGTCCGCCGCTCT	CTTCGCTCCTGTGAGTGGACGT
Irf4	TGAAACACGCGGGCAAGCA	TGGCTTGTCGATCCCTTCTCGGA
SpiB	AGGAGTCTTCTACGACCTGGA	GAAGGCTTCATAGGGAGCGAT
κ GT	GGACGTTCGGTGGAGGC	GGAAGATGGATACAGTTGGT

Immunoblot

Cells were lysed in RIPA buffer supplemented with Complete Protease Inhibitor Cocktail (Roche). Cell debris was cleared by centrifugation and soluble protein quantified with Bradford Reagent (Bio-Rad). Laemmli SDS loading buffer was added to 20-40ug of protein per sample prior to separation on 8-10% SDS-PAGE gels. Following transfer to Immobilon-FL PVDF membranes (Millipore) and blocking with 5% vol/vol milk/PBS solution, blots were probed with primary and secondary antibodies and analyzed with the Odyssey Infrared Imaging System (LI-COR Biosciences). Primary antibodies used: anti-EBF-1 (R&D Systems AF5156 and Millipore AB10523), anti-Myb (Millipore 05-175), anti-Pax5 (Santa Cruz sc-1974), anti-Stat5 (Santa Cruz sc-835), anti-Foxo1 (Cell Signaling L27), anti-Lamin B1 (Abcam ab16048), anti-Tubulin (Calbiochem CP06), and anti-FLAG M2 (Sigma-Aldrich). Infrared dye–conjugated secondary antibodies were from Molecular Probes–Invitrogen. Quantification was performed using ImageJ.

Chromatin immunoprecipitation

Chromatin immunoprecipitation (ChIP) was performed as previously described (Lee et al., 2006). Briefly, 80 million cells per experimental condition were harvested, fixed, lysed, and sonicated using a Branson 450 Digital Sonifier. Following centrifugation to remove insoluble material, chromatin was quantified and equal amounts used in experimental and control immunoprecipitations. 5mg of anti-FLAG M2 (Sigma-Aldrich), anti-Foxo1 (Abcam ab70382), anti-Pax5 (Santa Cruz sc-1974X), anti-Ebf1 (Sigma-Aldrich SAB2501166), or IgG control antibodies (GeneScript) were conjugated to Protein G Dynabeads (Invitrogen) and added to samples. Following overnight immunoprecipitation, beads were collected and washed three times with low salt buffer (0.1% SDS, 1% Triton X-100, 2 mM EDTA, 20 mM Tris pH 8.1, 150 mM NaCl), once with high salt buffer (0.1% SDS, 1% Triton X-100, 2 mM EDTA, 20 mM Tris pH 8.1, 500 mM NaCl), once with LiCl buffer (250 mM LiCl, 1% NP40, 1% sodium deoxycholate, 1 mM EDTA, 10 mM Tris pH 8.1) and twice with TE buffer. DNA-protein complexes were

eluted from beads with TE elution buffer (TE w/ 1% SDS), and crosslinks reversed overnight at 65°C. Following RNAse A (Quiagen) and Proteinase K (Invitrogen) treatment, chromatin was isolated using QIAquick columns (Quiagen) and subjected to qPCR analysis. Primer sequences were as follows (forward and reverse primers for each site shown 5' to 3'):

Foxo1 and Pax5 ChIP

I*rag2*	CATGGCTGAACGAACACTGC	GGTAAGCTGCTCCACGAGAA
E*rag* *Rag2*	CGTTTCCAACTTCCTCCAGC	GCCCTGCGCAGTTATTTTCT
Pax5BS	GGAACACCCTGGTGGGTTTCTG	GGCTGCAGGGTAGAGTGTTTGTGT
Pc*rag1*	CGGGGGACCCATTACTGAAC	AATTGCCATGGAGGAGAGCC
Pb*rag1*	GGAAGTTTAGCTGGGGGACC	CCACCGTAGGCATTCTCAGG
Pa*rag1*	TCCATTGCTCACTGCCCTTT	GGAGGTGGAGACAGGAGGAT
I*rag1*	TGTCTGCCTCTATGTCCCCA	TCATGAGTGGCAGGAGAGGA
I*Blnk*	TGTAAACACCCCCTGTCGTG	TCCAGGTGCTGTGACAAACA
Ib*Syk*	TCCTTAAACTGTGCTGGGCT	TTCCCGACAAAGGGGAACTG

Ebf1 ChIP

P*foxo1*	GAAAAATACCCCACCGCCCC	AATGGACGCGCGAAGTCTC
I*foxo1* A	CTCCCTGTGCCTTTTTAGCC	CTTCGACATTGTTCGTGGCG
I*foxo1* B	TCCACCTTGGAGGAAATAAGGC	GGAAGCTAGACACGCCAAGT
P*gfi1b*	GGGAGCTGTCCCTCTTCTGA	CTCATAACGTTGACCGAGCC
I*rag2*dist	AGATGAGGGACACATTGGCA	TGCAGGTTTCCTTCCTGAAC
I*rag2*prox	CCTAGAAAAGCATTAGGAACCTGC	TGCATAAACCACCAGACTGT
Pa*rag2*	TGAGTGATGGAAGAAAAAGCCC	TGTCATTCAGTCAGCTTCCACA
Pb*rag2*	TGGCCTTGCTTAAAGGTGACT	CAGGTCCAGCATCCTTGGTG

References

Amin, R.H., and M.S. Schlissel. 2008. Foxo1 directly regulates the transcription of recombination-activating genes during B cell development. *Nat. Immunol.* 9:613-622.

Banerjee, A., D. Northrup, H. Boukarabila, S.E. Jacobsen, and D. Allman. 2013. Transcriptional repression of gata3 is essential for early B cell commitment. *Immunity* 38:930-942.

Bertolino, E., K. Reddy, K.L. Medina, E. Parganas, J. Ihle, and H. Singh. 2005. Regulation of interleukin 7-dependent immunoglobulin heavy-chain variable gene rearrangements by transcription factor STAT5. *Nat. Immunol.* 6:836-843.

Cooper, A.B., C.M. Sawai, E. Sicinska, S.E. Powers, P. Sicinski, M.R. Clark, and I. Aifantis. 2006. A unique function for cyclin D3 in early B cell development. *Nat. Immunol.* 7:489-497.

Corcoran, A.E., A. Riddell, D. Krooshoop, and A.R. Venkitaraman. 1998. Impaired immunoglobulin gene rearrangement in mice lacking the IL-7 receptor. *Nature* 391:904-907.

Danial, N.N., A. Pernis, and P.B. Rothman. 1995. Jak-STAT signaling induced by the v-abl oncogene. *Science* 269:1875-1877.

Dengler, H.S., G.V. Baracho, S.A. Omori, S. Bruckner, K.C. Arden, D.H. Castrillon, R.A. DePinho, and R.C. Rickert. 2008. Distinct functions for the transcription factor Foxo1 at various stages of B cell differentiation. *Nat. Immunol.* 9:1388-1398.

Dias, S., H. Silva Jr, A. Cumano, and P. Vieira. 2005. Interleukin-7 is necessary to maintain the B cell potential in common lymphoid progenitors. *J. Exp. Med.* 201:971-979.

Fahl, S.P., R.B. Crittenden, D. Allman, and T.P. Bender. 2009. c-Myb is required for pro-B cell differentiation. *J. Immunol.* 183:5582-5592.

Fields, S., K. Ternyak, H. Gao, R. Ostraat, J. Akerlund, and J. Hagman. 2008. The 'zinc knuckle' motif of Early B cell Factor is required for transcriptional activation of B cell-specific genes. *Mol. Immunol.* 45:3786-3796.

Fleming, H.E., and C.J. Paige. 2001. Pre-B cell receptor signaling mediates selective response to IL-7 at the pro-B to pre-B cell transition via an ERK/MAP kinase-dependent pathway. *Immunity* 15:521-531.

Goetz, C.A., I.R. Harmon, J.J. O'Neil, M.A. Burchill, and M.A. Farrar. 2004. STAT5 activation underlies IL7 receptor-dependent B cell development. *J. Immunol.* 172:4770-4778.

Grawunder, U., T.M. Leu, D.G. Schatz, A. Werner, A.G. Rolink, F. Melchers, and T.H. Winkler. 1995. Down-regulation of RAG1 and RAG2 gene expression in preB cells after functional immunoglobulin heavy chain rearrangement. *Immunity* 3:601-608.

Greig, K.T., C.A. de Graaf, J.M. Murphy, M.R. Carpinelli, S.H. Pang, J. Frampton, B.T. Kile, D.J. Hilton, and S.L. Nutt. 2010. Critical roles for c-Myb in lymphoid priming and early B-cell development. *Blood* 115:2796-2805.

Gyory, I., S. Boller, R. Nechanitzky, E. Mandel, S. Pott, E. Liu, and R. Grosschedl. 2012. Transcription factor Ebf1 regulates differentiation stage-specific signaling, proliferation, and survival of B cells. *Genes Dev.* 26:668-682.

Hagman, J., C. Belanger, A. Travis, C.W. Turck, and R. Grosschedl. 1993. Cloning and functional characterization of early B-cell factor, a regulator of lymphocyte-specific gene expression. *Genes Dev.* 7:760-773.

Hagman, J., A. Travis, and R. Grosschedl. 1991. A novel lineage-specific nuclear factor regulates mb-1 gene transcription at the early stages of B cell differentiation. *EMBO J.* 10:3409-3417.

Heltemes-Harris, L.M., M.J. Willette, K.B. Vang, and M.A. Farrar. 2011. The role of STAT5 in the development, function, and transformation of B and T lymphocytes. *Ann. N. Y. Acad. Sci.* 1217:18-31.

Heng, T.S., M.W. Painter, and Immunological Genome Project Consortium. 2008. The Immunological Genome Project: networks of gene expression in immune cells. *Nat. Immunol.* 9:1091-1094.

Herzog, S., E. Hug, S. Meixlsperger, J.H. Paik, R.A. DePinho, M. Reth, and H. Jumaa. 2008. SLP-65 regulates immunoglobulin light chain gene recombination through the PI(3)K-PKB-Foxo pathway. *Nat. Immunol.* 9:623-631.

Herzog, S., M. Reth, and H. Jumaa. 2009. Regulation of B-cell proliferation and differentiation by pre-B-cell receptor signalling. *Nat. Rev. Immunol.* 9:195-205.

Hoelbl, A., B. Kovacic, M.A. Kerenyi, O. Simma, W. Warsch, Y. Cui, H. Beug, L. Hennighausen, R. Moriggl, and V. Sexl. 2006. Clarifying the role of Stat5 in lymphoid development and Abelson-induced transformation. *Blood* 107:4898-4906.

Hsu, L.Y., J. Lauring, H.E. Liang, S. Greenbaum, D. Cado, Y. Zhuang, and M.S. Schlissel. 2003. A conserved transcriptional enhancer regulates RAG gene expression in developing B cells. *Immunity* 19:105-117.

Igarashi, H., S.C. Gregory, T. Yokota, N. Sakaguchi, and P.W. Kincade. 2002. Transcription from the RAG1 locus marks the earliest lymphocyte progenitors in bone marrow. *Immunity* 17:117-130.

Johnson, K., J. Chaumeil, M. Micsinai, J.M. Wang, L.B. Ramsey, G.V. Baracho, R.C. Rickert, F. Strino, Y. Kluger, M.A. Farrar, and J.A. Skok. 2012. IL-7 functionally segregates the pro-B cell

stage by regulating transcription of recombination mediators across cell cycle. *J. Immunol.* 188:6084-6092.

Johnson, K., T. Hashimshony, C.M. Sawai, J.M. Pongubala, J.A. Skok, I. Aifantis, and H. Singh. 2008. Regulation of immunoglobulin light-chain recombination by the transcription factor IRF-4 and the attenuation of interleukin-7 signaling. *Immunity* 28:335-345.

Kikuchi, K., A.Y. Lai, C.L. Hsu, and M. Kondo. 2005. IL-7 receptor signaling is necessary for stage transition in adult B cell development through up-regulation of EBF. *J. Exp. Med.* 201:1197-1203.

Kishi, H., Z.X. Jin, X.C. Wei, T. Nagata, T. Matsuda, S. Saito, and A. Muraguchi. 2002. Cooperative binding of c-Myb and Pax-5 activates the RAG-2 promoter in immature B cells. *Blood* 99:576-583.

Kuppers, R., and R. Dalla-Favera. 2001. Mechanisms of chromosomal translocations in B cell lymphomas. *Oncogene* 20:5580-5594.

Lee, G.S., M.B. Neiditch, S.S. Salus, and D.B. Roth. 2004. RAG proteins shepherd double-strand breaks to a specific pathway, suppressing error-prone repair, but RAG nicking initiates homologous recombination. *Cell* 117:171-184.

Lee, J., and S. Desiderio. 1999. Cyclin A/CDK2 regulates V(D)J recombination by coordinating RAG-2 accumulation and DNA repair. *Immunity* 11:771-781.

Lee, T.I., S.E. Johnstone, and R.A. Young. 2006. Chromatin immunoprecipitation and microarray-based analysis of protein location. *Nat. Protoc.* 1:729-748.

Li, Z., D.I. Dordai, J. Lee, and S. Desiderio. 1996. A conserved degradation signal regulates RAG-2 accumulation during cell division and links V(D)J recombination to the cell cycle. *Immunity* 5:575-589.

Lidonnici, M.R., F. Corradini, T. Waldron, T.P. Bender, and B. Calabretta. 2008. Requirement of c-Myb for p210(BCR/ABL)-dependent transformation of hematopoietic progenitors and leukemogenesis. *Blood* 111:4771-4779.

Lin, H., and R. Grosschedl. 1995. Failure of B-cell differentiation in mice lacking the transcription factor EBF. *Nature* 376:263-267.

Lin, Y.C., S. Jhunjhunwala, C. Benner, S. Heinz, E. Welinder, R. Mansson, M. Sigvardsson, J. Hagman, C.A. Espinoza, J. Dutkowski, T. Ideker, C.K. Glass, and C. Murre. 2010. A global network of transcription factors, involving E2A, EBF1 and Foxo1, that orchestrates B cell fate. *Nat. Immunol.* 11:635-643.

Lukin, K., S. Fields, L. Guerrettaz, D. Straign, V. Rodriguez, S. Zandi, R. Mansson, J.C. Cambier, M. Sigvardsson, and J. Hagman. 2011. A dose-dependent role for EBF1 in repressing non-B-cell-specific genes. *Eur. J. Immunol.* 41:1787-1793.

Malin, S., S. McManus, C. Cobaleda, M. Novatchkova, A. Delogu, P. Bouillet, A. Strasser, and M. Busslinger. 2010. Role of STAT5 in controlling cell survival and immunoglobulin gene recombination during pro-B cell development. *Nat. Immunol.* 11:171-179.

Mandal, M., S.E. Powers, M. Maienschein-Cline, E.T. Bartom, K.M. Hamel, B.L. Kee, A.R. Dinner, and M.R. Clark. 2011. Epigenetic repression of the Igk locus by STAT5-mediated recruitment of the histone methyltransferase Ezh2. *Nat. Immunol.* 12:1212-1220.

Mandal, M., S.E. Powers, K. Ochiai, K. Georgopoulos, B.L. Kee, H. Singh, and M.R. Clark. 2009. Ras orchestrates exit from the cell cycle and light-chain recombination during early B cell development. *Nat. Immunol.* 10:1110-1117.

Mansson, R., E. Welinder, J. Ahsberg, Y.C. Lin, C. Benner, C.K. Glass, J.S. Lucas, M. Sigvardsson, and C. Murre. 2012. Positive intergenic feedback circuitry, involving EBF1 and FOXO1, orchestrates B-cell fate. *Proc. Natl. Acad. Sci. U. S. A.* 109:21028-21033.

Marshall, A.J., H.E. Fleming, G.E. Wu, and C.J. Paige. 1998. Modulation of the IL-7 dose-response threshold during pro-B cell differentiation is dependent on pre-B cell receptor expression. *J. Immunol.* 161:6038-6045.

Muljo, S.A., and M.S. Schlissel. 2003. A small molecule Abl kinase inhibitor induces differentiation of Abelson virus-transformed pre-B cell lines. *Nat. Immunol.* 4:31-37.

Ochiai, K., M. Maienschein-Cline, M. Mandal, J.R. Triggs, E. Bertolino, R. Sciammas, A.R. Dinner, M.R. Clark, and H. Singh. 2012. A self-reinforcing regulatory network triggered by limiting IL-7 activates pre-BCR signaling and differentiation. *Nat. Immunol.* 13:300-307.

Onishi, M., T. Nosaka, K. Misawa, A.L. Mui, D. Gorman, M. McMahon, A. Miyajima, and T. Kitamura. 1998. Identification and characterization of a constitutively active STAT5 mutant that promotes cell proliferation. *Mol. Cell. Biol.* 18:3871-3879.

Pongubala, J.M., D.L. Northrup, D.W. Lancki, K.L. Medina, T. Treiber, E. Bertolino, M. Thomas, R. Grosschedl, D. Allman, and H. Singh. 2008. Transcription factor EBF restricts alternative lineage options and promotes B cell fate commitment independently of Pax5. *Nat. Immunol.* 9:203-215.

Roessler, S., I. Gyory, S. Imhof, M. Spivakov, R.R. Williams, M. Busslinger, A.G. Fisher, and R. Grosschedl. 2007. Distinct promoters mediate the regulation of Ebf1 gene expression by interleukin-7 and Pax5. *Mol. Cell. Biol.* 27:579-594.

Schatz, D.G., and P.C. Swanson. 2011. V(D)J recombination: mechanisms of initiation. *Annu. Rev. Genet.* 45:167-202.

Schlissel, M.S. 2003. Regulating antigen-receptor gene assembly. *Nat. Rev. Immunol.* 3:890-899.

Schulz, D., L. Vassen, K.T. Chow, S.M. McWhirter, R.H. Amin, T. Moroy, and M.S. Schlissel. 2012. Gfi1b negatively regulates Rag expression directly and via the repression of FoxO1. *J. Exp. Med.* 209:187-199.

Stegmeier, F., G. Hu, R.J. Rickles, G.J. Hannon, and S.J. Elledge. 2005. A lentiviral microRNA-based system for single-copy polymerase II-regulated RNA interference in mammalian cells. *Proc. Natl. Acad. Sci. U. S. A.* 102:13212-13217.

Timblin, G.A., and M.S. Schlissel. 2013. Ebf1 and c-Myb repress rag transcription downstream of Stat5 during early B cell development. *J. Immunol.* 191:4676-4687.

Treiber, T., E.M. Mandel, S. Pott, I. Gyory, S. Firner, E.T. Liu, and R. Grosschedl. 2010. Early B cell factor 1 regulates B cell gene networks by activation, repression, and transcription-independent poising of chromatin. *Immunity* 32:714-725.

Tsapogas, P., S. Zandi, J. Ahsberg, J. Zetterblad, E. Welinder, J.I. Jonsson, R. Mansson, H. Qian, and M. Sigvardsson. 2011. IL-7 mediates Ebf-1-dependent lineage restriction in early lymphoid progenitors. *Blood* 118:1283-1290.

Vilagos, B., M. Hoffmann, A. Souabni, Q. Sun, B. Werner, J. Medvedovic, I. Bilic, M. Minnich, E. Axelsson, M. Jaritz, and M. Busslinger. 2012. Essential role of EBF1 in the generation and function of distinct mature B cell types. *J. Exp. Med.* 209:775-792.

Waldron, T., M. De Dominici, A.R. Soliera, A. Audia, I. Iacobucci, A. Lonetti, G. Martinelli, Y. Zhang, R. Martinez, T. Hyslop, T.P. Bender, and B. Calabretta. 2012. c-Myb and its target Bmi1 are required for p190BCR/ABL leukemogenesis in mouse and human cells. *Leukemia* 26:644-653.

Wang, Q.F., J. Lauring, and M.S. Schlissel. 2000. c-Myb binds to a sequence in the proximal region of the RAG-2 promoter and is essential for promoter activity in T-lineage cells. *Mol. Cell. Biol.* 20:9203-9211.

Zandi, S., R. Mansson, P. Tsapogas, J. Zetterblad, D. Bryder, and M. Sigvardsson. 2008. EBF1 is essential for B-lineage priming and establishment of a transcription factor network in common lymphoid progenitors. *J. Immunol.* 181:3364-3372.

Zhang, L., T.L. Reynolds, X. Shan, and S. Desiderio. 2011. Coupling of V(D)J recombination to the cell cycle suppresses genomic instability and lymphoid tumorigenesis. *Immunity* 34:163-174.

Figures

Figure 2.1

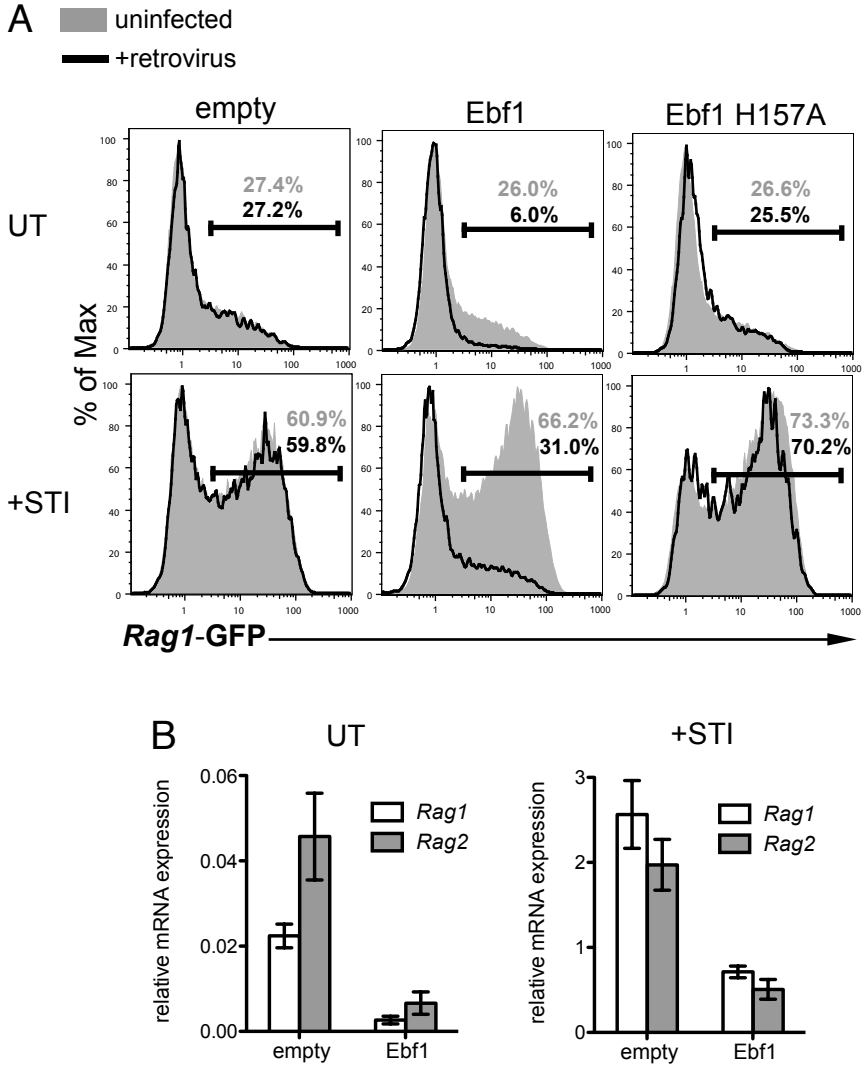

Figure 2.1. Ebf1 overexpression negatively regulates *Rag* transcription in AMuLV cells. **(A)** Flow cytometry analysis of GFP expression in an AMuLV-transformed B cell line generated from heterozygous *Rag1*-GFP knock-in mice, where GFP reports transcription from the endogenous *Rag* locus. Cells were infected with empty retroviral vector, Ebf1 retrovirus, or Ebf1 H157A DNA-binding mutant retrovirus (Fields et al., 2008). Uninfected cells (shaded histogram) were distinguished from transduced cells (black line) by staining with anti-hCD4 (retroviral marker). Analysis was performed on untreated (UT, top row) or STI-treated (+STI, bottom row) cells. Numbers above gate indicate the percentage of GFP+ uninfected cells (top) or transduced cells (bottom). **(B)** Quantitative realtime PCR (qPCR) measuring *Rag1* and *Rag2* transcript levels in sorted empty vector-transduced or Ebf1-overexpressing AMuLV-transformed B cells in normal culture conditions (left) or treated with STI (right).

Figure 2.2

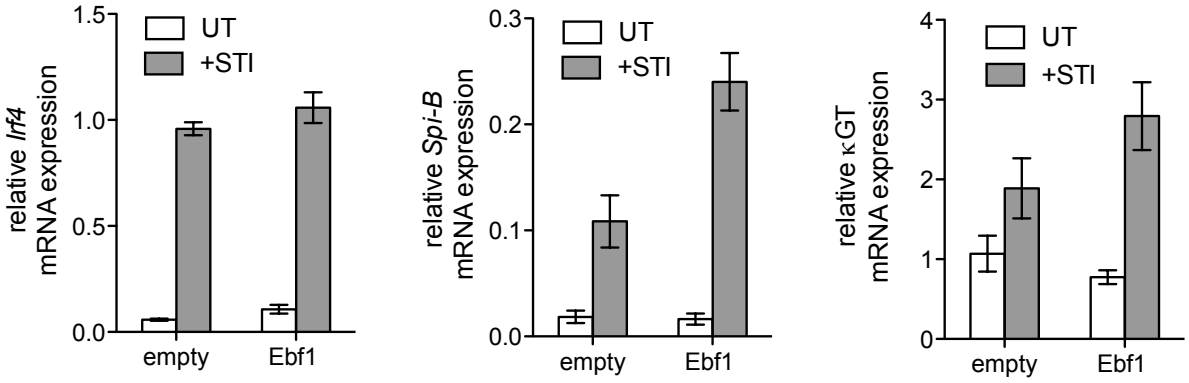

Figure 2.2. Ebf1 overexpression does not repress other genes upregulated during pre-B cell differentiation. qPCR measuring *Irf4*, *Spi-B* and *kappa* germline (κGT) transcript levels in sorted empty vector-transduced or Ebf1-overexpressing AMuLV-transformed B cells in normal culture conditions (white bars) or treated with STI (gray bars).

Figure 2.3

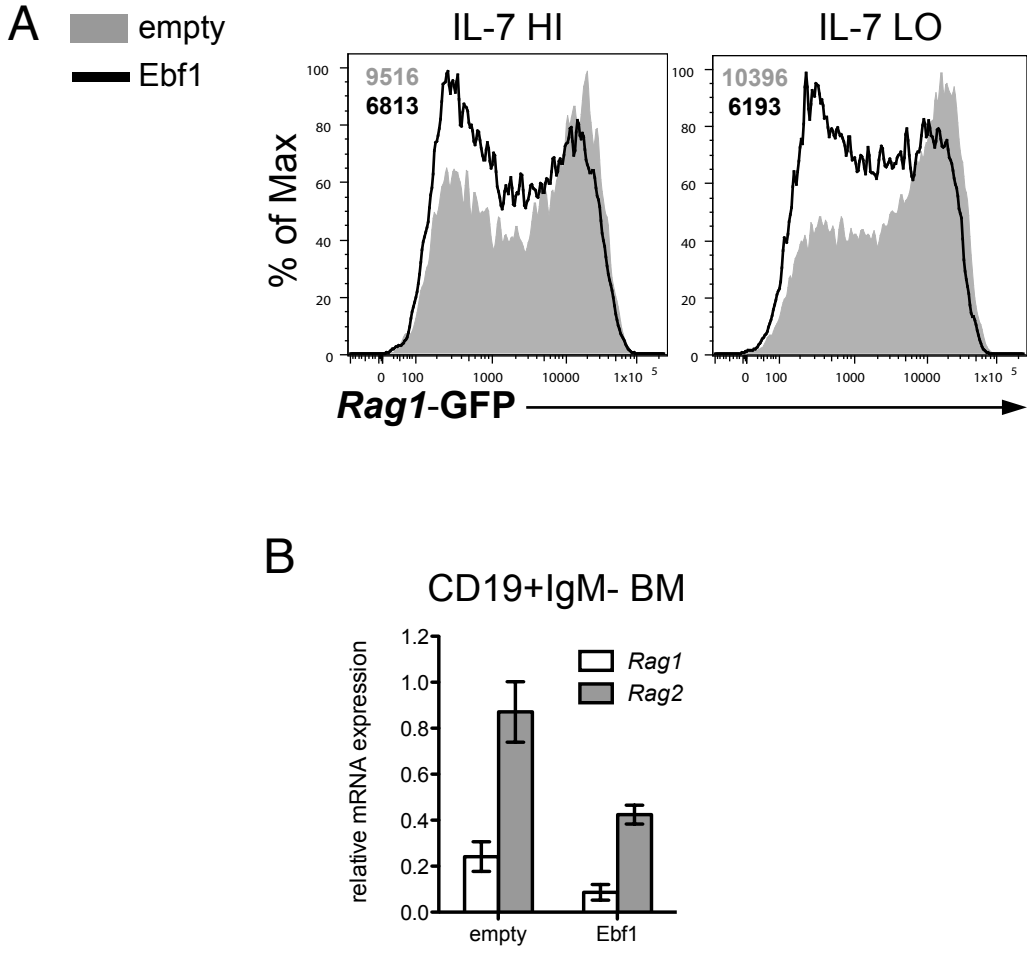

Figure 2.3. Ebf1 overexpression negatively regulates *Rag* transcription in primary B cells. **(A)** GFP expression in CD19+IgM- primary B cells from heterozygous *Rag1*-GFP knock-in mice transduced with empty retroviral vector (filled histogram) or Ebf1 retrovirus (black line) and cultured in high (left) or low (right) concentrations of IL-7. Numbers indicate the GFP mean fluorescence intensity (MFI) of the empty vector-transduced cells (top) or Ebf1-overexpressing cells (bottom). **(B)** qPCR measuring *Rag1* and *Rag2* transcript levels in sorted CD19+IgM- primary B cells from wildtype C57/B6 mice transduced with empty retroviral vector or Ebf1 retrovirus.

Figure 2.4

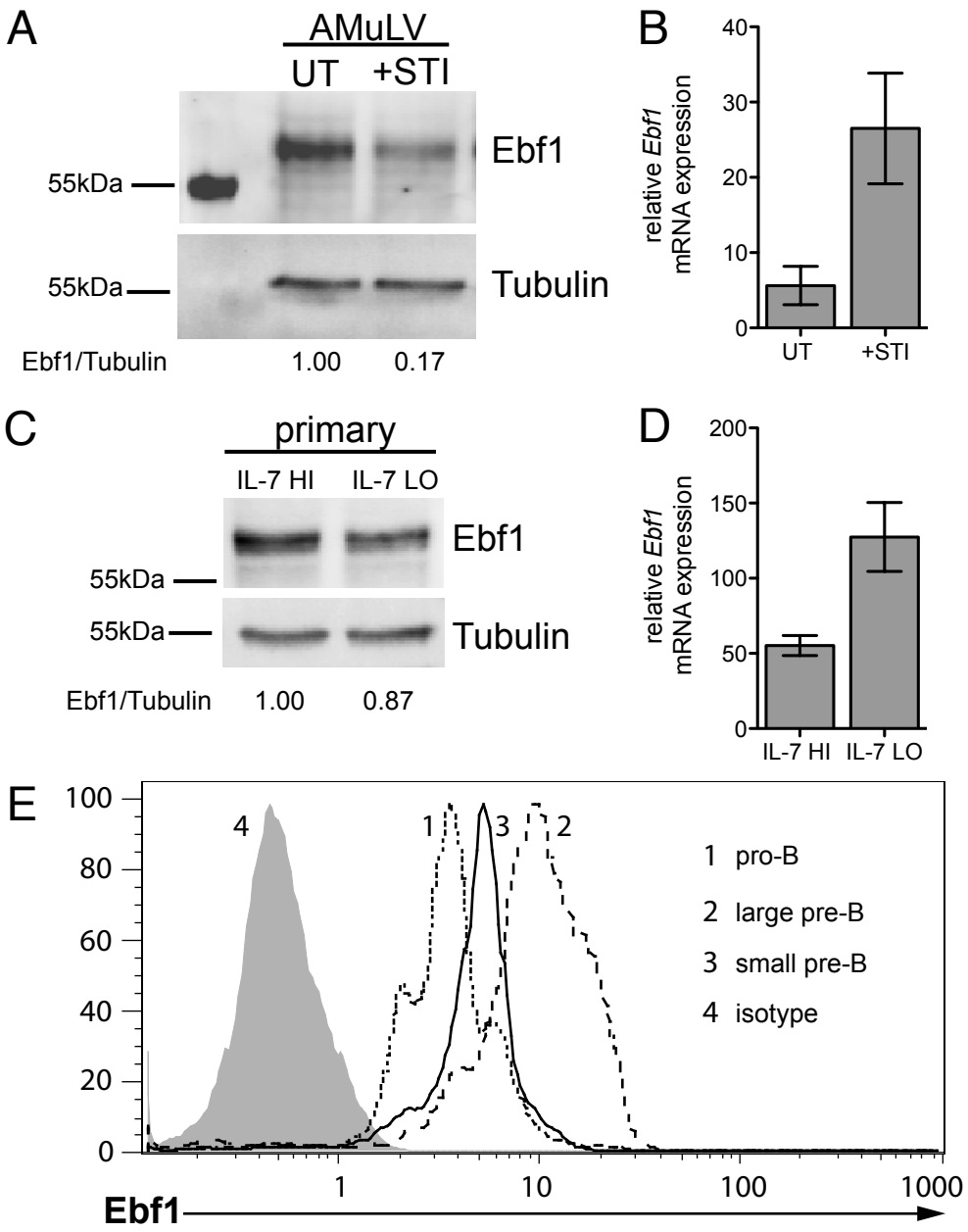

Figure 2.4. Ebf1 protein levels are inversely correlated with *Rag* expression. (A-D) Immunoblot measuring Ebf1 protein levels **(A,C)** and qPCR measuring *Ebf1* transcript levels **(B,D)** in AMuLV-transformed B cells in normal culture conditions or treated with STI (top), and in CD19+IgM- IL-7-cultured primary B cells before and after IL-7 withdrawal (bottom). Tubulin immunoblot serves as a protein loading control. Numbers below lanes indicate Ebf1/Tubulin ratio for each sample. **(E)** Flow cytometry analysis of intracellular Ebf1 expression in pro-B cells (1, dotted line), large cycling pre-B cells (2, dashed), and small resting pre-B cells (3, solid) isolated from wildtype C57/B6 mouse bone marrow. Shaded histogram represents total pre-B cell isotype control staining.

Figure 2.5

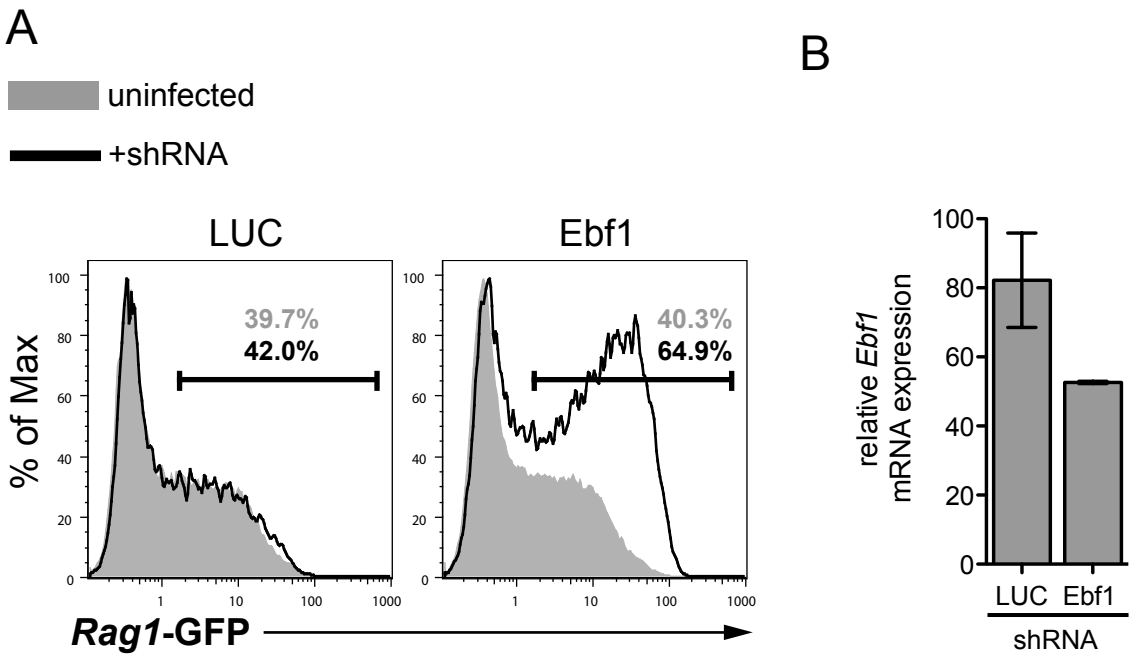

Figure 2.5. Ebf1 knockdown is sufficient to induce *Rag* transcription.
(A) GFP expression in AMuLV-transformed *Rag1*-GFP reporter B cells transduced with luciferase (LUC, left) or Ebf1 (right) shRNA retrovirus. Uninfected cells (shaded histogram) were distinguished from shRNA-expressing cells (black line) by staining with anti-hCD2 (retroviral marker). Numbers above each gate indicate the percentage of GFP+ uninfected cells (top) or shRNA-expressing cells (bottom) in each culture. **(B)** qPCR measuring *Ebf1* transcript levels in sorted AMuLV-transformed B cells transduced with luciferase or Ebf1 shRNA.

Figure 2.6

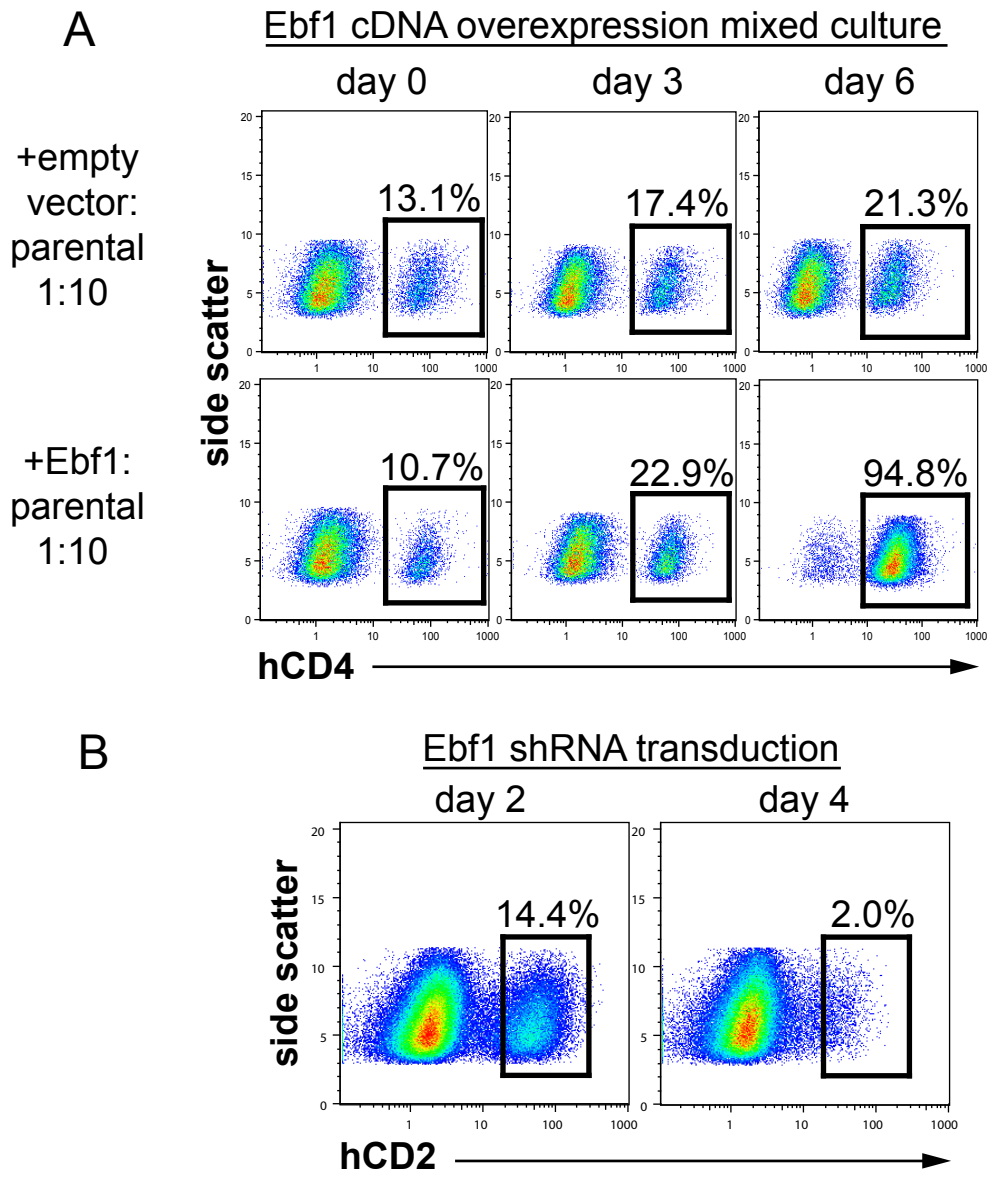

Figure 2.6. Ebf1 overexpression enhances proliferation, and Ebf1 knockdown is detrimental to growth and survival of AMuLV-transformed B cells. (A) AMuLV-transformed B cells transduced with empty (top) or Ebf1 (bottom) retrovirus were sorted 3 days post-transduction, expanded for 3 days, and mixed 1:10 with untransduced parental cells. Following staining with anti-hCD4 (retroviral marker), flow cytometry analysis was performed to determine the percentage of infected cells in the co-cultures at the indicated time points**. (B)** Flow cytometry analysis of hCD2 retroviral marker expression in AMuLV-transformed B cells transduced with Ebf1 shRNA retrovirus. Cells were stained with anti-hCD2 antibody and the percentage of Ebf1 shRNA-expressing cells in the cultures assessed at day 2 and day 4 post-transduction.

Figure 2.7

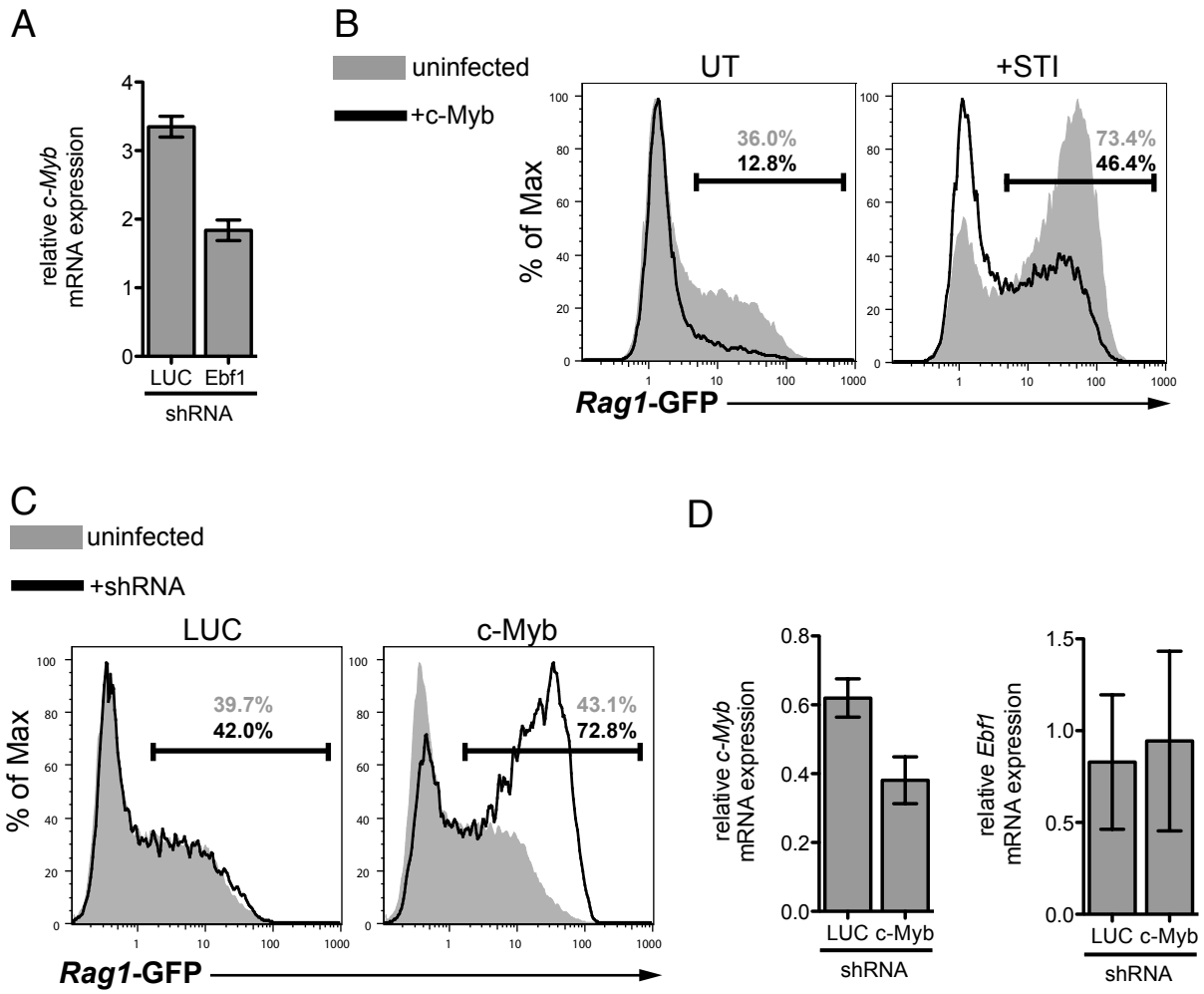

Figure 2.7. c-Myb negatively regulates *Rag* transcription downstream of Ebf1.
(A) qPCR measuring *c-Myb* transcript levels in sorted AMuLV-transformed B cells transduced with luciferase (LUC) or Ebf1 shRNA. **(B)** GFP expression in AMuLV-transformed *Rag1*-GFP reporter B cells transduced with c-Myb retrovirus. Uninfected cells (shaded histogram) were distinguished from c-Myb-overexpressing cells (black line) by staining with anti-hCD4 (retroviral marker). Analysis was performed on untreated (UT) or STI-treated (+STI) cells. Numbers above gate indicate the percentage of GFP+ uninfected cells (top) or c-Myb-overexpressing cells (bottom). **(C)** GFP expression in AMuLV-transformed *Rag1*-GFP reporter B cells transduced with luciferase (left) or c-Myb (right) shRNA. Uninfected cells (shaded histograms) were distinguished from shRNA-expressing cells (black line) by staining with anti-hCD2 (retroviral marker). Numbers above gate represent the percentage of GFP+ uninfected cells (top) or shRNA-expressing cells (bottom). **(D)** qPCR measuring c-*Myb* (left) and *Ebf1* (right) transcript levels in sorted AMuLV-transformed B cells transduced with luciferase or c-Myb shRNA.

Figure 2.8

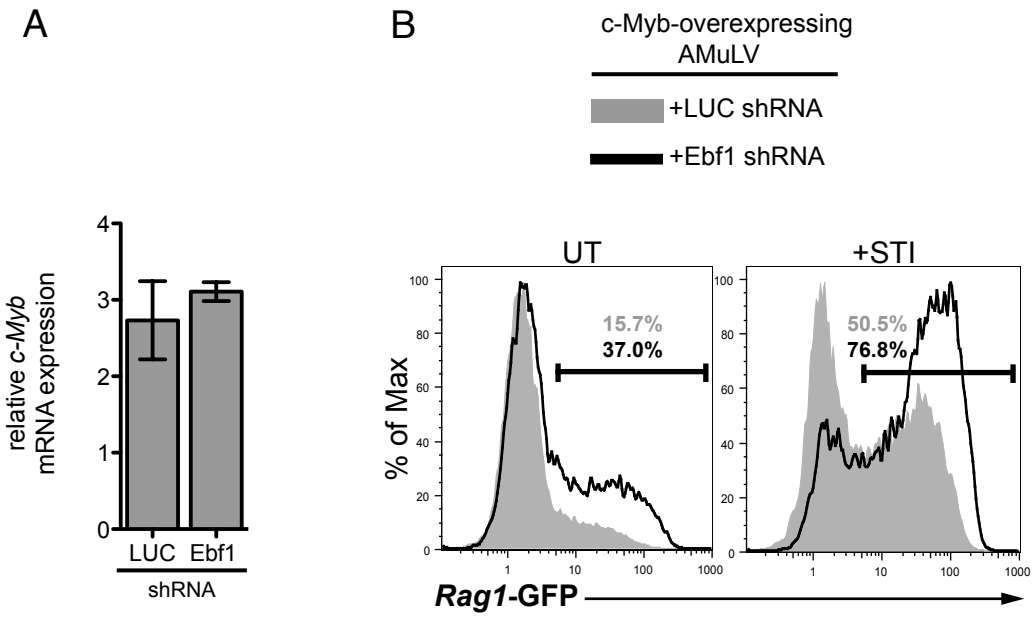

Figure 2.8. Ebf1 negatively regulates *Rag* transcription independent of c-Myb.
(A) qPCR measuring *c-Myb* transcript levels in sorted c-Myb-overexpressing AMuLV-transformed *Rag1*-GFP reporter B cells transduced with luciferase (LUC) or Ebf1 shRNA. **(B)** GFP expression in cells from **A** under normal culture conditions (UT) or treated with STI (+STI).

Figure 2.9

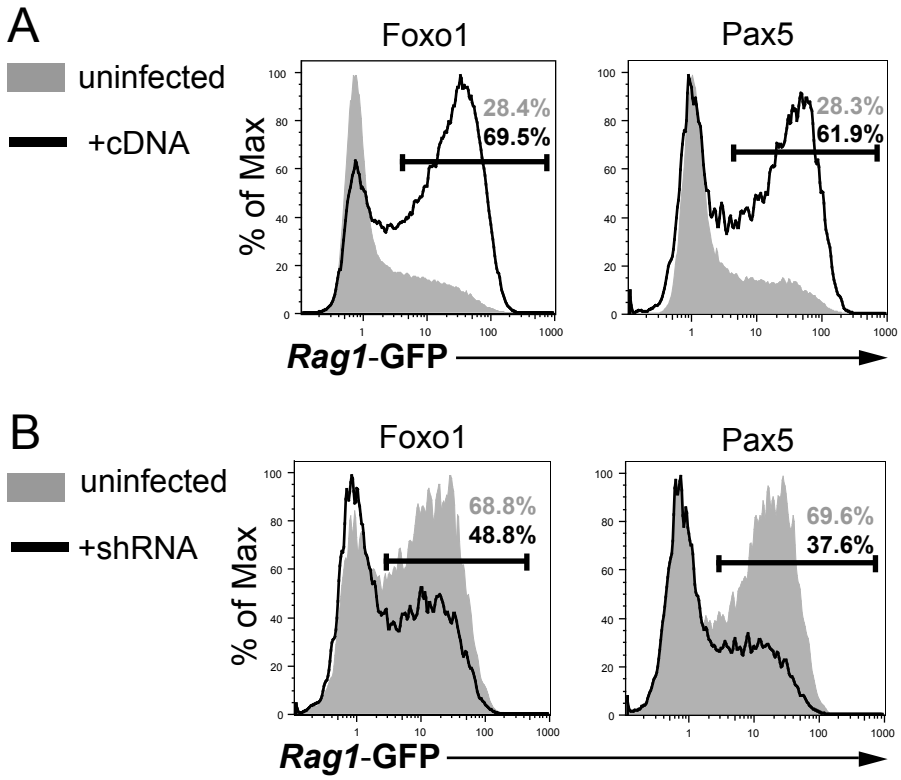

Figure 2.9. Foxo1 and Pax5 positively regulate *Rag* transcription.
(A) GFP expression in AMuLV-transformed *Rag1*-GFP reporter B cells transduced with Foxo1 or Pax5 cDNA retrovirus. Uninfected cells (shaded histogram) were distinguished cDNA-overexpressing cells (black line) by staining with anti-Thy1.1 (retroviral marker). Numbers above gate indicate the percentage of GFP+ uninfected cells (top) or cDNA-overexpressing cells (bottom). **(B)** GFP expression in AMuLV-transformed *Rag1*-GFP reporter B cells transduced with Foxo1 or Pax5 shRNA and treated with STI. Uninfected cells (shaded histogram) were distinguished from shRNA-expressing cells (black line) by staining with anti-hCD2 (retroviral marker). Numbers above gate indicate the percentage of GFP+ uninfected cells (top) or shRNA-expressing cells (bottom).

Figure 2.10

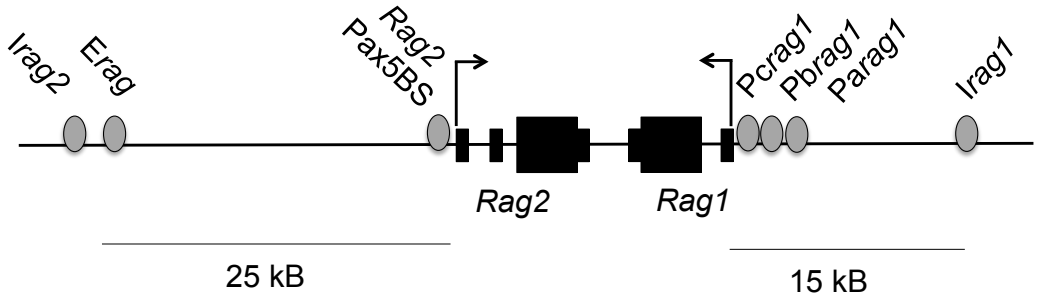

Figure 2.10. Foxo1 and Pax5 binding sites in the *Rag* locus.
Schematic of the *Rag* locus showing approximate locations of sites bound by Foxo1 and Pax5 upon pre-B cell differentiation (Ochiai et al., 2012). "P" and "I" denote promoter and intergenic binding sites, respectively.

Figure 2.11

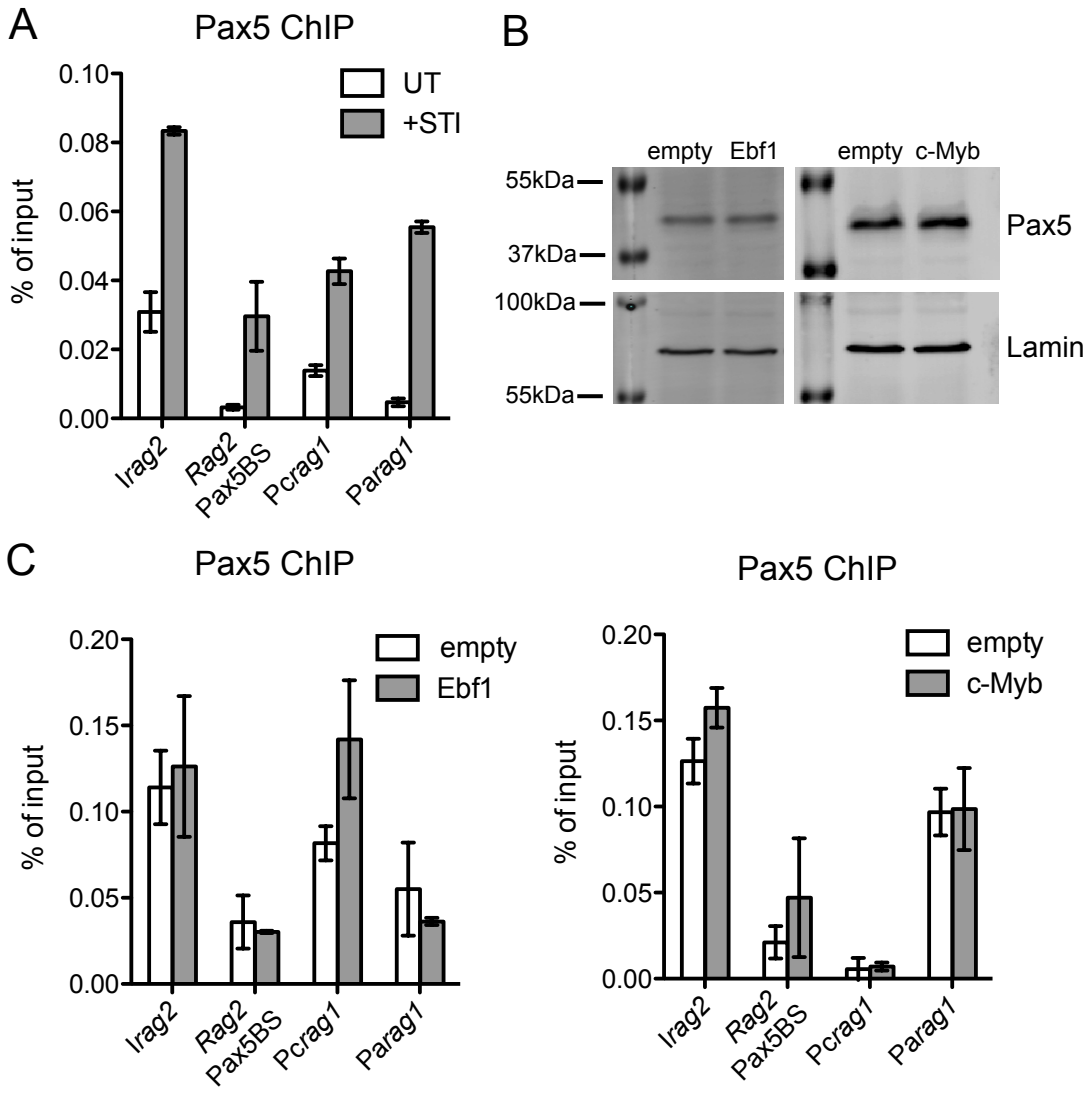

Figure 2.11. Ebf1 and c-Myb overexpression do not affect Pax5 binding to the *Rag* locus during pre-B cell differentiation. (A) ChIP in AMuLV-transformed B cells with anti-Pax5 antibody. Cells were cultured under normal conditions (white bars) or treated with STI (gray bars) prior to harvest. qPCR was performed with recovered chromatin to assess Pax5 occupancy at *Rag* locus sites depicted in **Figure 2.10** (Ochiai et al., 2012). **(B)** Immunoblot measuring Pax5 protein levels in sorted AMuLV-transformed B cells transduced with empty retroviral vector, Ebf1 retrovirus (left) or c-Myb retrovirus (right). Lamin serves as loading control. **(C)** ChIP in AMuLV-transformed B cells with anti-Pax5 or IgG control antibody. Empty vector-transduced, Ebf1-overexpressing (left), and c-Myb-overexpressing (right) cells were treated with STI and harvested. qPCR was performed with recovered chromatin to assess Pax5 occupancy at the binding sites depicted in **Figure 2.10.**

Figure 2.12

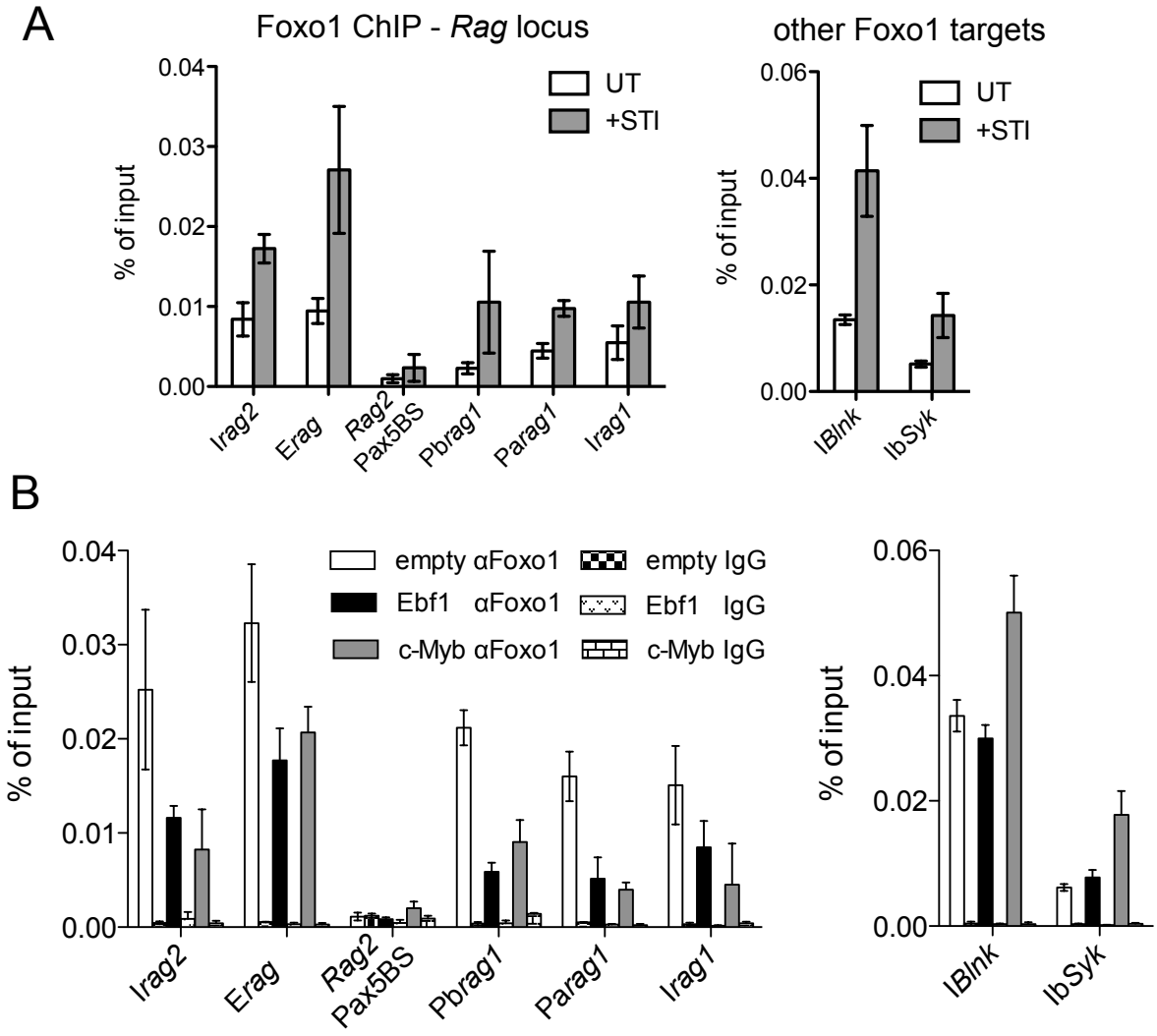

Figure 2.12. Ebf1 and c-Myb antagonize Foxo1 binding to the *Rag* locus during pre-B cell differentiation. (A) ChIP in AMuLV-transformed B cells with anti-Foxo1 antibody. Cells were cultured under normal conditions (white bars) or treated with STI (gray bars) prior to harvest. qPCR was performed with recovered chromatin to assess Foxo1 occupancy *Rag* locus sites depicted in **Figure 2.10**, or at binding sites near other Foxo1 target genes (Ochiai et al., 2012). "*Rag2*Pax5BS" serves as negative control as Foxo1 does not bind this site. **(B)** ChIP in AMuLV-transformed B cells with anti-Foxo1 or IgG control antibody. Empty vector-transduced, Ebf1-overexpressing, and c-Myb-overexpressing cells were treated with STI and harvested. qPCR was performed with recovered chromatin to assess Foxo1 occupancy at the binding sites depicted in **Figure 2.10.**

Figure 2.13

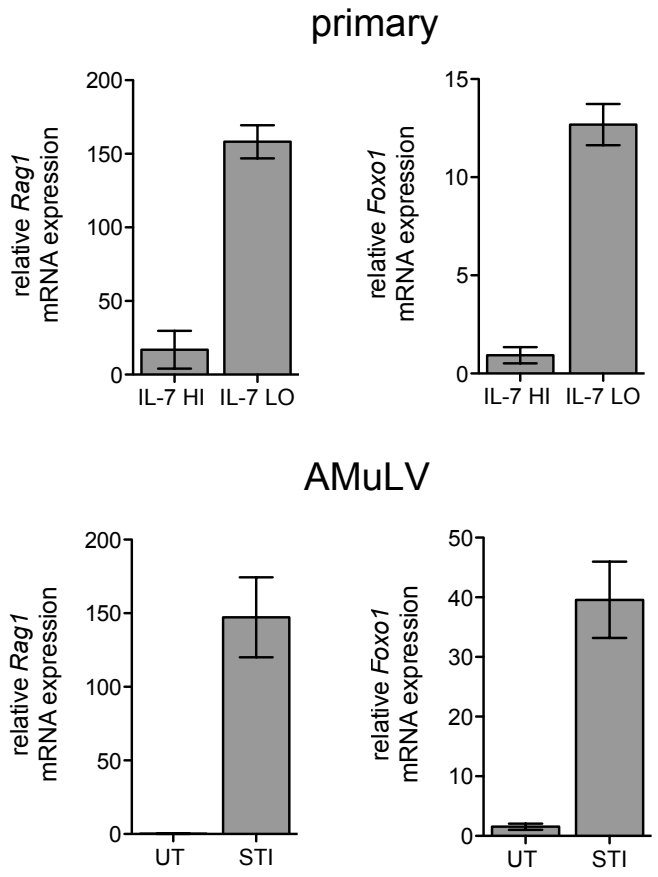

Figure 2.13. *Foxo1* mRNA expression increases during pre-B cell differentiation.
qPCR measuring *Rag1* and *Foxo1* transcript levels upon IL-7 withdrawal-induced differentiation of primary B cells from C57/B6 mouse bone marrow (top), and STI-induced differentiation of AMuLV-transformed B cells (bottom).

Figure 2.14

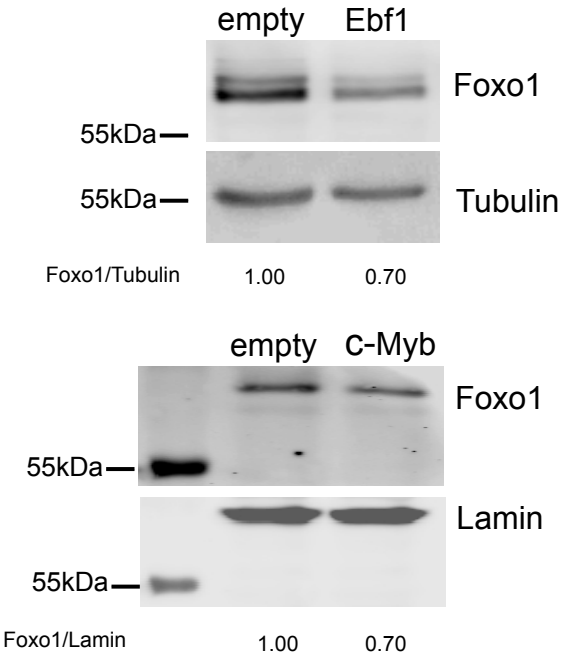

Figure 2.14. Ebf1 and c-Myb overexpression decrease Foxo1 expression.
Immunoblot measuring Foxo1 protein levels in sorted AMuLV-transformed B cells transduced with empty retroviral vector, Ebf1 retrovirus (top) or c-Myb retrovirus (bottom). Tubulin and Lamin serve as loading controls. Numbers below lanes indicate Ebf1/loading control ratio for each sample.

Figure 2.15

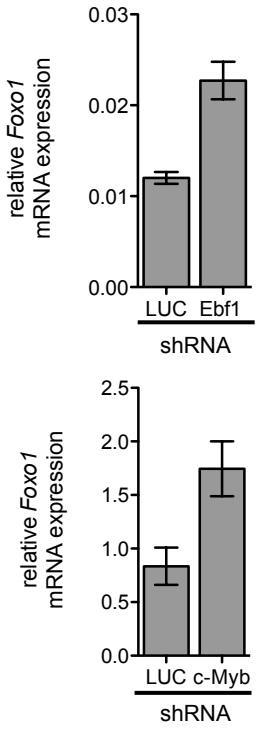

Figure 2.15. Ebf1 and c-Myb knockdown increase *Foxo1* expression.
qPCR measuring *Foxo1* transcript levels in sorted AMuLV-transformed B cells transduced with luciferase shRNA (LUC), and either Ebf1 (top) or c-Myb shRNA (bottom).

Figure 2.16

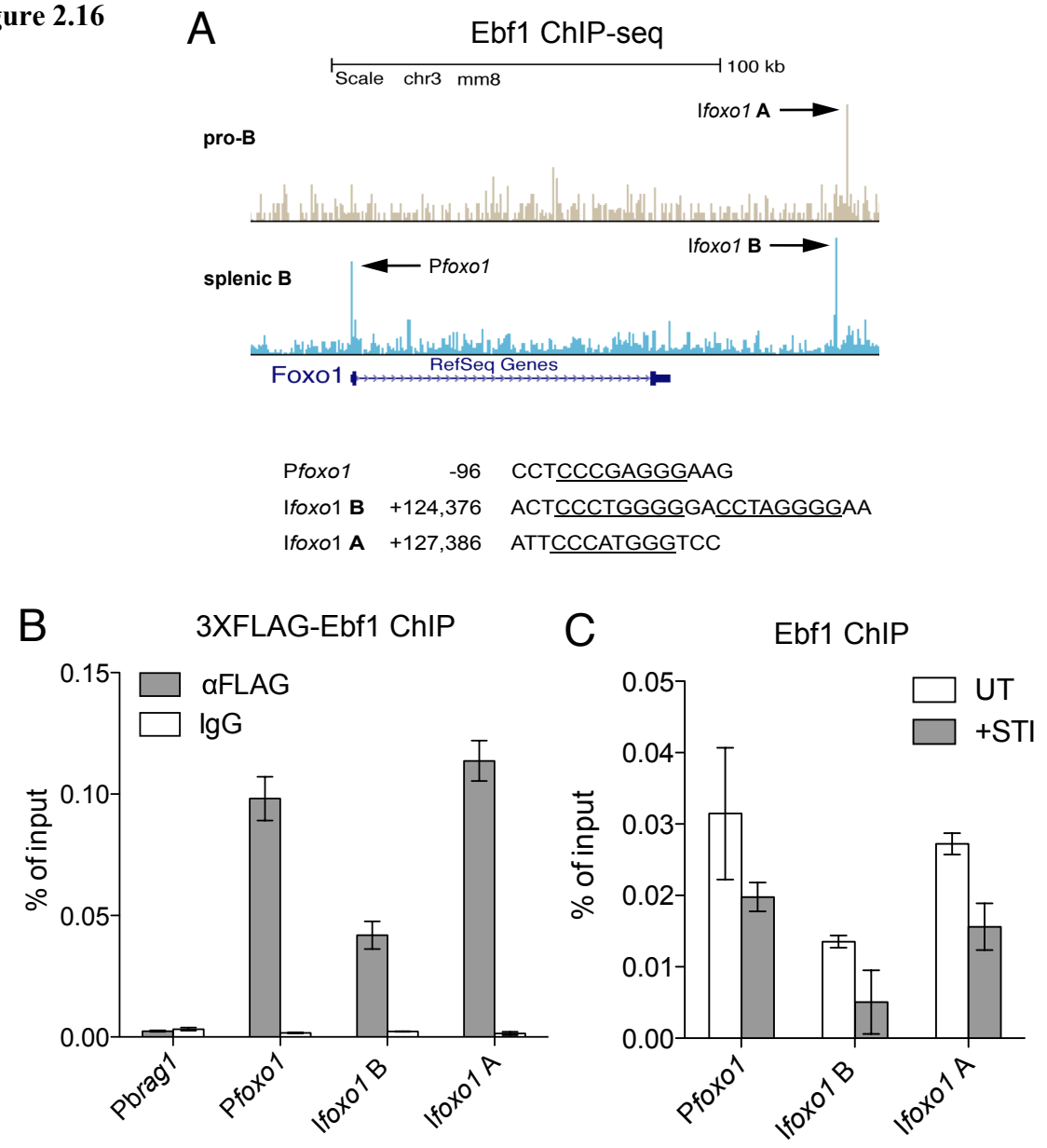

Figure 2.16. Ebf1 binds to sites the *Foxo1* locus.
(A) Published Ebf1 ChIP-seq data (Lin et al., 2010, Gyory et al., 2012) visualized in the UCSC Genome Browser at the *Foxo1* locus. "P" and "I" denote promoter and intergenic Ebf1 peaks, respectively. Ebf1 binding sites (5'-CCCNNGGG-3') identified within each peak are shown below, along with their location relative to the *Foxo1* TSS. **(B)** ChIP in AMuLV-transformed B cells overexpressing a 3XFLAG-tagged Ebf1 protein with anti-FLAG or IgG control antibody. qPCR was performed with recovered chromatin to assess 3XFLAG-Ebf1 occupancy at sites in the *Foxo1* locus described in **A** compared to a negative control site in the *Rag1* promoter. **(C)** ChIP in AMuLV-transformed B cells with anti-Ebf1 antibody. Cells were cultured in normal conditions (white bars) or treated with STI (gray bars) prior to harvest. qPCR was performed on recovered chromatin to assess Ebf1 occupancy at sites in the *Foxo1* locus described in **A**.

Figure 2.17

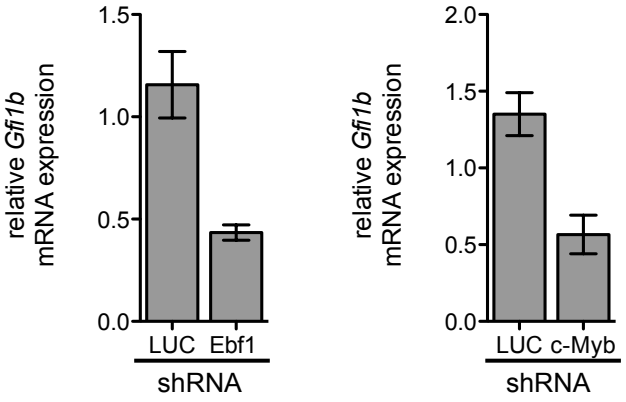

Figure 2.17. Ebf1 and c-Myb knockdown increase *Gfi1b* expression.
qPCR measuring *Gfi1b* transcript levels in sorted AMuLV-transformed B cells transduced with luciferase shRNA (LUC), and either Ebf1 (left) or c-Myb shRNA (right).

Figure 2.18

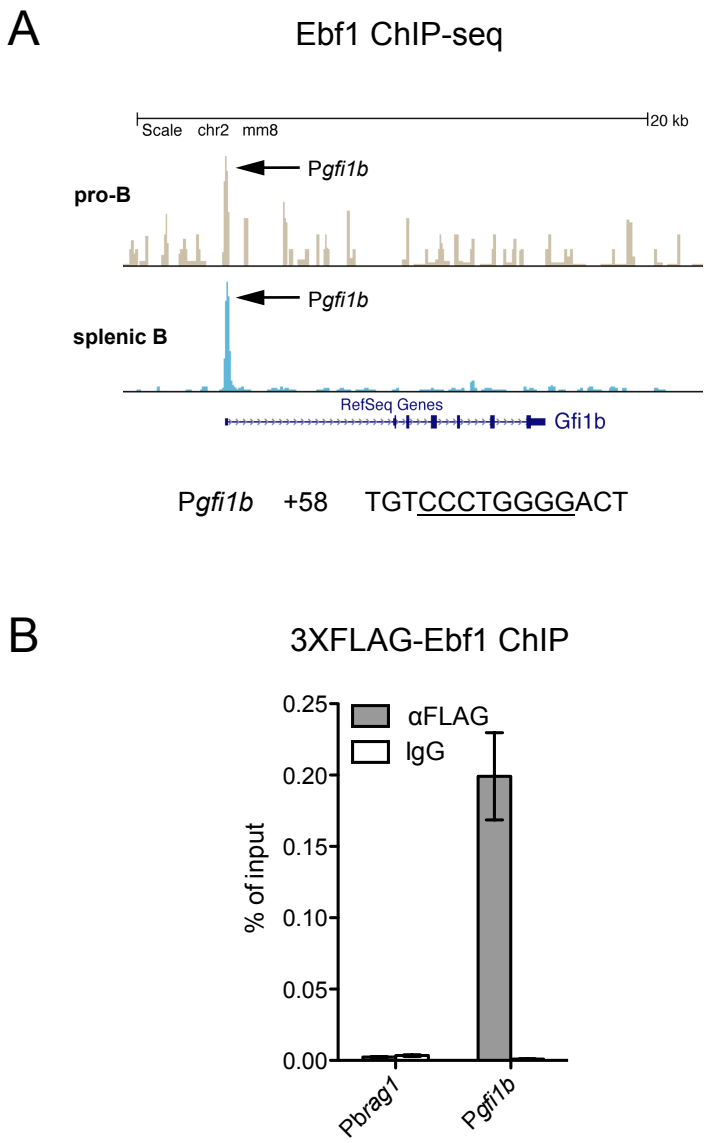

Figure 2.18. Ebf1 binds the *Gfi1b* promoter.
(A) Published Ebf1 ChIP-seq data (Lin et al., 2010, Gyory et al., 2012) visualized in the UCSC Genome Browser at the *Gfi1b* locus. An Ebf1 binding site (5'-CCCNNGGG-3') identified within the *Gfi1b* promoter peak is shown below, along with its location relative to the *Gfi1b* TSS. **(B)** ChIP in AMuLV-transformed B cells overexpressing a 3XFLAG-tagged Ebf1 protein with anti-FLAG or IgG control antibody. qPCR was performed on recovered chromatin to assess Ebf1 occupancy at the *Gfi1b* promoter site described in **A** compared to a negative control site in the *Rag1* promoter.

Figure 2.19

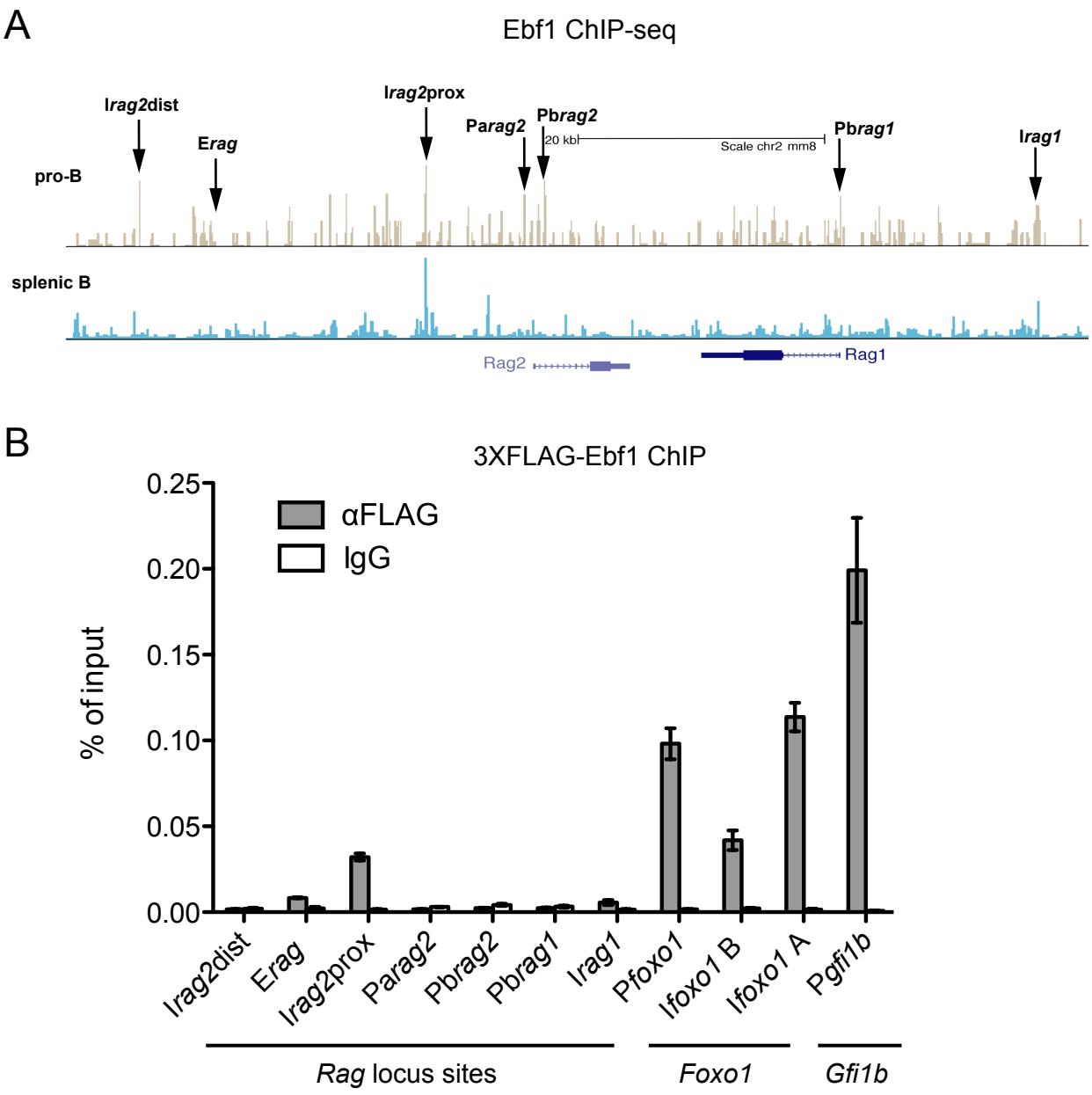

Figure 2.19. Ebf1 does not bind to sites in the *Rag* locus.
(A) Published Ebf1 ChIP-seq data (Lin et al., 2010, Gyory et al., 2012) visualized in the UCSC Genome Browser at the *Rag* locus. Potential Ebf1 binding sites are indicated by arrows. **(B)** ChIP in AMuLV-transformed B cells overexpressing a 3XFLAG-tagged Ebf1 protein with anti-FLAG or IgG control antibody. qPCR was performed on recovered chromatin to assess Ebf1 occupancy at the *Rag* locus sites described in **A.** Ebf1 binding sites in the *Foxo1* and *Gfi1b* loci serve as positive controls.

Figure 2.20

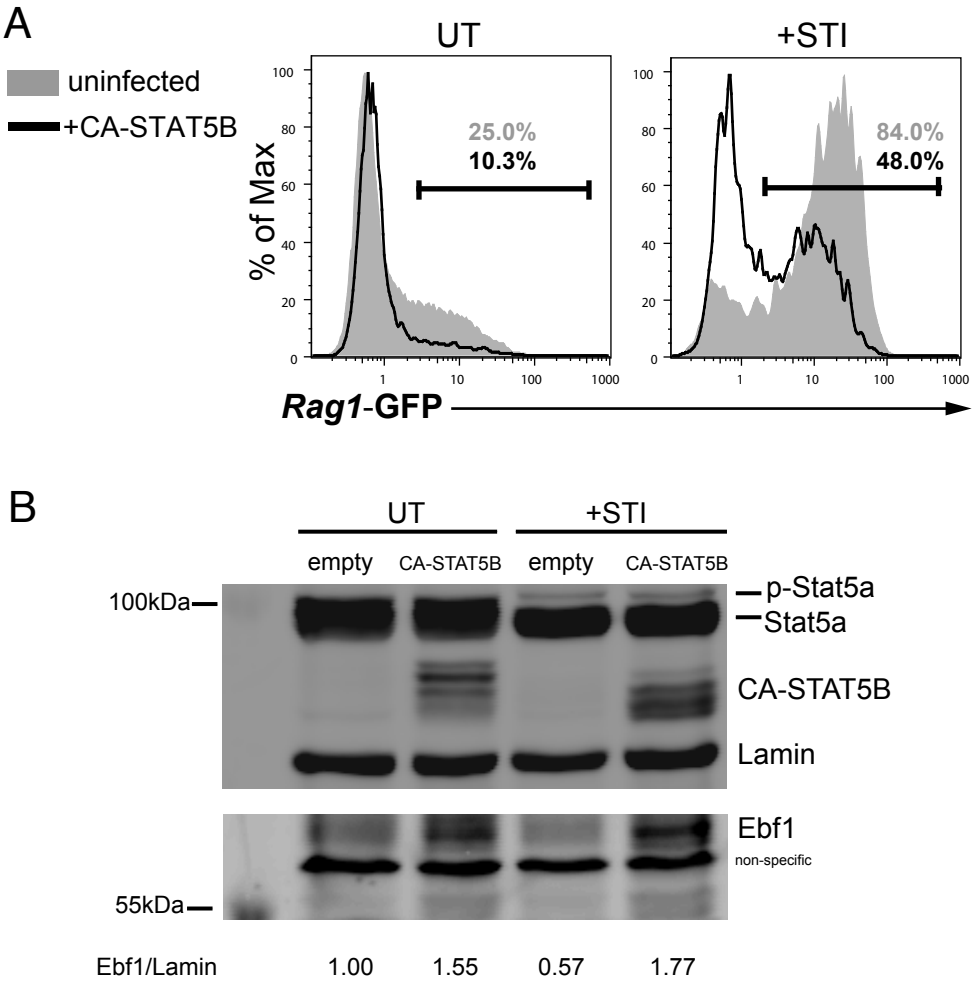

Figure 2.20. Stat5 represses *Rag* transcription through upregulation of Ebf1.
(A) GFP expression in AMuLV-transformed *Rag1*-GFP reporter B cells transduced with constitutively active STAT5B (CA-STAT5B) retrovirus. Uninfected cells (shaded histogram) were distinguished from CA-STAT5B-overexpressing cells (black line) by staining with anti-hCD4 (retroviral marker). Analysis was performed on cells in normal culture conditions (UT) or treated with STI (+STI). Numbers above gate indicate the percentage of GFP+ uninfected cells (top) or CA-STAT5-overexpressing cells (bottom). **(B)** Immunoblot measuring Stat5 and Ebf1 protein levels in sorted AMuLV-transformed B cells transduced with empty vector or CA-STAT5B retrovirus. Cells were cultured under normal conditions (UT) or treated with STI (+STI) prior to harvest. Lamin serves as protein loading control. Endogenous Stat5a is distinguished from exogenous CA-STAT5B based on molecular weight. Slower-migrating Stat5a species is the phosphorylated form of the protein (denoted "p-Stat5a"). Numbers below lanes indicate Ebf1/Lamin ratio for each sample. Non-specific band below Ebf1 arises from anti-Stat5 probing.

Figure 2.21

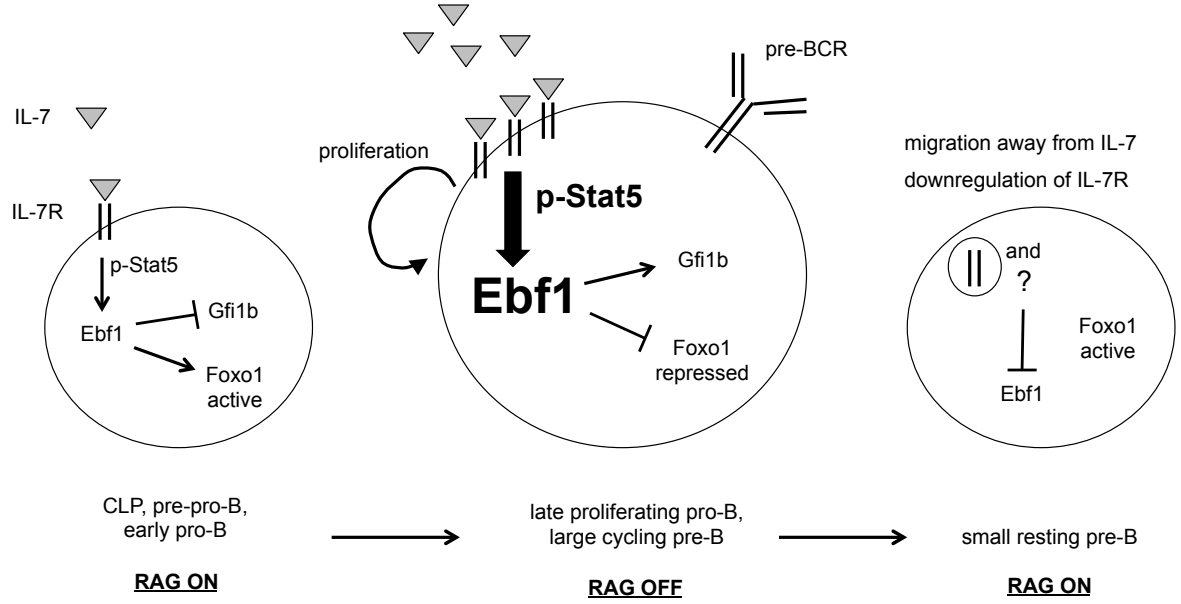

Figure 2.21. Model for stage-specific repression of *Rag* transcription by Ebf1 during B cell development.

Chapter 3

Dual mechanism of *Rag* gene repression by c-Myb revealed through studies of M303V c-Myb mutant

Background

Expression of the recombination activating genes *Rag1* and *Rag2* (*Rag*) during lymphocyte development is essential for generation of the diverse B and T cell receptor repertoires required for effective adaptive immune responses (Schlissel., 2003). This process involves the generation of double stranded DNA breaks in the antigen receptor loci (Schatz and Swanson., 2011). If generated during S phase, these breaks have the potential to be repaired by homologous recombination, resulting in chromosomal translocations sometimes leading to oncogenic transformation. Thus both RAG protein and *Rag* mRNA expression in developing lymphocytes, which undergo periods of proliferation and clonal expansion, is restricted to cells in the G_0-G_1 phases of cell cycle (Lee et al., 2004, Kuppers and Dalla-Favera., 2001, Zhang et al., 2011). Identifying the factors responsible for this temporal control of *Rag* expression is critical for our understanding of tumor suppression and proper immune system development.

Developing B lymphocytes in the bone marrow undergo a period of clonal expansion following successful immunoglobulin heavy chain (Ig H) locus recombination during the pro-B cell stage (Grawunder et al., 1995). While the mechanism of RAG protein downregulation in these large cycling pre-B cells is well-characterized (Li et al., 1996), the transcription factors responsible for the repression of *Rag* mRNA expression are less defined. Moreover, little is known about how the activity of these repressive factors is controlled as cells cease proliferating, differentiate into small pre-B cells, and re-express the *Rag* genes for recombination of the immunoglobulin light chain (Ig L) loci.

We previously used Abelson Murine Leukemia Virus (AMuLV) transformed B cell lines to screen for novel repressors of *Rag* transcription. The v-Abl oncogene selectively transforms developing B cells in a large cycling pre-B cell-like state where *Rag* transcription is repressed. This developmental block can be reversed by inhibiting v-Abl kinase activity with STI-571 (STI), which induces cell cycle exit, differentiation to a small pre-B cell-like state, and robust *Rag* transcription (Muljo and Schlissel., 2003). We identified Ebf1 and c-Myb, two well-studied transcription factors in the context of B cell development, as repressors of *Rag* transcription in these highly proliferative cells (Timblin and Schlissel., 2013). shRNA knockdown of either factor was sufficient to induce *Rag* transcription in AMuLV B cells independent of v-Abl inhibition with STI. Experiments suggested that Ebf1 does not represses *Rag* transcription directly, but rather through controlling expression of Foxo1 and Gfi1b, two factors previously identified as positive and negative regulators of *Rag* transcription, respectively (Amin and Schlissel., 2008, Dengler et al., 2008, Schulz et al., 2012). However, the mechanism by which c-Myb repressed *Rag* transcription (directly or via other factors) was less clear.

Here we set out to learn more about the mechanism of *Rag* repression by c-Myb using AMuLV-transformed B cells. To do so we compared the repressive activity of wild-type c-Myb (WT) to that of a previously described c-Myb mutant (M303V) (Sandberg et al., 2005) that has impaired repressive activity (Zhao et al., 2011). Experiments comparing the WT and mutant proteins reveal c-Myb represses *Rag* transcription by a dual mechanism: indirectly through repression of Foxo1 expression, and directly by occupying the E*rag*

enhancer in the *Rag* locus and antagonizing Foxo1 binding to this *cis* regulatory element. This work provides important insight into c-Myb biology and the mechanism by which this factor represses *Rag* transcription during B cell development.

Results

M303V mutation impairs the ability of c-Myb to repress *Rag* transcription

To investigate the mechanism of *Rag* repression by c-Myb, we used a previously described AMuLV-transformed *Rag1*-GFP reporter B cell line (Kuwata et al., 1999, Amin and Schlissel., 2008). Figure 3.1A shows that *Rag1*-GFP levels are low in these cells, and that treatment with STI induces differentiation and robust *Rag* expression. We previously showed that protein levels of the *Rag* repressor Ebf1 decrease drastically upon STI-induced differentiation (Timblin and Schlissel., 2013), allowing for the upregulation of *Rag* expression. In contrast, c-Myb protein expression levels are similar in untreated and STI-treated cells (Figure 3.1B), suggesting that mechanisms are in place to control c-Myb repressive activity upon differentiation and allow for *Rag* upregulation.

We hypothesized that interactions with corepressors might control c-Myb activity. A previous study showed that B cell development in mice homozygous for a c-Myb point mutation (M303V) is blocked at the stage (large cycling pre-B cell, Hardy Fraction C') during which cells undergo a proliferative burst and *Rag* transcription is repressed (Sandberg et al., 2005). Biochemical analysis revealed the M303V mutation disrupts c-Myb interaction with p300, a protein traditionally viewed as a coactivator. However, a subsequent study of a similar c-Myb mutant (L302A) defective in its ability to interact with p300 showed that this mutation abrogates the ability of c-Myb to both activate and repress target genes during myeloid differentiation (Zhao et al., 2011). Thus we wanted to test if M303V mutation impairs the previously described ability of c-Myb to repress *Rag* transcription in AMuLV-transformed B cells (Timblin and Schlissel., 2013).

Figure 3.2 shows AMuLV-transformed *Rag1*-GFP reporter B cell cultures transduced with WT c-Myb or M303V c-Myb retroviruses. Looking at GFP expression in untreated cells (top row), while M303V c-Myb is still able to decrease GFP levels compared to control untransduced cells in the same culture (top right), the effect is not as strong as for WT c-Myb (top left), suggesting the M303V mutant has impaired repressive activity. This is more evident upon STI-induced differentiation (bottom row), as *Rag* induction is much more robust in cells transduced with M303V c-Myb (bottom right) than WT c-Myb (bottom left) compared to control untransduced cells in each culture.

To rule out the possibility that differences in the expression level of WT c-Myb and M303V c-Myb might account for this phenotype, we transduced cells with 3XFLAG-tagged versions of these proteins and sorted infected cells to obtain pure cultures. Figure 3.3A shows that the sorted 3XFLAG M303V c-Myb cells have higher *Rag* expression levels than sorted 3XFLAG WT c-Myb cells in the untreated condition (left), and that *Rag* induction upon STI treatment is much more robust in the 3XFLAG M303V c-Myb cells than the 3XFLAG WT c-Myb cells (right). FLAG immunoblot using lysates prepared from these sorted cell lines shows the expression levels of the 3XFLAG-tagged c-Myb proteins is similar (Figure 3.3B). Taken together, these experiments show that the M303V mutation impairs the ability of c-Myb to repress *Rag* transcription.

M303V c-Myb is defective in repression of Foxo1

Our previous work suggested that c-Myb represses *Rag* transcription at least in part through repression of Foxo1 expression, as WT c-Myb-overexpressing cell lines have reduced Foxo1 protein levels compared to control cell lines (Timblin and Schlissel., 2013). Figure 3.4A shows GFP expression in sorted *Rag*1-GFP reporter cells transduced with empty vector (VEC), 3XFLAG WT c-Myb (WT), or 3XFLAG M303V c-Myb (M303V) retrovirus. To test whether M303V c-Myb represses Foxo1, we examined Foxo1 expression levels in these three cell lines. Figure 3.4B shows that compared to control empty vector-transduced cells, 3XFLAG WT c-Myb-transduced cells have reduced Foxo1 protein levels, confirming our previous result. Interestingly, Foxo1 protein levels in the 3XFLAG M303V c-Myb cell line are rescued and comparable to Foxo1 levels in the empty vector control cell line. This result shows that the M303V mutation impairs the ability of c-Myb to repress Foxo1 expression.

Our previous work identified a region in the *Foxo1* promoter (P*foxo1*) and intergenic regions downstream of the *Foxo1* gene (I*foxo1* A and I*foxo1* B) bound strongly by Ebf1 (Timblin and Schlissel., 2013), suggesting that Ebf1 directly represses Foxo1 expression. Given that Ebf1 and c-Myb overexpression have similar effects on Foxo1 levels (Timblin and Schlissel., 2013), we hypothesized that c-Myb might also bind to these regions to negatively regulate *Foxo1* in a direct manner similar to Ebf1. To test this we performed FLAG ChIP using the 3XFLAG WT c-Myb and 3XFLAG M303V c-Myb cell lines. Figure 3.5 shows that both 3XFLAG WT c-Myb and 3XFLAG M303V c-Myb bind the regions in the *Foxo1* locus but not a negative control region in the *Rag1* promoter where we detect no c-Myb binding. This result suggests that c-Myb directly represses Foxo1 expression by co-occupying *cis* regulatory elements in the *Foxo1* locus with Ebf1. It also suggests that the defect in Foxo1 repression observed for M303V c-Myb is not due to a reduction the DNA binding ability of the mutant, as occupancy at regions in the *Foxo1* locus is comparable between the 3XFLAG WT c-Myb and 3XFLAG M303V c-Myb proteins. This result is consistent with gel shift experiments showing WT c-Myb and M303V c-Myb proteins have similar DNA binding ability *in vitro* (Sandberg et al., 2005).

Foxo1 expression is also negatively regulated by the transcriptional repressor Gfi1b (Schulz et al., 2012). We previously demonstrated that shRNA knockdown of c-Myb resulted in a decrease in *Gfi1b* mRNA levels, suggesting c-Myb positively regulates Gfi1b (Timblin and Schlissel., 2013). FLAG ChIP clearly shows that both 3XFLAG WT c-Myb and 3XFLAG M303V c-Myb strongly bind to the region in the *Gfi1b* promoter also bound by Ebf1 (P*gfi1b*, Figure 3.5), suggesting that positive regulation of Gfi1b by c-Myb is direct. And as observed for elements in the *Foxo1* locus, *Gfi1b* promoter binding levels are comparable between the 3XFLAG WT c-Myb and 3XFLAG M303V c-Myb proteins.

In conclusion, these experiments show that unlike WT c-Myb, M303V c-Myb is unable to repress Foxo1 expression, providing an explanation for the defect in *Rag* repression observed for the mutant protein. They also show that c-Myb co-occupies regulatory regions in the *Foxo1* and *Gfi1b* loci with the *Rag* repressor Ebf1. Comparable levels of DNA binding

to these regions are observed for WT c-Myb and M303V c-Myb, suggesting the defect in repression observed for M303V c-Myb is not due to a decrease in DNA binding ability.

Both WT and M303V c-Myb antagonize Foxo1 binding to the E*rag* enhancer

Figure 3.4A shows that despite the mutation, M303V c-Myb possesses some residual repressive activity as *Rag*1-GFP expression is reduced compared to control empty vector transduced cells (22.4% versus 33.7%). This residual repressive activity is evident upon STI treatment of these cell lines as shown in Figure 3.6A. While *Rag1*-GFP induction is much greater in M303V c-Myb cells (63.3%) compared to WT c-Myb cells (21.5%), it is reduced compared to control empty vector-transduced cells (79.9%).

We previously showed that Foxo1 inducibly binds to the well-characterized E*rag* enhancer (Hsu et al., 2003) upon STI treatment, and that WT c-Myb overexpression results in reduced Foxo1 binding (Timblin and Schlissel., 2013). To test if M303V c-Myb, while unable to repress Foxo1 expression (Figure 3.4B), is still capable of antagonizing Foxo1 binding to the *Rag* locus, we performed Foxo1 ChIP using the STI-treated cells in Figure 3.6A. Figure 3.6B shows robust binding of Foxo1 to the E*rag* enhancer, but not to a downstream negative control region between the enhancer and *Rag2* promoter, in the STI-treated empty vector control cell line. As shown previously, Foxo1 binding to E*rag* is reduced in the WT c-Myb cell line. Interestingly, Foxo1 binding is also reduced in the M303V c-Myb cell line, suggesting that while the mutant protein is unable to repress Foxo1 expression, M303V c-Myb retains the ability to antagonize Foxo1 binding the E*rag* enhancer.

We hypothesized that the ability of M303V c-Myb to antagonize Foxo1 binding to E*rag*, despite being unable to repress Foxo1 expression, could be a direct effect. To test if c-Myb binds the E*rag* enhancer, we again performed FLAG ChIP using the WT and M303V cell lines. Figure 3.7 shows that both 3XFLAG WT c-Myb and 3XFLAG M303V c-Myb bind to E*rag*, but not to a control region in the *Rag1* promoter. As with the previous ChIP for regions in the *Foxo1* and *Gfi1b* loci (Figure 3.5), the E*rag* ChIP signal suggests WT c-Myb and M303V c-Myb possess similar DNA binding ability. It also shows that despite not being able to repress Foxo1 expression, the M303V c-Myb mutant can antagonize STI-induced Foxo1 binding to the E*rag* enhancer through its own ability to bind this important regulatory element, at least partially explaining its residual repressive activity. Finally, these results reveal two separate modes by which WT c-Myb antagonizes *Rag* expression: indirectly through repression of Foxo1 expression, and directly through occupying E*rag* and antagonizing Foxo1 binding.

Disruption of Foxo1 binding to E*rag* is sufficient to repress STI-induced *Rag* expression

Targeted deletion of E*rag*, a 1.7 kb enhancer element lying 23 kb upstream of the *Rag*2 promoter, results in impaired B cell development owing to reduced *Rag* expression and subsequent defects in V(D)J recombination (Hsu et al., 2003). Experiments from our lab have shown *Rag* expression is extremely Foxo1-dependent, as genetic deletion of *Foxo1* abolishes STI-induced *Rag* expression in AMuLV B cells (Chow et al., 2013). While a

consensus Foxo1 binding site exists within the E*rag* ChIP amplicon analyzed in this study (Figure 3.8A), Foxo1 also binds to other regions in the *Rag* locus that may be important for activating *Rag* gene expression (Ochiai et al., 2012).

We sought to test the importance of Foxo1 binding to this particular site within E*rag*, where both WT and M303V c-Myb act as binding antagonists, for *Rag* expression. To do so we utilized CRISPR/Cas9 transcriptional interference technology (Gilbert et al., 2013). We created stable cell lines in which a catalytically inactive Cas9 protein (dCas9) fused to a Kruppel-associated box (KRAB) repressor domain is targeted to E*rag* by co-expressed small guide RNAs (sgRNAs) (Figure 3.8A, top). More specifically, we designed the sgRNAs such that the dCas9-KRAB repressor is targeted to the Foxo1 E*rag* site, or to four adjacent c-Myb binding sites (Figure 3.8A, bottom). As a control we created cells co-expressing the fusion protein and a sgRNA against an irrelevant sequence such that no dCas9-KRAB will be targeted to the *Rag* locus.

Figure 3.8B shows dCas9-KRAB is expressed in each of the cell lines, and that STI treatment induces robust *Rag* transcription in control sgRNA-expressing cells as expected. In the cells where dCas9-KRAB is targeted to the Foxo1 consensus binding site in E*rag*, the induction of *Rag* expression upon STI treatment is severely blunted. The same negative effect on *Rag* expression is observed when dCas9-KRAB is targeted to the c-Myb binding sites adjacent to the Foxo1 site.

These experiments suggest Foxo1 binding to this E*rag* site is crucial *Rag* expression, as targeting a transcriptional repressor to the site and disrupting Foxo1 binding severely inhibits *Rag* induction upon STI-induced differentiation. They also show that targeting the repressor to adjacent c-Myb binding sites is sufficient to inhibit *Rag* induction. As our ChIP data shows c-Myb binds this region and affects both Foxo1 binding and *Rag* expression, we surmise the latter experiments could mimic the physiological mechanism by which c-Myb achieves *Rag* repression. Whether corepressor recruitment to these sites by c-Myb is necessary for repression, or if c-Myb can achieve repression at these sites through steric hindrance of Foxo1, remains to be tested (see discussion).

c-Myb overexpression does not alter p300 recruitment to the E*rag* enhancer

Characterization of the M303V mutation showed it disrupted the ability of c-Myb to interact with p300 (Sandberg et al., 2005), and both subsequent work (Zhao et al., 2011) and the data presented here show M303V c-Myb is defective in gene repression. This suggests c-Myb co-opts p300, normally thought of as a coactivator, for gene repression. The previous studies, however, do not rule out the possibility that the M303V mutation disrupts c-Myb interactions with other proteins. In an attempt to establish a connection between c-Myb, p300, and *Rag* gene repression, we studied p300 binding dynamics at the E*rag* enhancer, which our ChIP experiments show is bound by c-Myb.

p300 ChIP using the *Rag*1-GFP reporter cell line reveals that in the untreated condition, p300 occupancy is nonexistent at both the E*rag* enhancer and *Rag1* promoter (Figure 3.9). Upon STI treatment, strong p300 binding is observed at E*rag* but not the *Rag1* promoter,

consistent with studies showing that p300 occupies active tissue-specific enhancer elements (Heintzman et al., 2007, Visel et al., 2009). Thus, p300 occupancy at E*rag* is undetectable in untreated cells, and strong p300 binding upon STI treatment is directly correlated with the induction *Rag* expression. These results are inconsistent with a role for p300 as a *Rag* repressor that is recruited to E*rag* by c-Myb in the untreated cells.

To further confirm that p300 is not a cofactor utilized by c-Myb to repress *Rag* expression, we measured p300 occupancy at E*rag* in the context of WT c-Myb and M303V c-Myb overexpression. If c-Myb recruits p300 as a co-repressor to negatively regulated target genes, overexpression of WT c-Myb, but not M303V c-Myb, would enhance p300 occupancy at E*rag* in untreated cells. However, our ChIP results show no p300 occupancy at the E*rag* enhancer in both WT c-Myb-overexpressing and M303V c-Myb-overexpressing cells (Figure 3.10, UT), suggesting that *Rag* repression by c-Myb does not require p300 recruitment.

It is possible that WT c-Myb represses *Rag* by interacting with and sequestering p300 from binding and activating the E*rag* enhancer. This model would predict that upon STI treatment, p300 binding to E*rag* would be reduced in cells overexpressing WT c-Myb, but not M303V c-Myb. However we observed robust and comparable p300 binding to E*rag* in both WT c-Myb-overexpressing and M303V c-Myb-overexpressing cells following STI treatment (Figure 3.10, +STI), suggesting p300 interaction is not required by c-Myb for its repressive activity.

These experiments show that p300 binding to the E*rag* enhancer is directly correlated with *Rag* expression in our system. They also show that enforced c-Myb expression, which has clear repressive effects on *Rag* transcription, does not alter p300 binding at E*rag* in either the untreated condition or following STI-induced differentiation. Together these results suggest that if c-Myb and p300 cooperate for *Rag* repression, they do so in a manner that does not involve alteration of normal p300 binding dynamics at the E*rag* enhancer.

Discussion

c-Myb has been well-studied in the context of early B cell development where it plays an important role in B lymphoid priming through activation of lineage-specific genes in progenitor cells (Fahl et al., 2009, Greig et al., 2010). Using the AMuLV-transformed B cell system, we sought to learn more about c-Myb function during later stages of B cell development, specifically at the pro-to-pre-B cell transition where we identified c-Myb as a repressor of *Rag* transcription in these highly proliferative cells (Timblin and Schlissel., 2013). Comparing the activity of WT c-Myb to a c-Myb point mutant (M303V) that is defective in gene repression revealed that repression of *Rag* transcription by c-Myb proceeds through both indirect and direct mechanisms.

Our previous work showed that c-Myb overexpression in AMuLV cells impaired binding of the *Rag* activator Foxo1 to the *Rag* locus upon differentiation with STI (Timblin and Schlissel., 2013). Subsequent experiments suggested this occurred because of the ability of c-Myb to repress Foxo1 expression, as 1) c-Myb overexpression repressed Foxo1 protein levels, and 2) shRNA knockdown of c-Myb increased *Foxo1* mRNA expression. Overexpression and knockdown of Ebf1, a factor we and others identified as being upstream of c-Myb in AMuLV cells (Gyory et al., 2012), had identical effects on Foxo1 expression. Identification of elements bound by Ebf1 in the *Foxo1* locus suggested repression of Foxo1 by Ebf1 is direct (Timblin and Schlissel., 2013). Here we tested the possibility that c-Myb might co-occupy these regions with Ebf1 and also directly repress Foxo1. This is indeed the case as we detect robust binding of c-Myb to the same regions in the *Foxo1* locus bound by Ebf1 (Figure 3.5), suggesting that Ebf1 and c-Myb co-occupy *cis* regulatory elements to achieve Foxo1 repression and negative regulation of the *Rag* genes.

Our previous work also showed a role for Ebf1 and c-Myb in the positive regulation of Gfi1b expression in AMuLV B cells, as knockdown of either factor resulted in a strong decrease in *Gfi1b* mRNA levels (Timblin and Schlissel., 2013). Given ChIP experiments showed strong Ebf1 binding to the *Gfi1b* promoter, we wanted to test here whether c-Myb might co-occupy this region and co-regulate Gfi1b expression with Ebf1. This is indeed the case as we were able to detect strong binding of c-Myb to the *Gfi1b* promoter (Figure 3.5).

The combination of overexpression, knockdown, and ChIP experiments suggest c-Myb (along with Ebf1) is a direct negative regulator of Foxo1, and direct positive regulator of Gfi1b. Together these activities result in the reduced Foxo1 protein levels observed in c-Myb-overexpressing cell lines compared to control cell lines (Figure 3.4B, VEC versus WT). Because the M303V mutation clearly impairs the ability of c-Myb to repress Foxo1 (Figure 3.4B, WT versus M303V) but does not affect c-Myb binding to elements in the *Foxo1* and *Gfi1b* loci (Figure 3.5), this suggests the M303V mutation prevents c-Myb from interacting with and recruiting coactivators and corepressors to the *Foxo1* and *Gfi1b* loci to achieve repression or activation. Whether p300 is one such cofactor remains to be definitively shown (see discussion below).

M303V c-Myb possesses some repressive activity despite its inability to repress Foxo1 expression (Figure 3.4A, Figure 3.6A). Interestingly we found that like WT c-Myb, the

M303V c-Myb mutant can antagonize Foxo1 binding to the *Rag* locus, as reduced Foxo1 binding to the E*rag* enhancer upon STI treatment is observed in both WT and M303V c-Myb-overexpressing cells compared to control cells (Figure 3.6B). Given we can detect binding of both WT and M303V c-Myb to E*rag* by ChIP (Figure 3.7), we believe the mutant protein retains the ability to directly repress *Rag*, providing an explanation for its residual repressive activity. Moreover, these experiments reveal a distinct mode of direct *Rag* repression by WT c-Myb, as without them we would have attributed the reduced Foxo1 binding to E*rag* in WT c-Myb-overexpressing cells simply to be a consequence of reduced Foxo1 levels alone.

The mechanism of direct *Rag* repression by c-Myb binding to E*rag* could be through the recruitment of corepressors, whose interaction is not perturbed by the M303V mutation, that modify chromatin and make the region inaccessible to Foxo1. When we targeted a transcriptional repressor to c-Myb binding sites adjacent the previously identified consensus Foxo1 site in the E*rag* enhancer that is strongly bound by Foxo1 upon pre-B cell differentiation (Ochiai et al., 2012), we observed strong *Rag* repression (Figure 3.8). Thus binding these sites and recruiting corepressors such as histone deacetylases (Nomura et al., 2004, Zhao et al., 2012) is a plausible mechanism by which c-Myb could achieve *Rag* repression through the E*rag* enhancer.

Alternatively, direct repression by c-Myb could be achieved independent of corepressor recruitment through occupying E*rag* sites and sterically inhibiting Foxo1 binding. To test this, one could target sgRNA/dCas9 complexes lacking corepressor recruitment ability to the c-Myb binding sites in E*rag* in an experiment similar to that shown in Figure 3.8. If this complex can sterically hinder the binding of Foxo1 to E*rag*,, it would suggest that c-Myb binding alone is sufficient for *Rag* repression. Our results strongly suggest that Foxo1 binding to this site is crucial for *Rag* expression (Figure 3.8), supporting previous work from our lab that *Rag* transcription in AMuLV cells is Foxo1-dependent (Chow et al., 2013). However more work is necessary to fully understand the interplay between Foxo1 and c-Myb at E*rag* and its importance in the regulation of *Rag* expression.

The experiments performed raise interesting questions about Foxo1 binding kinetics and how they are regulated during pre-B cell differentiation. Despite the difference in Foxo1 expression between the WT and M303V cells (Figure 3.4B), similar Foxo1 ChIP signals are observed at E*rag* (Figure 3.6B). A long formaldehyde crosslinking time (10 minutes) was used in the ChIP procedure. Thus, even though concentrations of DNA-binding competent Foxo1 may differ between WT and M303V cells, this long crosslinking period could allow capture of a similar number of Foxo1/E*rag* complexes between the two population of cells as studies have suggested that formaldehyde addition does not affect the ability of unbound transcription factors to bind target sites (Poorey et al., 2013).

Additionally, while the WT and M303V cell lines display similar levels of Foxo1 occupancy at the E*rag* enhancer upon STI treatment (Figure 3.6B), they have different levels of *Rag1*-GFP expression (Figure 3.6A). One explanation might be that the off-rate for Foxo1 in the Foxo1/E*rag* complex might be lower in the M303V cells versus WT cells, allowing for more stable Foxo1/enhancer complex formation and thus more rounds of *Rag* transcriptional

initiation in these cells. Such a difference in off-rate would not be detected by ChIP occupancy measurements (Poorey et al., 2013). An alternative explanation is that WT but not M303V c-Myb may perturb the binding of additional activators to the *Rag* locus upon STI treatment, resulting in stronger *Rag* repression in WT but not M303V-overexpressing cells.

Mutational studies identified residues within an amphipathic helix in the transactivation domain of c-Myb necessary for interaction with the KIX domain of the coactivators CBP and p300 (Parker et al., 1999). Given its proximity to these residues, characterization of the M303V mutation focused on c-Myb interaction with p300, which was shown to be disrupted by the mutation (Sandberg et al., 2005). This led the authors to conclude that the defects in B cell development and other aspects of hematopoiesis in *c-Myb*$^{M303V/M303V}$ mice were due to the disruption of c-Myb/p300 interactions, although a formal connection between p300 and the development defects was not shown. However, previous work with mice homozygous for mutations in the KIX domain of p300 (but not CBP) that disrupt interaction with c-Myb caused similar defects in both B cell development and hematopoiesis (Kasper et al., 2002), though it is unclear if disruption of other interactions affected by the KIX mutations (ex. p300/CREB) contributed to the phenotype.

More recent experiments with one of the originally described c-Myb mutants (L302A) revealed that in the context of myeloid differentiation, this mutation affects the ability of c-Myb to both activate and repress target genes (Zhao et al., 2011). Further support that c-Myb and p300 cooperate for repression came in a study showing p300 and CBP KIX domain mutations affect the ability of c-Myb to both activate and repress genes in MEFs and T cells (Kasper et al., 2013). While we attempted to formally establish a role for p300 in gene repression in our system, overexpression and knockdown of p300 in AMuLV B cells failed to show any conclusive effect on *Rag* transcription (unpublished observations). Moreover, p300 ChIP experiments showed a direct correlation between p300 occupancy at E*rag* and *Rag* expression (Figure 3.9), and no perturbation of p300 binding was observed upon c-Myb overexpression (Figure 3.10). Thus if c-Myb and p300 are cooperating for *Rag* repression in AMuLV cells, our experiments suggest repression is not achieved through c-Myb-dependent recruitment of p300 to the E*rag* enhancer. Alternatively, none of the aforementioned studies investigated if the M303V mutation disrupts c-Myb interaction with other proteins. Thus it is possible the M303V mutation impairs the ability of c-Myb to repress *Rag* transcription through disrupting interactions with a novel corepressor. Coimmunoprecipitation and mass spectrometry experiments could be used to identify differential interacting proteins between WT c-Myb and the M303V mutant and generate a list of candidates that could be tested for a potential role in *Rag* repression.

M303V c-Myb failed to rescue cell survival upon deletion of endogenous c-Myb in an AMuLV B cell line with floxed c-Myb alleles (unpublished observations). In the context of B cell development, the failure of rescue is consistent with the observation that *c-Myb*$^{M303V/M303V}$ mice completely lack cells in the large cycling pre-B cell/Hardy Fraction C' compartment (Sandberg et al., 2005). Thus besides *Rag* repression, c-Myb and its M303-dependent activities play a crucial role in directing the gene expression program required for the survival and clonal expansion of B cell progenitors. In the context of leukemic

transformation, the rescue failure suggests that the M303-dependent activities of c-Myb are required for maintaining the AMuLV-transformed state. Previous studies have described the need for c-Myb in transformation by ABL oncogenes (Lidonnici et al., 2008) and implicated c-Myb as a therapeutic target in cancers including pre-B cell Acute Lymphoblastic Leukemia (ALL) (Waldron et al., 2012, Sarvaiya et al., 2012). Identifying more genes regulated in an M303-dependent matter, and all of the protein-protein interactions mediated by M303, will reveal important insight into the role of c-Myb in oncogenic transformation and identify additional therapeutic targets.

Materials and Methods

Cell culture and chemicals

AMuLV-transformed B cells were cultured in RPMI 1640 (Gibco) supplemented with 5% vol/vol FCS (Gemini), 100 mg/mL penicillin and streptomycin (Gibco), and 55nM 2-mercaptoethanol (Gibco). GP2 retroviral packaging cells were cultured in DMEM (Gibco) supplemented with 5% vol/vol FCS, 100 mg/mL penicillin and streptomycin, and 1mM sodium pyruvate (Gibco). All cells were grown at 37°C in 5% CO_2. STI-571 (Novartis) was used at a final concentration of 2.5 uM for 16-20h in all experiments.

Retroviral expression plasmids

MSCV-based cDNA retroviral expression constructs were previously described(Amin and Schlissel., 2008). Murine c-Myb transcript variant 2 (NM_010848.3) ORF was PCR-amplified from a primary B cell cDNA library with Platinum Pfx DNA Polymerase (Invitrogen) and cloned into a multiple cloning site (MCS) upstream of an internal ribosome entry site (IRES). This IRES is followed by coding sequence for human CD4 (hCD4) cell surface protein to mark infected cells.

M303V c-Myb mutant was created by cloning WT c-Myb into pBSK plasmid. Mutagenesis was then performed using QuickChange Multi Site-Directed Mutagenesis kit (Agilent) according to manufacture's instructions and the following mutagenesis primer: 5'-GCTGGAGTTGCTCCTGGTGTCAACAGAGAACGA-3'.

C-terminal 3XFLAG-tagged WT c-Myb and M303V c-Myb constructs were created by PCR amplifying the ORFs lacking an stop codon and cloning them upstream of a 3XFLAG sequence inserted into the MCS of CMSCV IRES hCD4.

Retrovirus production and infection

GP2 packaging cells were transfected with a 5:3 ratio of retroviral:VSVG plasmids using Lipofectamine 2000 (Invitrogen) and placed at 37°C. Cells were moved to 32°C at 24h. At 48h, retroviral supernatant was collected and concentrated (1.5 h, 16,800g, 4°C) using a SW 41 Ti rotor and L8-M ultracentrifuge (Beckman). Retroviral pellets were resuspended in media supplemented with 4 ug/mL polybrene (Sigma-Aldrich). Target cells were cultured in concentrated retrovirus at 32°C for 24h, and then moved to 37°C and expanded. Analysis and sorting were performed 2-4 days post-infection.

Cell sorting and flow cytometry

Single-cell suspensions were prepared and when necessary, cells were labeled with anti-hCD4 PE-conjugated antibody (eBioscience) using standard techniques. A FC500 (Beckman Coulter) or LSRII (BD Biosciences) flow cytometer was used for analysis, while a MoFlo or Influx cell sorter (Dako-Cytomation) was used for sorting. Data were analyzed with FlowJo software (Tree Star).

sgRNA/dCas9-KRAB E*rag* targeting

Small guide RNAs were designed using the MIT CRISPR Design Tool (http://crispr.mit.edu/) and custom oligos ordered from Integrated DNA Technologies. Oligos were annealed and

directionally cloned into the BsmBI site of a modified PiggyBac dual expression vector downstream of a U6 promoter and upstream of an EF1α promoter driving expression of a catalytically inactive *S. pyogenes* Cas9 (dCas9) KRAB fusion protein. Individual sgRNA/dCas9-KRAB constructs were co-transfected with Super PiggyBac transposase expression vector using Lipofectamine 2000 (Invitrogen) and cells were G418 selected (800 ug/mL) for approximately 2 weeks to generate stable sgRNA/dCas9-KRAB-expressing cell lines. sgRNA oligos were as follows (top and bottom oligos for each site shown 5' to 3'):

c-Myb site 1
CACCGCGTTTCCAACTTCCTCCAGC
AAACGCTGGAGGAAGTTGGAAACGC

c-Myb site 2
CACCGATCGCCTGCTGGAGGAAGT
AAACACTTCCTCCAGCAGGCGATC

c-Myb site 3
CACCGCAACTGGCAGATCGCCTGC
AAACGCAGGCGATCTGCCAGTTGC

Foxo1 site
CACCGTCAAAACAATGCTAAGCCCT
AAACAGGGCTTAGCATTGTTTTGAC

c-Myb site 4
CACCGTCGACAGAAAATAACTGCGC
AAACGCGCAGTTATTTTCTGTCGAC

Immunoblot
Cells were lysed in RIPA buffer supplemented with Complete Protease Inhibitor Cocktail (Roche). Cell debris was cleared by centrifugation and soluble protein quantified with Bradford Reagent (Bio-Rad). Laemmli SDS loading buffer was added to 20ug of protein per sample prior to separation on 8% SDS-PAGE gels. Following transfer to Immobilon-FL PVDF (Millipore) or Protran BA85 nitrocellulose (GE Whatman) membranes and blocking with 5% vol/vol milk/PBS solution, blots were probed with primary and secondary antibodies and analyzed with the Odyssey Infrared Imaging System (LI-COR Biosciences). Primary antibodies used: anti-Myb (Millipore 05-175), anti-Foxo1 (Cell Signaling L27), anti-Lamin B1 (Abcam ab16048), and anti-FLAG M2 (Sigma-Aldrich). Infrared dye–conjugated secondary antibodies were from Molecular Probes–Invitrogen.

Chromatin immunoprecipitation
Chromatin immunoprecipitation (ChIP) was performed as previously described (Lee et al., 2006). Briefly, approximately 100 million cells per experimental condition were harvested, fixed, lysed, and sonicated using a Covaris S220 ultrasonicator. Following centrifugation to remove insoluble material, chromatin was quantified and equal amounts used in experimental and control immunoprecipitations. 5mg of anti-FLAG M2 (Sigma-Aldrich),

anti-Foxo1 (Abcam ab70382), anti-p300 (Santa Cruz SC-585 X), or IgG control antibodies (GeneScript) were conjugated to Protein G Dynabeads (Invitrogen) and added to samples. Following overnight immunoprecipitation, beads were collected and washed three times with low salt buffer (0.1% SDS, 1% Triton X-100, 2 mM EDTA, 20 mM Tris pH 8.1, 150 mM NaCl), once with high salt buffer (0.1% SDS, 1% Triton X-100, 2 mM EDTA, 20 mM Tris pH 8.1, 500 mM NaCl), once with LiCl buffer (250 mM LiCl, 1% NP40, 1% sodium deoxycholate, 1 mM EDTA, 10 mM Tris pH 8.1) and twice with TE buffer. DNA-protein complexes were eluted from beads with TE elution buffer (TE w/ 1% SDS), and crosslinks reversed overnight at 65°C. Following RNAse A (Fermentas) and Proteinase K (Invitrogen) treatment, chromatin was isolated using QIAquick columns (Quiagen) and subjected to qPCR analysis (see below).

Quantitative realtime PCR (qPCR)

Quantitative realtime PCR was carried out on an Applied Biosystems 7300 thermocycler using SYBR Select Master Mix (Applied Biosystems). PCR conditions were as follows: 50°C 2 min, 95°C 10 min, 40 cycles of 95°C 15s, 60°C 1 min. For ChIP qPCR, data is presented as a percentage of ChIP input. Error bars on all ChIP qPCR plots represent the standard deviation of triplicate qPCR assays. ChIP primer sequences were as follows (forward and reverse primers for each site shown 5' to 3'):

P*foxo1*	GAAAAATACCCCACCGCCCC	AATGGACGCGCGAAGTCTC
I*foxo1* A	CTCCCTGTGCCTTTTTAGCC	CTTCGACATTGTTCGTGGCG
I*foxo1* B	TCCACCTTGGAGGAAATAAGGC	GGAAGCTAGACACGCCAAGT
P*gfi1b*	GGGAGCTGTCCCTCTTCTGA	CTCATAACGTTGACCGAGCC
E*rag*	CGTTTCCAACTTCCTCCAGC	GCCCTGCGCAGTTATTTTCT
Pb*rag1*	GGAAGTTTAGCTGGGGGACC	CCACCGTAGGCATTCTCAGG
control	CTCTGTATAGCCCTGGCTGTCCAG	TGAAGCCGGGCAGTGGTG

References

Amin, R.H., and M.S. Schlissel. 2008. Foxo1 directly regulates the transcription of recombination-activating genes during B cell development. *Nat. Immunol.* 9:613-622.

Chow, K.T., G.A. Timblin, S.M. McWhirter, and M.S. Schlissel. 2013. MK5 activates Rag transcription via Foxo1 in developing B cells. *J. Exp. Med.* 210:1621-1634.

Dengler, H.S., G.V. Baracho, S.A. Omori, S. Bruckner, K.C. Arden, D.H. Castrillon, R.A. DePinho, and R.C. Rickert. 2008. Distinct functions for the transcription factor Foxo1 at various stages of B cell differentiation. *Nat. Immunol.* 9:1388-1398.

Fahl, S.P., R.B. Crittenden, D. Allman, and T.P. Bender. 2009. c-Myb is required for pro-B cell differentiation. *J. Immunol.* 183:5582-5592.

Gilbert, L.A., M.H. Larson, L. Morsut, Z. Liu, G.A. Brar, S.E. Torres, N. Stern-Ginossar, O. Brandman, E.H. Whitehead, J.A. Doudna, W.A. Lim, J.S. Weissman, and L.S. Qi. 2013. CRISPR-mediated modular RNA-guided regulation of transcription in eukaryotes. *Cell* 154:442-451.

Grawunder, U., T.M. Leu, D.G. Schatz, A. Werner, A.G. Rolink, F. Melchers, and T.H. Winkler. 1995. Down-regulation of RAG1 and RAG2 gene expression in preB cells after functional immunoglobulin heavy chain rearrangement. *Immunity* 3:601-608.

Greig, K.T., C.A. de Graaf, J.M. Murphy, M.R. Carpinelli, S.H. Pang, J. Frampton, B.T. Kile, D.J. Hilton, and S.L. Nutt. 2010. Critical roles for c-Myb in lymphoid priming and early B-cell development. *Blood* 115:2796-2805.

Gyory, I., S. Boller, R. Nechanitzky, E. Mandel, S. Pott, E. Liu, and R. Grosschedl. 2012. Transcription factor Ebf1 regulates differentiation stage-specific signaling, proliferation, and survival of B cells. *Genes Dev.* 26:668-682.

Heintzman, N.D., R.K. Stuart, G. Hon, Y. Fu, C.W. Ching, R.D. Hawkins, L.O. Barrera, S. Van Calcar, C. Qu, K.A. Ching, W. Wang, Z. Weng, R.D. Green, G.E. Crawford, and B. Ren. 2007. Distinct and predictive chromatin signatures of transcriptional promoters and enhancers in the human genome. *Nat. Genet.* 39:311-318.

Hsu, L.Y., J. Lauring, H.E. Liang, S. Greenbaum, D. Cado, Y. Zhuang, and M.S. Schlissel. 2003. A conserved transcriptional enhancer regulates RAG gene expression in developing B cells. *Immunity* 19:105-117.

Kasper, L.H., F. Boussouar, P.A. Ney, C.W. Jackson, J. Rehg, J.M. van Deursen, and P.K. Brindle. 2002. A transcription-factor-binding surface of coactivator p300 is required for haematopoiesis. *Nature* 419:738-743.

Kasper, L.H., T. Fukuyama, S. Lerach, Y. Chang, W. Xu, S. Wu, K.L. Boyd, and P.K. Brindle. 2013. Genetic interaction between mutations in c-Myb and the KIX domains of CBP and p300 affects multiple blood cell lineages and influences both gene activation and repression. *PLoS One* 8:e82684.

Kuppers, R., and R. Dalla-Favera. 2001. Mechanisms of chromosomal translocations in B cell lymphomas. *Oncogene* 20:5580-5594.

Kuwata, N., H. Igarashi, T. Ohmura, S. Aizawa, and N. Sakaguchi. 1999. Cutting edge: absence of expression of RAG1 in peritoneal B-1 cells detected by knocking into RAG1 locus with green fluorescent protein gene. *J. Immunol.* 163:6355-6359.

Lee, G.S., M.B. Neiditch, S.S. Salus, and D.B. Roth. 2004. RAG proteins shepherd double-strand breaks to a specific pathway, suppressing error-prone repair, but RAG nicking initiates homologous recombination. *Cell* 117:171-184.

Lee, T.I., S.E. Johnstone, and R.A. Young. 2006. Chromatin immunoprecipitation and microarray-based analysis of protein location. *Nat. Protoc.* 1:729-748.

Li, Z., D.I. Dordai, J. Lee, and S. Desiderio. 1996. A conserved degradation signal regulates RAG-2 accumulation during cell division and links V(D)J recombination to the cell cycle. *Immunity* 5:575-589.

Lidonnici, M.R., F. Corradini, T. Waldron, T.P. Bender, and B. Calabretta. 2008. Requirement of c-Myb for p210(BCR/ABL)-dependent transformation of hematopoietic progenitors and leukemogenesis. *Blood* 111:4771-4779.

Muljo, S.A., and M.S. Schlissel. 2003. A small molecule Abl kinase inhibitor induces differentiation of Abelson virus-transformed pre-B cell lines. *Nat. Immunol.* 4:31-37.

Nomura, T., J. Tanikawa, H. Akimaru, C. Kanei-Ishii, E. Ichikawa-Iwata, M.M. Khan, H. Ito, and S. Ishii. 2004. Oncogenic activation of c-Myb correlates with a loss of negative regulation by TIF1beta and Ski. *J. Biol. Chem.* 279:16715-16726.

Ochiai, K., M. Maienschein-Cline, M. Mandal, J.R. Triggs, E. Bertolino, R. Sciammas, A.R. Dinner, M.R. Clark, and H. Singh. 2012. A self-reinforcing regulatory network triggered by limiting IL-7 activates pre-BCR signaling and differentiation. *Nat. Immunol.* 13:300-307.

Parker, D., M. Rivera, T. Zor, A. Henrion-Caude, I. Radhakrishnan, A. Kumar, L.H. Shapiro, P.E. Wright, M. Montminy, and P.K. Brindle. 1999. Role of secondary structure in discrimination between constitutive and inducible activators. *Mol. Cell. Biol.* 19:5601-5607.

Poorey, K., R. Viswanathan, M.N. Carver, T.S. Karpova, S.M. Cirimotich, J.G. McNally, S. Bekiranov, and D.T. Auble. 2013. Measuring chromatin interaction dynamics on the second time scale at single-copy genes. *Science* 342:369-372.

Sandberg, M.L., S.E. Sutton, M.T. Pletcher, T. Wiltshire, L.M. Tarantino, J.B. Hogenesch, and M.P. Cooke. 2005. c-Myb and p300 regulate hematopoietic stem cell proliferation and differentiation. *Dev. Cell.* 8:153-166.

Sarvaiya, P.J., J.R. Schwartz, C.P. Hernandez, P.C. Rodriguez, and W.V. Vedeckis. 2012. Role of c-Myb in the survival of pre B-cell acute lymphoblastic leukemia and leukemogenesis. *Am. J. Hematol.* 87:969-976.

Schatz, D.G., and P.C. Swanson. 2011. V(D)J recombination: mechanisms of initiation. *Annu. Rev. Genet.* 45:167-202.

Schlissel, M.S. 2003. Regulating antigen-receptor gene assembly. *Nat. Rev. Immunol.* 3:890-899.

Schulz, D., L. Vassen, K.T. Chow, S.M. McWhirter, R.H. Amin, T. Moroy, and M.S. Schlissel. 2012. Gfi1b negatively regulates Rag expression directly and via the repression of FoxO1. *J. Exp. Med.* 209:187-199.

Timblin, G.A., and M.S. Schlissel. 2013. Ebf1 and c-Myb repress rag transcription downstream of Stat5 during early B cell development. *J. Immunol.* 191:4676-4687.

Visel, A., M.J. Blow, Z. Li, T. Zhang, J.A. Akiyama, A. Holt, I. Plajzer-Frick, M. Shoukry, C. Wright, F. Chen, V. Afzal, B. Ren, E.M. Rubin, and L.A. Pennacchio. 2009. ChIP-seq accurately predicts tissue-specific activity of enhancers. *Nature* 457:854-858.

Waldron, T., M. De Dominici, A.R. Soliera, A. Audia, I. Iacobucci, A. Lonetti, G. Martinelli, Y. Zhang, R. Martinez, T. Hyslop, T.P. Bender, and B. Calabretta. 2012. c-Myb and its target Bmi1 are required for p190BCR/ABL leukemogenesis in mouse and human cells. *Leukemia* 26:644-653.

Zhang, L., T.L. Reynolds, X. Shan, and S. Desiderio. 2011. Coupling of V(D)J recombination to the cell cycle suppresses genomic instability and lymphoid tumorigenesis. *Immunity* 34:163-174.

Zhao, H., S. Jin, and A.M. Gewirtz. 2012. The histone acetyltransferase TIP60 interacts with c-Myb and inactivates its transcriptional activity in human leukemia. *J. Biol. Chem.* 287:925-934.

Zhao, L., E.A. Glazov, D.R. Pattabiraman, F. Al-Owaidi, P. Zhang, M.A. Brown, P.J. Leo, and T.J. Gonda. 2011. Integrated genome-wide chromatin occupancy and expression analyses identify key myeloid pro-differentiation transcription factors repressed by Myb. *Nucleic Acids Res.* 39:4664-4679.

Figures

Figure 3.1

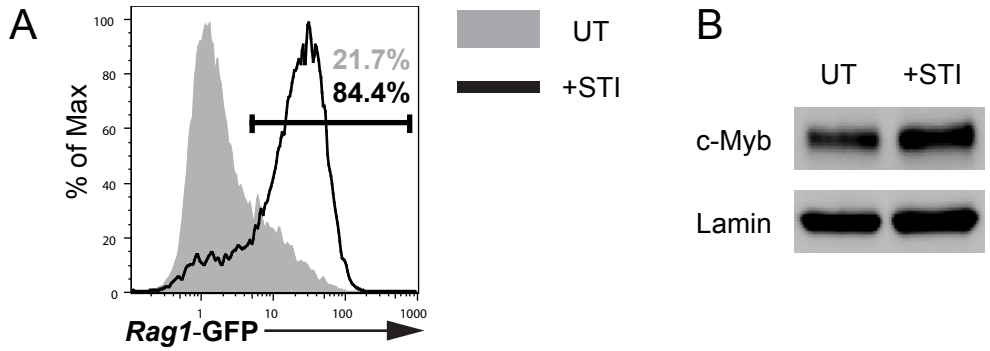

Figure 3.1. c-Myb protein levels are unchanged upon STI-induced differentiation of AMuLV B cells. (A) Flow cytometry analysis of GFP expression in an AMuLV-transformed B cell line generated from heterozygous *Rag1*-GFP knock-in mice, where GFP reports transcription from the endogenous *Rag* locus. Analysis was performed on untreated cells (UT, shaded histogram) or cells treated with STI-571 (+STI, black line). Numbers above gate indicate the percentage of GFP+ untreated cells (top) or STI-treated cells (bottom). **(B)** Immunoblot measuring c-Myb protein levels in UT and +STI cells from **A**. Lamin immunoblot serves as loading control.

Figure 3.2

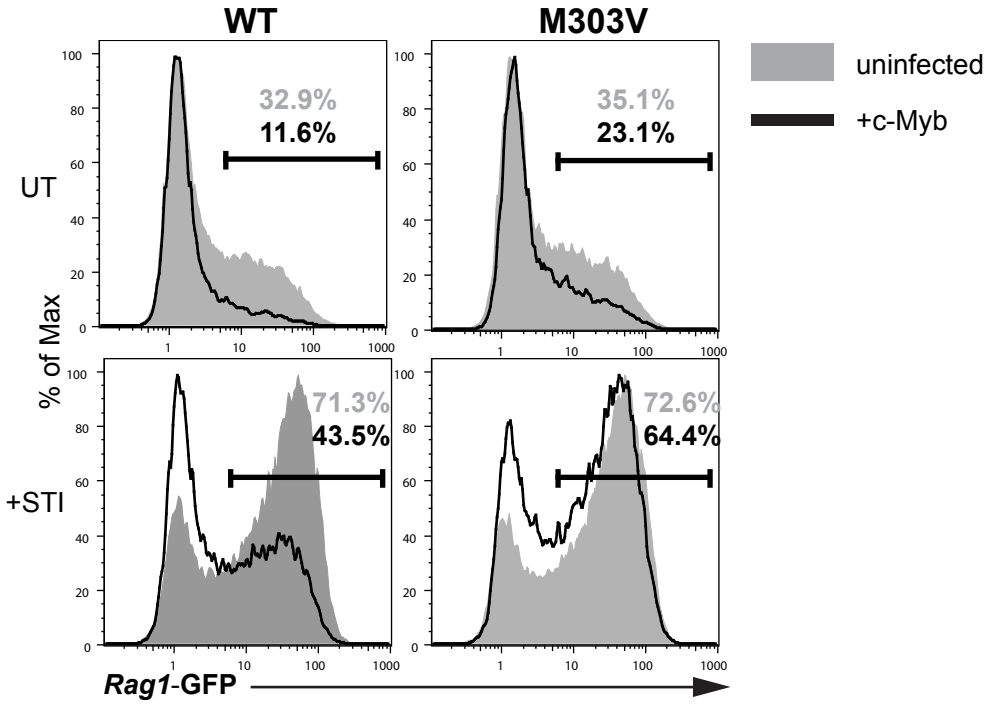

Figure 3.2. M303V mutation impairs ability of c-Myb to repress *Rag* transcription. GFP expression in *Rag1*-GFP reporter cell mixed cultures transduced with WT c-Myb (left column) or M303V c-Myb (right column) retrovirus. Uninfected cells (shaded histogram) were distinguished from transduced cells (black line) in each culture by staining with anti-hCD4 (retroviral marker). Analysis was performed on untreated (UT, top row) and STI-treated (+STI, bottom row) cells. Numbers above gate indicate the percentage of GFP+ uninfected cells (top) or transduced cells (bottom).

Figure 3.3

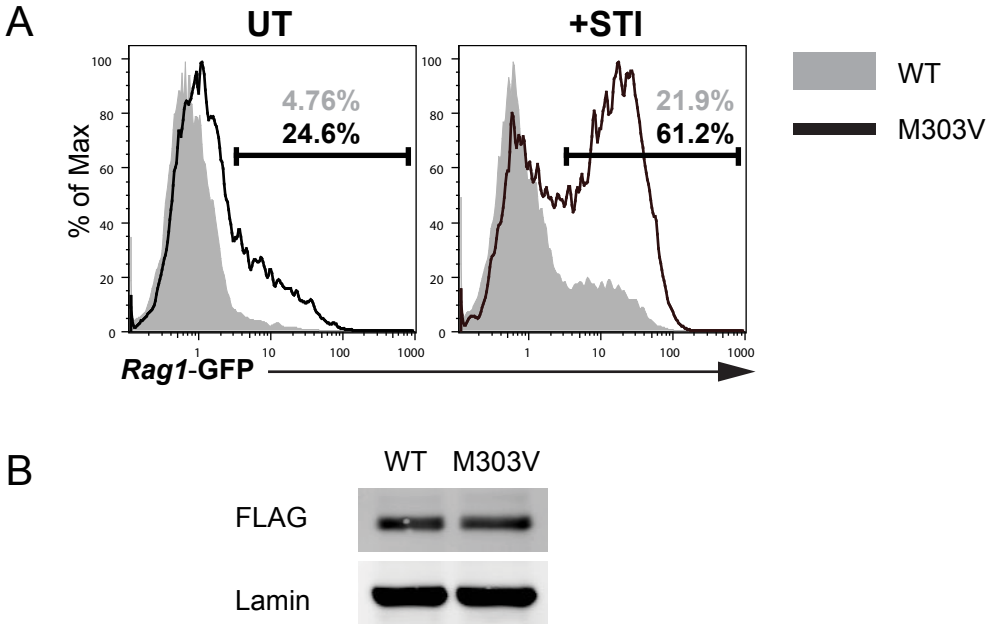

Figure 3.3. Expression levels of WT and M303V c-Myb are similar.
(A) GFP expression in sorted *Rag1*-GFP reporter cells transduced with 3XFLAG WT c-Myb (shaded histogram) or 3XFLAG M303V c-Myb (black line) retrovirus. Analysis was performed on untreated (UT, left) and STI-treated (+STI, right) cells. Numbers above gate indicate the percentage of GFP+ WT-transduced (top) or M303V-transduced (bottom) cells. **(B)** FLAG immunoblot measuring protein levels of 3XFLAG WT c-Myb and 3XFLAG M303V c-Myb in cells from **A**. Lamin immunoblot serves as a loading control.

Figure 3.4

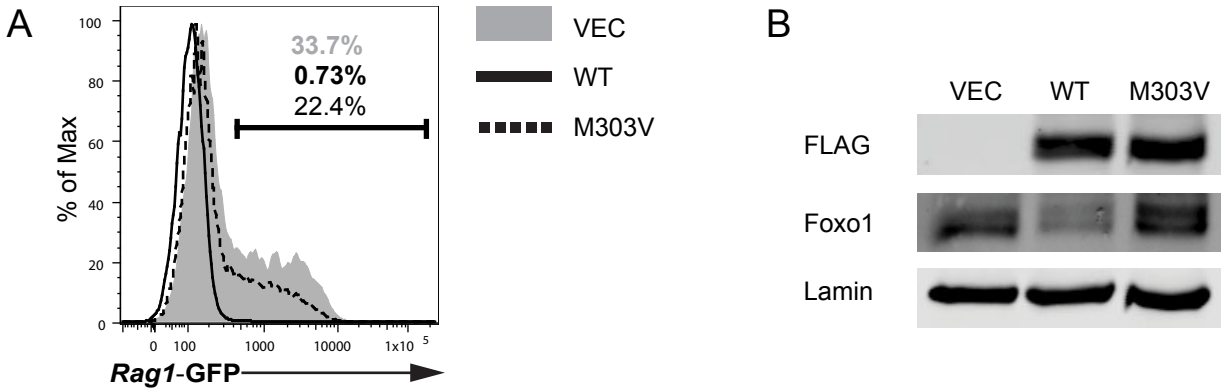

Figure 3.4. M303V c-Myb is defective in repression of Foxo1.
(A) GFP expression in sorted *Rag1*-GFP reporter cells transduced with empty (VEC, shaded histogram), 3XFLAG WT c-Myb (WT, black line), or 3XFLAG M303V c-Myb (M303V, dashed line) retrovirus. Numbers above gate indicate the percentage of GFP+ cells for each respective cell line in the untreated condition. **(B)** Immunoblot measuring Foxo1 protein levels in cell lines from **A**. FLAG immunoblot confirms expression of 3XFLAG-tagged c-Myb proteins. Lamin immunoblot serves as loading control.

Figure 3.5

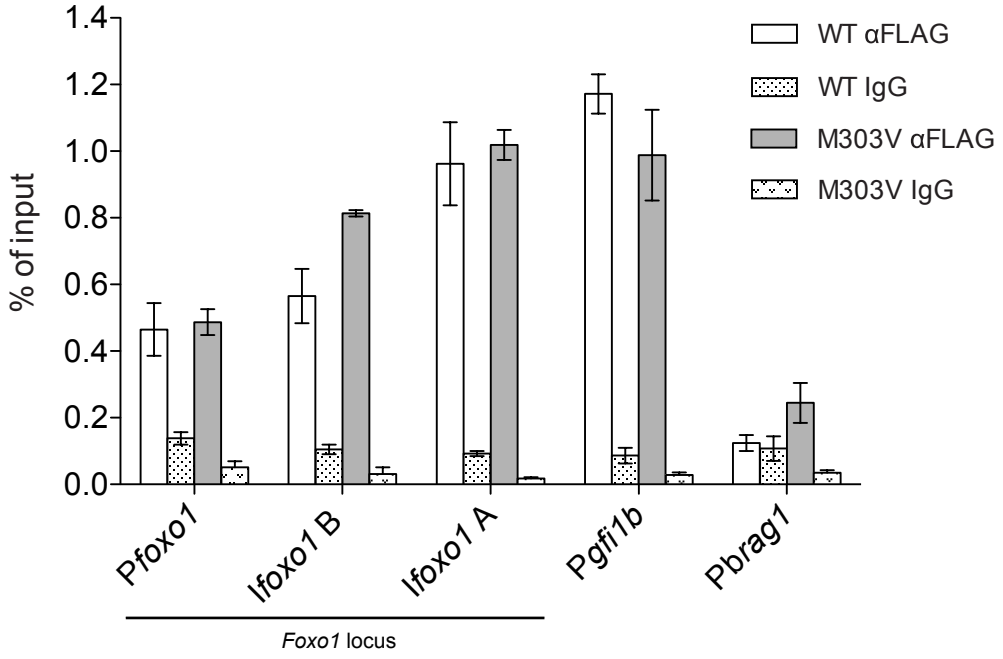

Figure 3.5. Both WT and M303V c-Myb bind regions in the *Foxo1* and *Gfi1b* loci.
ChIP using WT and M303V cell lines from **Figure 3.4A** with anti-FLAG or IgG control antibody. qPCR was performed with recovered chromatin to assess 3XFLAG WT c-Myb and 3XFLAG M303V c-Myb occupancy at regions in the *Foxo1* and *Gfi1b* loci described previously (Timblin and Schlissel., 2013) compared to a negative control region in the *Rag1* promoter.

Figure 3.6

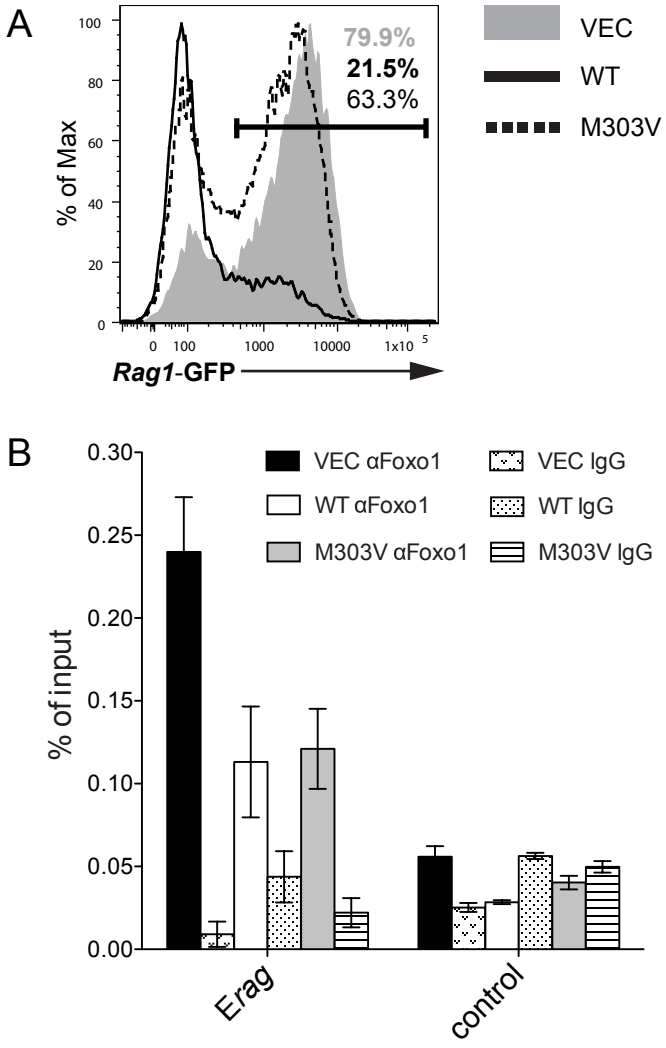

Figure 3.6. M303V c-Myb antagonizes Foxo1 binding to the E*rag* enhancer.
(A) GFP expression in sorted *Rag1*-GFP reporter cells transduced with empty (VEC, shaded histogram), 3XFLAG WT c-Myb (WT, black line), or 3XFLAG M303V c-Myb (M303V, dashed line) retrovirus. Numbers above gate indicate the percentage of GFP+ cells for each respective cell line following STI treatment. **(B)** ChIP using STI-treated cells from **A** with anti-Foxo1 or IgG control antibody. qPCR was performed with recovered chromatin to assess Foxo1 occupancy at the E*rag* enhancer as compared to a negative control region between E*rag* and the *Rag2* promoter.

Figure 3.7

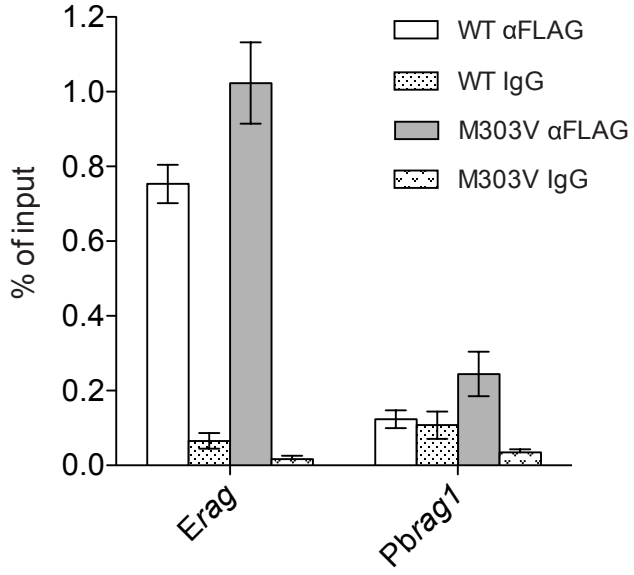

Figure 3.7. Both WT and M303V c-Myb bind the E*rag* enhancer.
ChIP using WT and M303V cell lines with anti-FLAG or IgG control antibody. qPCR was performed with recovered chromatin to assess 3XFLAG WT c-Myb and 3XFLAG M303V c-Myb occupancy at the E*rag* enhancer compared to a negative control region in the *Rag1* promoter.

Figure 3.8

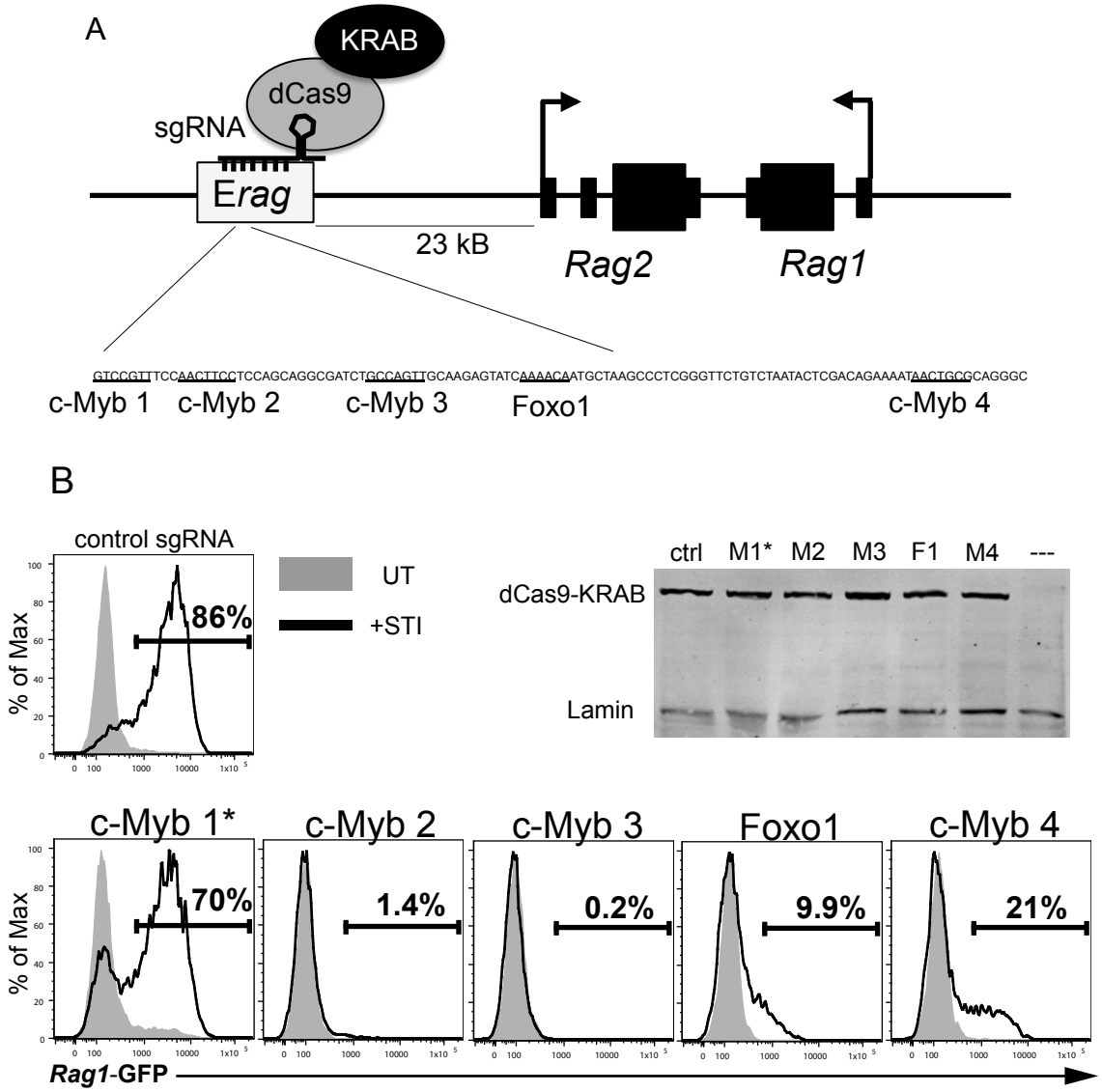

Figure 3.8. Inhibition of Foxo1 binding to E*rag* is sufficient to repress STI-induced *Rag* expression. (A) *Rag* locus schematic showing CRISPR/Cas9 transcriptional interference strategy. A catalytically inactive Cas9 protein fused to the KRAB repressor domain (dCas9-KRAB) was targeted to the E*rag* enhancer through co-expression of custom small guide RNAs (sgRNAs) complementary to sequences within the E*rag* ChIP amplicon analyzed in this study. Sequence of the amplicon is shown with a previously described consensus Foxo1 binding site (Ochiai et al., 2012) and four adjacent c-Myb binding sites (5'-ACCNGNC-3') underlined. **(B)** GFP expression in *Rag1*-GFP reporter cells expressing dCas9-KRAB along with a control sgRNA, or sgRNAs targeting the Foxo1 and c-Myb sites in denoted in **A**. Numbers above gate indicate the percentage of GFP+ cells for each respective cell line following STI treatment. V5 immunoblot with lamin loading control shows dCas9-KRAB expression is similar between the cell lines. (*note: sgRNA targeting the "c-Myb 1" site contains a seed sequence point mutation)

Figure 3.9

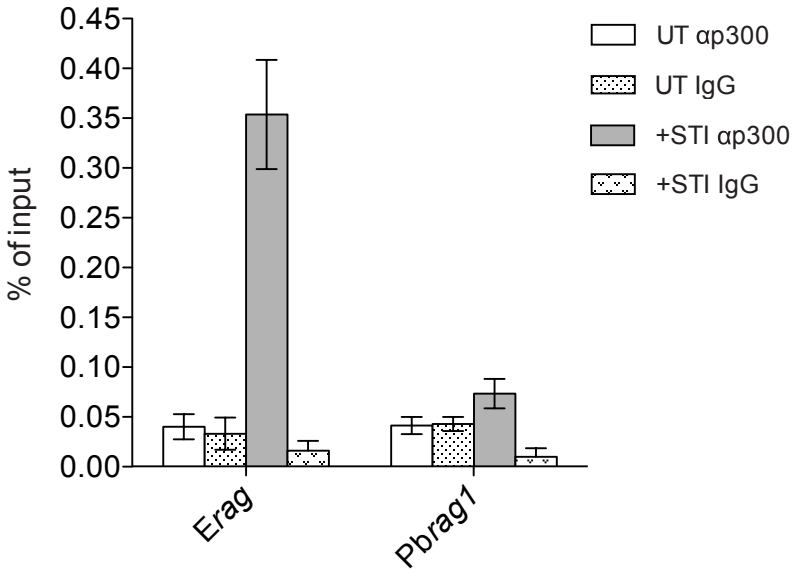

Figure 3.9. p300 binds to E*rag* upon STI-induced differentiation of AMuLV B cells.
ChIP using untreated (UT) and STI-treated (+STI) *Rag1*-GFP reporter cells with anti-p300 or IgG control antibody. qPCR was performed with recovered chromatin to assess p300 occupancy at the E*rag* enhancer compared to a negative control region in the *Rag1* promoter.

Figure 3.10

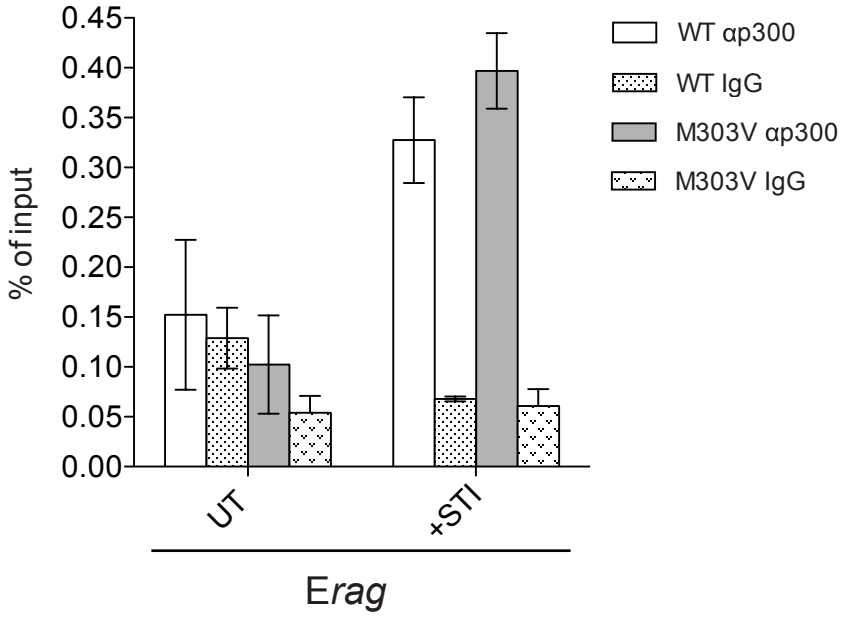

Figure 3.10. c-Myb overexpression does not alter p300 recruitment to the E*rag* enhancer. ChIP using WT and M303V cell lines with anti-p300 or IgG control antibody. qPCR was performed with recovered chromatin to compare p300 occupancy at the E*rag* enhancer in the context of 3XFLAG WT c-Myb overexpression versus 3XFLAG M303V c-Myb overexpression in the both the untreated condition (UT, left) and following STI treatment (+STI, right).

Chapter 4

Using *Rag* expression as a lineage reporter in the reprogramming of fibroblasts to B lymphocytes

Background

The differentiation of stem cells to more mature cell types, such as the differentiation of hematopoietic stem cells (HSCs) to B lymphocytes, has traditionally been viewed as a stringent, highly ordered, non-reversible process. C.H. Waddington's famous "epigenetic landscape" model with a marble atop a hill (representing a stem cell) rolling down one of many grooves in the slope (representing pathways towards different cell fates) suggests that cells are progressively more restricted in the gene expression characteristics they can acquire as they differentiate towards a particular cell fate at the bottom of the hill (Figure 4.1)(Ladewig et al., 2013). Moreover, the model implied that once at the bottom of the hill, it is difficult to go back up the hill and reacquire stem cell characteristics, or move laterally to a different groove and acquire the characteristics of a completely different terminally differentiated cell type. But as early as the 1950s, Gurdon's somatic nuclear transfer (SNCT) experiments showing that all information required for a differentiated cell to reacquire pluripotency were present in its nucleus suggested that cell fate was more plastic and manipulable than implied by Waddington's model (GURDON et al., 1958).

The ability to isolate and culture embryonic stem cells (ESCs) generated excitement in the regenerative medicine field as theoretically these cells could be readily isolated and differentiated to various lineages *in vitro*, and then administered to patients for therapeutic purposes (Thomson et al., 1998). However, ethical concerns over the use of embryos to derive ESC lines prompted scientists to investigate whether there were alternative ways to acquire pluripotent cells for therapeutic use. Experiments showing that fusion between ESCs and terminally differentiated fibroblasts could reprogram somatic nuclei to a pluripotent state suggested that discovering ways to manipulate and alter cell identity could provide a means to generate unlimited numbers of stem cells for regenerative medicine purposes (Cowan et al., 2005).

In 2006, a groundbreaking study by Takahashi and Yamanaka described the reprogramming of terminally differentiated somatic fibroblasts into induced pluripotent stem cells (iPSCs) by defined factors (Takahashi and Yamanaka., 2006). This astonishing breakthrough was achieved by a simple yet elegant approach. The authors transduced fibroblasts with pooled retroviruses expressing 24 different transcription factors, most of which had been described as being essential for pluripotency and/or specifically expressed in ESCs. Cells transduced with a combination of retroviruses that could induce reprogramming were selected on the basis of activation of an *Fbx15* reporter, a gene specifically expressed in ESCs. To identify the factors responsible, subsequent transductions were performed using a "minus one" approach whereby single factors were serially omitted from the retroviral pool, allowing the authors to determine which of the 20 were necessary for generating *Fbx15*-expressing iPSCs. It was ultimately determined that a set of four transcription factors, known as the "Yamanaka Factors", were responsible for iPSC reprogramming: Oct4, Sox2, Klf4, and c-Myc (Figure 4.2).

Soon after the advent of iPSCs, the question was raised as to whether one cell type could be directly reprogrammed (or transdifferentiated) into another without first passing through a pluripotent state (Figure 4.2). In other words, instead of moving Waddington's marble back up the hill and then down a different groove (analogous to creating iPSCs and differentiating them

to a particular cell type), could a cell be coerced to "jump over" one of the grooves on Waddington's hill and acquire a completely different identity (Figure 4.1). Several examples of transdifferentiation between closely related cell types had been previously described: the conversion of fibroblast to myocytes by MyoD (Davis et al., 1987), the conversion of B and T cells to macrophages by C/EPBα (Xie et al., 2004), and the reversion of B cells to macrophages and T cells upon loss of Pax5 (Mikkola et al., 2002). The reprogramming efficiency in these reports was much higher than in iPSC reprogramming, suggesting barriers to reprogramming were lower when converting between closely related cell types. However, it was not known if cells derived from one germ layer could be reprogrammed to cell types derived from another completely different germ layer.

This question was answered as direct reprogramming across lineages was soon described for the transdifferentiation of fibroblasts into neurons, cardiomyocytes, and hepatocytes (Ieda et al., 2010, Vierbuchen et al., 2010, Sekiya and Suzuki., 2011). In each study, the authors achieved reprogramming using a Yamanka-inspired approach: overexpression of defined factors known to be important for the proper development of their cell type of interest in primary fibroblasts, followed by selection of cells induced to undergo reprogramming by monitoring activation of a lineage-specific reporter gene (Figure 4.2).

During the differentiation of B lymphocytes from hematopoietic stem cells (HSCs) in the bone marrow, early B cell progenitors can be identified by the expression of B lineage-specific genes and cell surface markers (Bryder and Sigvardsson., 2010). The recombination activating genes *Rag1* and *Rag2* (collectively referred to as the *Rag* genes), which encode the V(D)J recombinase responsible for antigen receptor gene rearrangement, are among the earliest lineage-specific genes expressed in these cell progenitors (Igarashi et al., 2002). Moreover, *Rag* expression within the B cell progenitor compartment is closely tied with B lineage commitment, as cells with relatively higher levels of *Rag* expression are less amenable to differentiation to alternative (but closely related) cell fates (Mansson et al., 2010).

Based on these observations and the success of the aforementioned direct reprogramming studies, we hypothesized that a combination of defined factors important for proper B cell development could directly reprogram non-lymphoid cells such as fibroblasts into B lymphocytes. We reasoned that activation of the *Rag* locus in a fibroblast by a specific combination of B lineage factors might indicate that particular cell is undergoing a reprogramming event to the B lineage. Thus we set out to screen for factors capable of directly reprogramming fibroblasts to B lymphocytes using *Rag* expression as a marker for reprogramming.

Results

To select for potential reprogramming factors, we reviewed the literature for genes encoding transcription factors for which severe defects in B lymphocyte development arise when their expression is disrupted in mice. 20 factors were chosen (Figure 4.3A) and each was individually cloned into a retroviral vector. Infectious retrovirus for each factor was then prepared, pooled, and used to transduce primary adult ear fibroblasts from heterozygous *Rag1*-GFP mice, which have a GFP cDNA knocked-in to one copy of the endogenous *Rag1* locus (Figure 4.3B) (Kuwata et al., 1999). Following transduction, we detect a very small percentage of *Rag1*-GFP+ cells in fibroblasts transduced with 20 factors (20TF), but not in cells transduced with a random 10 factor control pool (10TF) (Figure 4.4A). To confirm that GFP expression faithfully reported *Rag* transcription in these cells, we sorted GFP+ cells and performed quantitative realtime PCR (qPCR) for *Rag1* mRNA transcripts. We could detect *Rag1* transcripts in the sorted 20TF GFP+ fibroblasts but not in cDNA prepared from the bulk unsorted fibroblasts, confirming that the 20TF GFP+ fibroblasts are *bona fide Rag*-expressing cells (Figure 4.4B).

To determine which of the 20 factors were responsible for inducing *Rag* expression in the rare GFP+ cells, we used the "minus one" approach in which factors were serially removed from the 20TF transduction pool. Reducing the complexity of the pool in this manner increased the percentage of *Rag1*-GFP positive cells generated via mixed retrovirus transduction by roughly an order of magnitude (compare Figure 4.4A 20TF to Figure 4.5 6TF). Moreover, the "minus one" approach revealed factors both inhibitory and essential in the generation GFP+ cells. For example, removal of Ebf1 from the 6TF pool enhanced the percentage of GFP+ cells generated, while removal of Foxo1 from the pool greatly diminished their appearance (Figure 4.5). Ultimately transduction with two factors (2TF - Foxo1 and E47) was found to be most efficient at producing GFP+ *Rag*-expressing cells (Figure 4.6).

Rag expression is not constant throughout B cell development as only bone marrow pro- and pre-B cells undergoing V(D)J recombination express the *Rag* genes. To test the stability of *Rag* expression, we sorted the rare GFP+ cells and expanded them in culture. While sorting did enrich for GFP expression , it was not stable as over time the percentage of GFP+ cells in the sorted cultures was greatly diminished (Figure 4.7).

Given *Rag* expression is transient and represents a only a single B lineage gene, we decided to test if the GFP+ cells also expressed B cell surface markers such as IL7R and CD19. Expression of these B lineage markers could not be detected on either the GFP+ cells or other cells in the 2TF cultures (Figure 4.8). Thus while we had optimized our system for inducing expression of an important B lineage gene in non-lymphoid cells, we failed to detect any evidence of a transdifferentiation event involving activation of multiple B lineage genes occurring in the *Rag*-expressing fibroblasts.

Discussion

Recent studies have shown that direct reprogramming between distantly-related cell types can be achieved through overexpression of lineage-specific transcription factors. This is an exciting advance for the field of regenerative medicine as easily isolated cells such as fibroblasts could be harvested from a patient, directly reprogrammed to different cell types *in vitro*, and readministered to the patient for therapeutic purposes. Such a system could provide an essentially unlimited supply of patient-specific cells for treatment, thus avoiding complications with locating immunocompatible donors. Patients with certain immunodeficiencies, autoimmune disorders, or malignant conditions might benefit from replacement of their B cell repertoire with a healthy population of B cells capable of mediating effective immune responses without contributing to disease. Thus we set out to test if a defined set of transcription factors important for B cell development could directly reprogram fibroblasts to the B lineage, as such a system could provide an unlimited source of patient-specific B lymphocytes.

Given the close ties between *Rag* gene expression and lineage commitment in early B cell progenitors (Igarashi et al., 2002, Mansson et al., 2010), we utilized fibroblast from *Rag1*-GFP reporter mice as the target cell in our system. We reasoned activation that of the *Rag* genes in these non-lymphoid cells upon overexpression of a specific combination of B lineage transcription factors could mark cells undergoing a direct reprogramming event to the B lineage. We were successful inducing *Rag1*-GFP expression in a small number of target fibroblast transduced with our 20TF pool (Figure 4.4). Ultimately we found that transduction with two factors, Foxo1 and E47, was most efficient at generating *Rag1*-GFP+ fibroblasts (Figure 4.6). This is not surprising as both Foxo1 and E47 have been shown to bind the E*rag* enhancer and activate *Rag* transcription during normal B cell development (Hsu et al., 2003, Amin and Schlissel., 2008, Dengler et al., 2008). Although reports of *Rag* expression in non-lymphoid tissues and tumors are somewhat controversial, one such report implicates Foxo1 and E47 in activation of the *Rag* locus in various cancer cell lines (Chen et al., 2011). Our results suggest that Foxo1 and E47 possess pioneer factor activity in that they can bind chromatin in a cellular context where it would be predicted to be closed and recruit factors necessary for transcriptional activation (Zaret and Carroll., 2011). This is consistent with the previously reported ability of E47 to bind and activate transcription at the immunoglobulin loci in non-lymphoid cells, an activity dependent on E47's recruitment of p300 for histone acetylation and the opening of chromatin (Romanow et al., 2000, Sakamoto et al., 2012).

Unfortunately while we optimized our system for the generation of *Rag*-expressing cells, we did not detect activation of additional B lineage genes (Figure 4.8), suggesting we failed to induce global gene expression changes indicative of a direct reprogramming event. It is possible that besides Foxo1 and E47, additional factors may be necessary for inducing a more global B lineage gene expression program in fibroblasts. Such factors might include additional sequence-specific DNA binding transcription factors important for B cell development not included in our original 20TF pool, as the list of such factors is ever-expanding (Kosan et al., 2010, Satoh et al., 2013). Co-expression of components of the ATP-dependent BAF chromatin remodeling complex with the Yamanaka factors was shown to greatly enhance iPSC reprogramming (Singhal et al., 2010). Thus overexpressing more general chromatin remodeling factors along with Foxo1 and E47 in fibroblasts might be helpful in inducing a more global direct reprogramming event.

It is also possible that further manipulating culture conditions will be necessary for inducing reprogramming. Co-culture with bone marrow-derived stromal cells and supplementation with cytokines including Flt3L and IL-7 is necessary for robust differentiation of ESCs to the B lineage (Cho et al., 1999). Thus co-culture of our retrovirally transduced fibroblasts with stromal cells in cytokine-enriched media might provide cell-cell interactions and soluble factors crucial for the induction of reprogramming that were not present in our initial reprogramming attempts.

Previous work suggests addition to cultures of small molecules that influence global chromatin structure might assist in achieving direst reprogramming in our system. Histone deacetylase (HDAC) inhibitors were found to greatly enhance the efficiency of fibroblast-to-iPSC reprogramming, presumably by making chromatin at promoters and enhancers of pluripotency genes more accessible to exogenously introduced factors such as Oct4 and Sox2 during the early stages of reprogramming (Huangfu et al., 2008). While Foxo1 and E47 may be able to bind and activate the *Rag* locus in fibroblasts, perhaps barriers to binding and activating other B lineage genes are too great and could be lowered through use of small molecules.

In conclusion, while we failed to achieve our goal of direct reprogramming fibroblasts to B lymphocytes, we did establish a system in which we could activate a lineage-specific gene crucial for B cell development and function in a relatively robust manner in non-lymphoid cells. This provides a platform to further investigate fibroblast-to-B cell reprogramming through isolation and further manipulation of these cells with additional exogenous factors and refined culture conditions.

Materials and Methods

Cell culture

Primary ear fibroblasts were isolated from 4-6 week old heterozygous *Rag1*-GFP mice as follows. Ear tissue was harvest and incubated 2 h at 37 C in McCoy's serum-free media (Gibco) supplemented with collagenase and pronase (Sigma) according to manufacture's instructions. Digested tissue and cell debris was isolated by centrifugation and plated out in McCoy's supplemented with 10% vol/vol FCS and 2.5 ug/mL Fungizone (Gibco). Media was changed to DMEM (Gibco) supplemented with 10% vol/vol FCS, 100 mg/mL penicillin and streptomycin, and 1mM sodium pyruvate (Gibco), following outgrowth of fibroblast approximately one week after plating of digested tissue. GP2 retroviral packaging cells were cultured in DMEM (Gibco) supplemented with 5% vol/vol FCS, 100 mg/mL penicillin and streptomycin, and 1mM sodium pyruvate (Gibco).

Expression plasmids

MSCV-based cDNA retroviral expression constructs were previously described (Amin and Schlissel., 2008). cDNAs were either isolated by restriction digested from existing plasmids, or PCR-amplified from plasmid templates with Platinum Pfx DNA Polymerase (Invitrogen), and cloned into the multiple cloning site (MCS) lying upstream of an internal ribosome entry site (IRES). This IRES is followed by coding sequence for a human CD4 (hCD4) cell surface protein to mark infected cells. All cDNA open reading frames (ORFs) were sequenced to confirm the absence of mutations.

Retrovirus production and infection

GP2 packaging cells were transfected with a 5:3 ratio of retroviral:VSVG plasmids using Lipofectamine 2000 (Invitrogen) and placed at 37°C. Cells were moved to 32°C at 24 h. At 48 h, retroviral supernatant was collected and concentrated (1.5 h, 16,800g, 4°C) using a SW 41 Ti rotor and L8-M ultracentrifuge (Beckman). Retroviral pellets were resuspended in media supplemented with 4 ug/mL polybrene (Sigma-Aldrich). Target cells were cultured in concentrated retrovirus at 32°C for 24 h, and then moved to 37°C and expanded.

Flow cytometry and cell sorting

Single-cell suspensions were prepared and cells labeled with fluorochrome-conjugated antibodies using standard techniques. A FC500 (Beckman Coulter) or LSRII (BD Biosciences) flow cytometer was used for analysis, while a MoFlo or Influx cell sorter (Dako-Cytomation) was used for sorting. Data were analyzed with FlowJo software (Tree Star).

Anti-hCD4 (RPA-T4) was used to label cells tranduced with retrovirus. Ig2a isotype control (eBM2a), anti-CD127 (A7R34), and anti-CD19 (1D3) antibodies were used in B cell marker staining experiments. Anti-CD19 was obtained from BD Pharmingen, while all other antibodies were purchased from eBiosciences.

Quantitative realtime PCR (qPCR)

GFP+ cells were sorted directly into Trizol LS (Invitrogen). RNA was prepared and reverse transcription performed with MMLV-RT (Invitrogen) using random hexamer priming. Quantitative realtime PCR was carried out on an Applied Biosystems 7300 thermocycler using JumpStart Taq (Sigma) and EvaGreen (Biotium). PCR conditions were as follows: 50°C 2 min, 95°C 10 min, 40 cycles of 95°C 15s, 60°C 1 min. Transcript levels *Rag1* were normalized to *Hprt*. Error bars represent the standard deviation of triplicate qPCR assays. Primer sequences were as follows:

Rag1 F 5'-CATTCTAGCACTCTGGCCGG-3'
Rag1 R 5'-TCATCGGGTGCAGAACTGAA-3'
Hprt F 5'-CTGGTGAAAAGGACCTCTCG-3'
Hprt R 5'-TGAAGTACTCATTATAGTCAAGGCA-3'

References

Amin, R.H., and M.S. Schlissel. 2008. Foxo1 directly regulates the transcription of recombination-activating genes during B cell development. *Nat. Immunol.* 9:613-622.

Bryder, D., and M. Sigvardsson. 2010. Shaping up a lineage--lessons from B lymphopoesis. *Curr. Opin. Immunol.* 22:148-153.

Chen, Z., Y. Xiao, J. Zhang, J. Li, Y. Liu, Y. Zhao, C. Ma, J. Luo, Y. Qiu, G. Huang, C. Korteweg, and J. Gu. 2011. Transcription factors E2A, FOXO1 and FOXP1 regulate recombination activating gene expression in cancer cells. *PLoS One* 6:e20475.

Cho, S.K., T.D. Webber, J.R. Carlyle, T. Nakano, S.M. Lewis, and J.C. Zuniga-Pflucker. 1999. Functional characterization of B lymphocytes generated in vitro from embryonic stem cells. *Proc. Natl. Acad. Sci. U. S. A.* 96:9797-9802.

Cowan, C.A., J. Atienza, D.A. Melton, and K. Eggan. 2005. Nuclear reprogramming of somatic cells after fusion with human embryonic stem cells. *Science* 309:1369-1373.

Davis, R.L., H. Weintraub, and A.B. Lassar. 1987. Expression of a single transfected cDNA converts fibroblasts to myoblasts. *Cell* 51:987-1000.

Dengler, H.S., G.V. Baracho, S.A. Omori, S. Bruckner, K.C. Arden, D.H. Castrillon, R.A. DePinho, and R.C. Rickert. 2008. Distinct functions for the transcription factor Foxo1 at various stages of B cell differentiation. *Nat. Immunol.* 9:1388-1398.

GURDON, J.B., T.R. ELSDALE, and M. FISCHBERG. 1958. Sexually mature individuals of Xenopus laevis from the transplantation of single somatic nuclei. *Nature* 182:64-65.

Hsu, L.Y., J. Lauring, H.E. Liang, S. Greenbaum, D. Cado, Y. Zhuang, and M.S. Schlissel. 2003. A conserved transcriptional enhancer regulates RAG gene expression in developing B cells. *Immunity* 19:105-117.

Huangfu, D., R. Maehr, W. Guo, A. Eijkelenboom, M. Snitow, A.E. Chen, and D.A. Melton. 2008. Induction of pluripotent stem cells by defined factors is greatly improved by small-molecule compounds. *Nat. Biotechnol.* 26:795-797.

Ieda, M., J.D. Fu, P. Delgado-Olguin, V. Vedantham, Y. Hayashi, B.G. Bruneau, and D. Srivastava. 2010. Direct reprogramming of fibroblasts into functional cardiomyocytes by defined factors. *Cell* 142:375-386.

Igarashi, H., S.C. Gregory, T. Yokota, N. Sakaguchi, and P.W. Kincade. 2002. Transcription from the RAG1 locus marks the earliest lymphocyte progenitors in bone marrow. *Immunity* 17:117-130.

Kosan, C., I. Saba, M. Godmann, S. Herold, B. Herkert, M. Eilers, and T. Moroy. 2010. Transcription factor miz-1 is required to regulate interleukin-7 receptor signaling at early commitment stages of B cell differentiation. *Immunity* 33:917-928.

Kuwata, N., H. Igarashi, T. Ohmura, S. Aizawa, and N. Sakaguchi. 1999. Cutting edge: absence of expression of RAG1 in peritoneal B-1 cells detected by knocking into RAG1 locus with green fluorescent protein gene. *J. Immunol.* 163:6355-6359.

Ladewig, J., P. Koch, and O. Brustle. 2013. Leveling Waddington: the emergence of direct programming and the loss of cell fate hierarchies. *Nat. Rev. Mol. Cell Biol.* 14:225-236.

Mansson, R., S. Zandi, E. Welinder, P. Tsapogas, N. Sakaguchi, D. Bryder, and M. Sigvardsson. 2010. Single-cell analysis of the common lymphoid progenitor compartment reveals functional and molecular heterogeneity. *Blood* 115:2601-2609.

Mikkola, I., B. Heavey, M. Horcher, and M. Busslinger. 2002. Reversion of B cell commitment upon loss of Pax5 expression. *Science* 297:110-113.

Romanow, W.J., A.W. Langerak, P. Goebel, I.L.M. Wolvers-Tettero, J.J.M. van Dongen, A.J. Feeney, and C. Murre. 2000. E2A and EBF Act in Synergy with the V(D)J Recombinase to Generate a Diverse Immunoglobulin Repertoire in Nonlymphoid Cells. *Mol. Cell* 5:343-353.

Sakamoto, S., K. Wakae, Y. Anzai, K. Murai, N. Tamaki, M. Miyazaki, K. Miyazaki, W.J. Romanow, T. Ikawa, D. Kitamura, I. Yanagihara, N. Minato, C. Murre, and Y. Agata. 2012. E2A and CBP/p300 act in synergy to promote chromatin accessibility of the immunoglobulin kappa locus. *J. Immunol.* 188:5547-5560.

Satoh, Y., T. Yokota, T. Sudo, M. Kondo, A. Lai, P.W. Kincade, T. Kouro, R. Iida, K. Kokame, T. Miyata, Y. Habuchi, K. Matsui, H. Tanaka, I. Matsumura, K. Oritani, T. Kohwi-Shigematsu, and Y. Kanakura. 2013. The Satb1 protein directs hematopoietic stem cell differentiation toward lymphoid lineages. *Immunity* 38:1105-1115.

Sekiya, S., and A. Suzuki. 2011. Direct conversion of mouse fibroblasts to hepatocyte-like cells by defined factors. *Nature* 475:390-393.

Singhal, N., J. Graumann, G. Wu, M.J. Arauzo-Bravo, D.W. Han, B. Greber, L. Gentile, M. Mann, and H.R. Scholer. 2010. Chromatin-Remodeling Components of the BAF Complex Facilitate Reprogramming. *Cell* 141:943-955.

Takahashi, K., and S. Yamanaka. 2006. Induction of Pluripotent Stem Cells from Mouse Embryonic and Adult Fibroblast Cultures by Defined Factors. *Cell* 126:663-676.

Thomson, J.A., J. Itskovitz-Eldor, S.S. Shapiro, M.A. Waknitz, J.J. Swiergiel, V.S. Marshall, and J.M. Jones. 1998. Embryonic stem cell lines derived from human blastocysts. *Science* 282:1145-1147.

Vierbuchen, T., A. Ostermeier, Z.P. Pang, Y. Kokubu, T.C. Sudhof, and M. Wernig. 2010. Direct conversion of fibroblasts to functional neurons by defined factors. *Nature* 463:1035-1041.

Xie, H., M. Ye, R. Feng, and T. Graf. 2004. Stepwise reprogramming of B cells into macrophages. *Cell* 117:663-676.

Zaret, K.S., and J.S. Carroll. 2011. Pioneer transcription factors: establishing competence for gene expression. *Genes Dev.* 25:2227-2241.

Figures

Figure 4.1

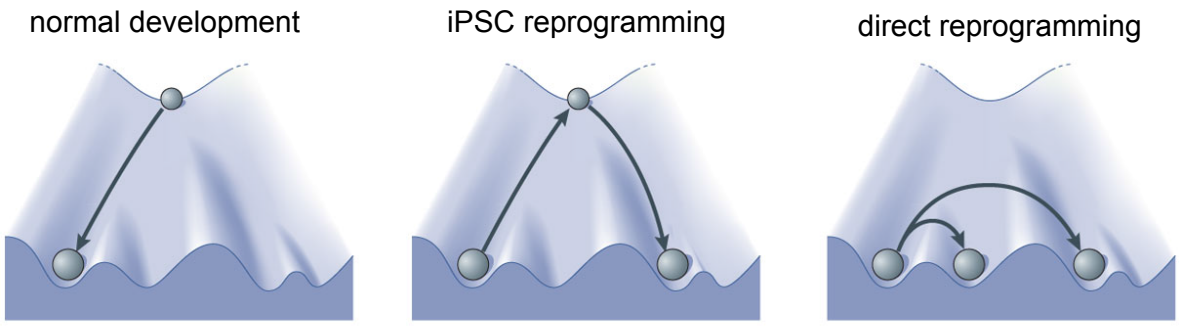

Figure 4.1. Waddington's epigenetic landscape and cellular reprogramming.
C.H. Waddington's epigenetic landscape model used to depict normal development (left), reprogramming of terminally differentiated cells to pluripotency (middle), and direct reprogramming or transdifferentiation (right). Marble at the top of the hill represents a multi- or pluripotent stem cell, while grooves in the slope represent pathways to various terminally differentiated cell fates at the bottom of the hill.

Figure 4.2

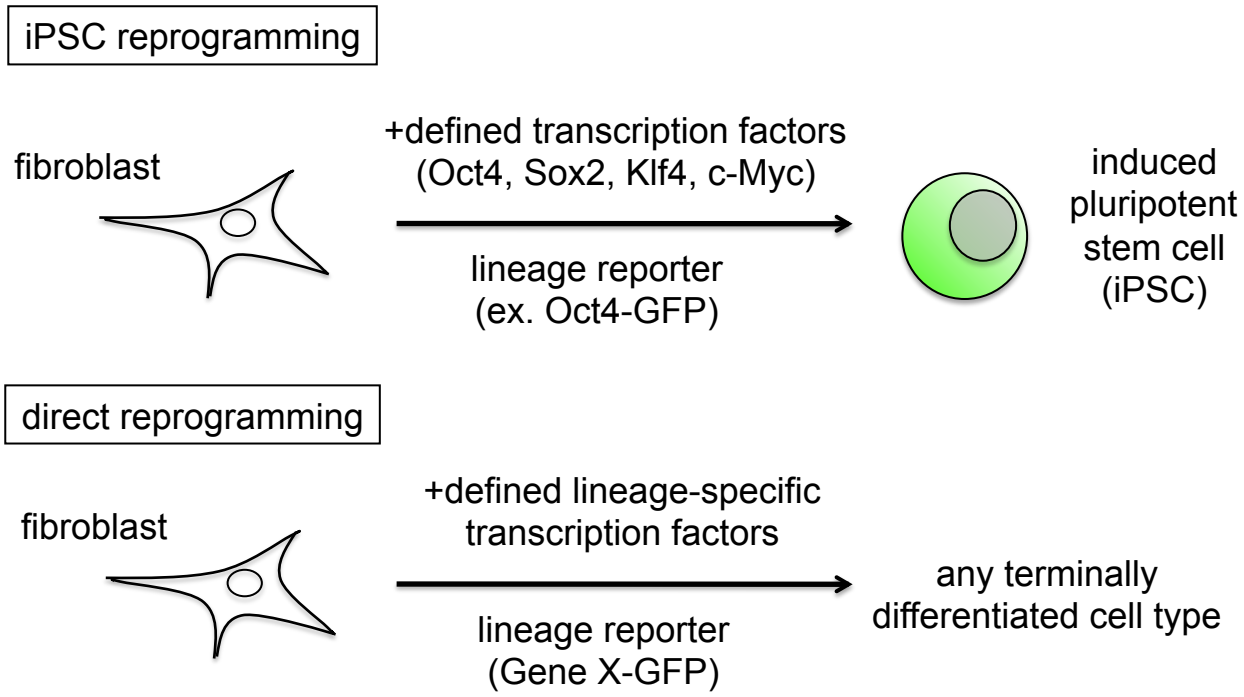

Figure 4.2. Reprogramming to pluripotency versus direct reprogramming.
Strategy used in the reprograming of terminally differentiated fibroblasts to induced pluripotent stem cells (iPSCs) is shown (top). Overexpression of the four Yamanaka Factors is sufficient to achieve reprogramming. Activation of a reporter gene such as Oct4-GFP is used to identify cells undergoing reprogramming to a pluripotent state. This is contrasted with the strategy for direct reprogramming or transdifferentiation (bottom). Instead of reverting fibroblasts to a multi- or pluripotent state, expression of lineage-specific factors in the target fibroblast is used to directly reprogram them to the desired cell type. A reporter for a gene expressed specifically in that cell type is used to identifying cells undergoing transdifferentiation.

Figure 4.3

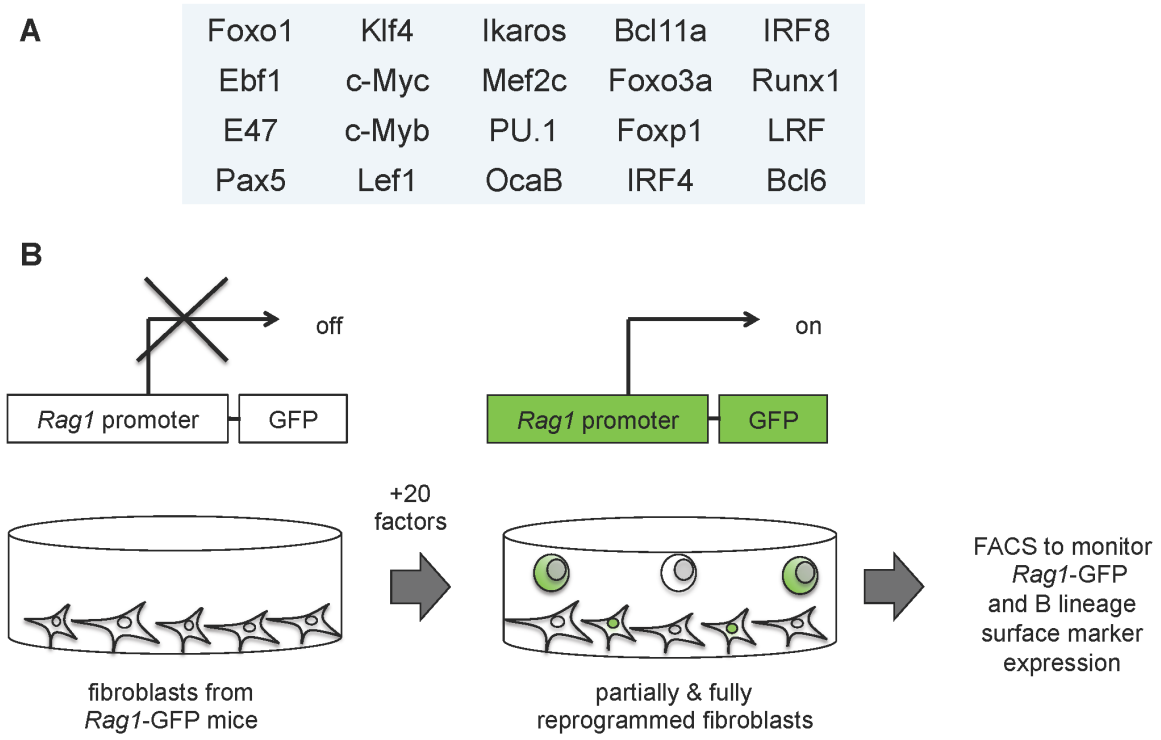

Figure 4.3. Strategy for the direct reprogramming of fibroblasts to B lymphocytes. (A) List of 20 transcription factors important for B cell development that were cloned into retroviruses and used in direct reprogramming experiments. **(B)** Schematic showing strategy for directly reprogramming fibroblasts to B lymphocytes. Infectious retrovirus for each factor in **A** is pooled and used to transduce primary fibroblast from heterozygous *Rag1*-GFP mice, where GFP expression reports transcription from the endogenous *Rag* locus. Flow cytometry is used to monitor *Rag1*-GFP expression and expression of B lineage cell surface markers in the cultures.

Figure 4.4

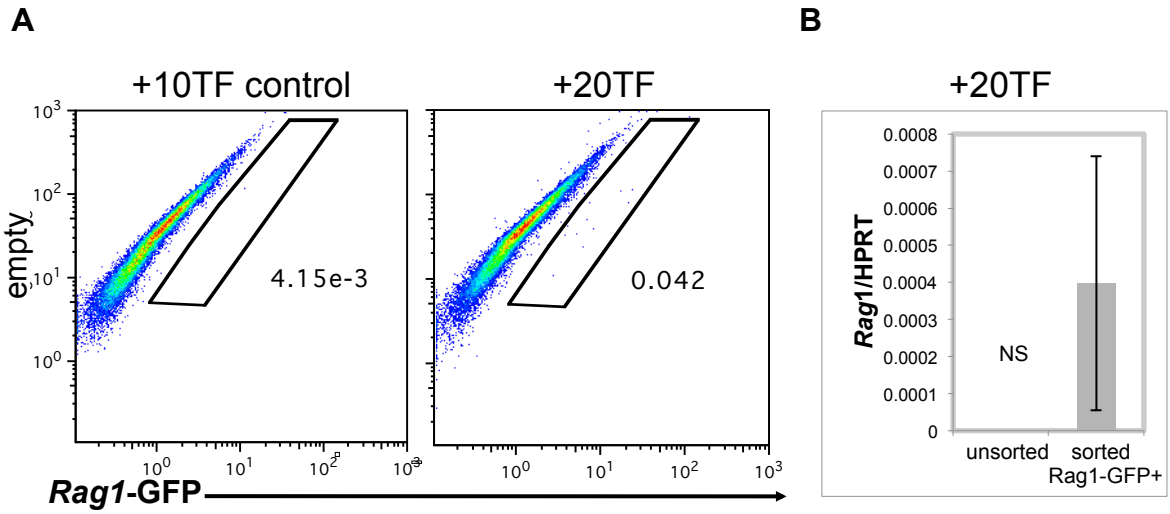

Figure 4.4. Transduction with 20TF pool induces *Rag* expression in fibroblasts.
(A) Flow cytometer analysis of GFP expression in primary *Rag*1-GFP fibroblasts transduced with 20 factor pool (20TF, right) or control 10 factor pool (10TF, left). **(B)** qPCR measuring *Rag1* transcript levels in sorted GFP+ 20TF fibroblast from **A** compared to unsorted cells from the same cultures. "NS" indicates no signal was detected.

Figure 4.5

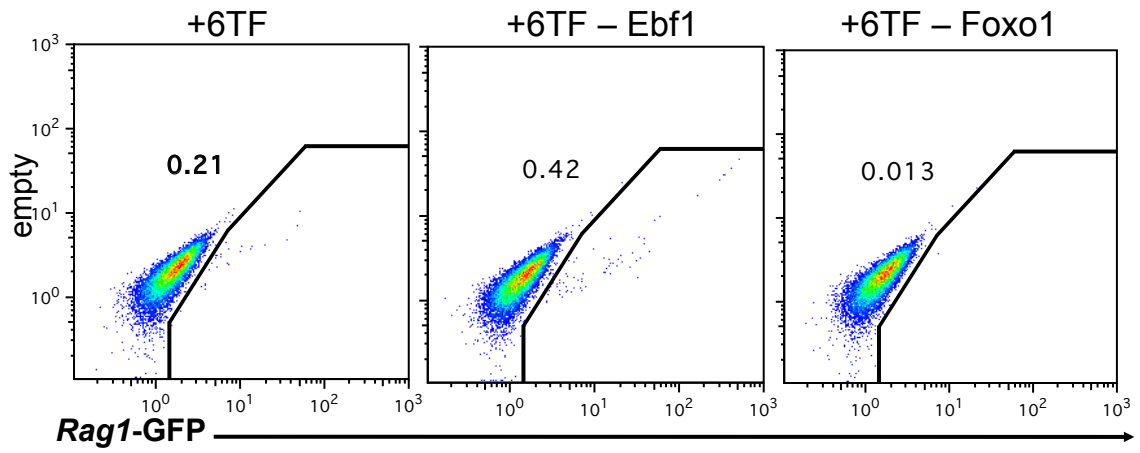

Figure 4.5. "Minus one" experiments reveal factors important for inducing *Rag* expression in fibroblasts. Flow cytometer analysis of GFP expression in primary *Rag*1-GFP fibroblasts transduced with 6 factor pool (6TF), or 6 factor pool with Ebf1 or Foxo1 retroviruses omitted.

Figure 4.6

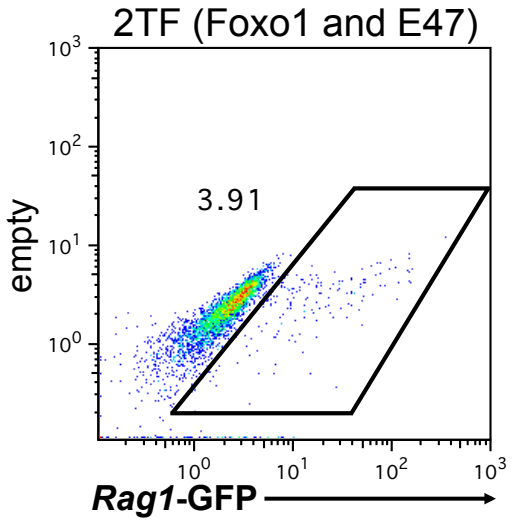

Figure 4.6. Foxo1 and E47 induce robust *Rag* expression in fibroblasts.
Flow cytometer analysis of GFP expression in primary *Rag*1-GFP fibroblasts transduced with mixed Foxo1 and E47 retroviruses (2TF).

Figure 4.7

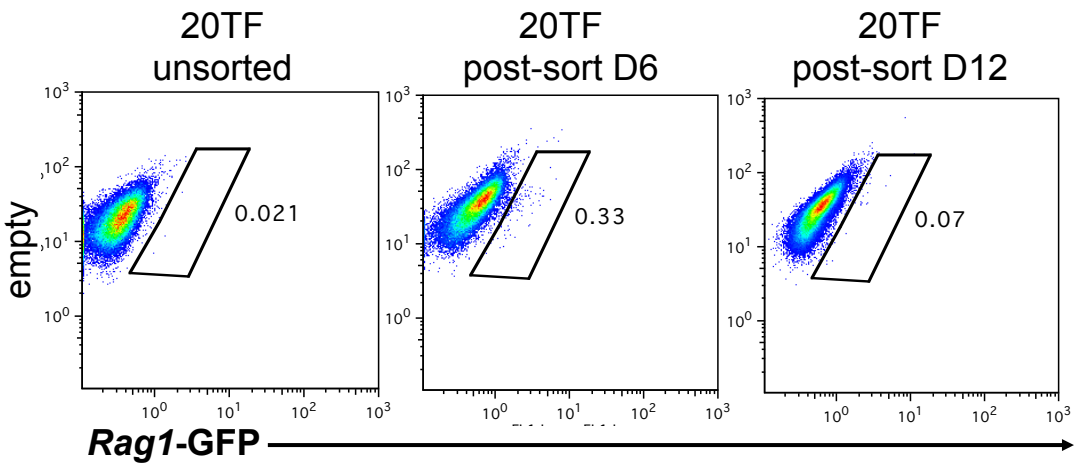

Figure 4.7. *Rag* expression in fibroblasts is not stable.
Flow cytometer analysis of GFP expression in primary *Rag*1-GFP fibroblasts transduced with 20 factor pool prior to sorting (20TF unsorted), or following sorting for rare GFP+ cells. GFP expression in expanded cultures are shown for day 6 (D6) and day 12 (D12) post-sorting.

Figure 4.8

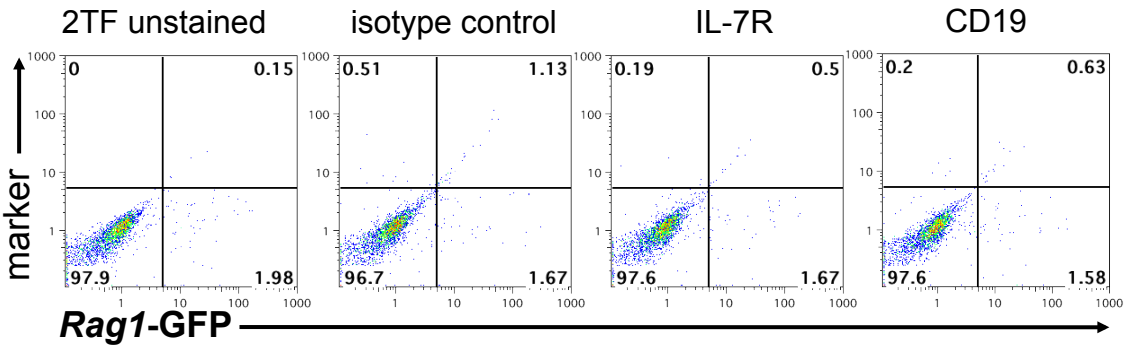

Figure 4.8. *Rag*-expressing fibroblast do not express B lineage cell surface markers. Flow cytometer analysis of B cell surface marker expression versus GFP expression in primary *Rag*1-GFP fibroblasts transduced with Foxo1 and E47 (2TF).